NERC ADVANCED TRAINING

British Geological Survey
NATURAL ENVIRONMENT RESEARCH COUNCIL

Multidisciplinary Fieldwork Training in a Professional Geoscience Environment: Quaternary mapping, landscape literacy and hazard identification

NERC SCIENCE OF THE ENVIRONMENT

BRITISH GEOLOGICAL SURVEY

TRAINING PROGRAMME

INTERNAL REPORT IR/14/054

Multidisciplinary Fieldwork Training in a Professional Geoscience Environment: Quaternary mapping, landscape literacy and hazard identification

A H Cooper, H Kessler, H Burke & J Chambers

Contributors

S Booth, J Lee, J Ford, S Price

Keywords

Report; Quaternary, Yorkshire, mapping, training, geological hazards, landslides.

National Grid Reference

SW corner 400000,400000
Centre point 470000,450000
NE corner 540000,500000

Map

Sheet Various, 1:50 000 scale, Harrogate, York, Leeds, Selby, Flamborough & Bridlington

Bibliographical reference

COOPER, A H, KESSLER, H, Burke, H & Chambers, J. 2014. Multidisciplinary Fieldwork Training in a Professional Geoscience Environment: Quaternary mapping, landscape literacy and hazard identification. *British Geological Survey Internal Report*, IR/14/054. 65pp.

Keyworth, Nottingham British Geological Survey 2014

BRITISH GEOLOGICAL SURVEY

The full range of our publications is available from BGS shops at Nottingham, Edinburgh, London and Cardiff (Welsh publications only) see contact details below or shop online at www.geologyshop.com

The London Information Office also maintains a reference collection of BGS publications, including maps, for consultation.

We publish an annual catalogue of our maps and other publications; this catalogue is available online or from any of the BGS shops.

The British Geological Survey carries out the geological survey of Great Britain and Northern Ireland (the latter as an agency service for the government of Northern Ireland), and of the surrounding continental shelf, as well as basic research projects. It also undertakes programmes of technical aid in geology in developing countries.

The British Geological Survey is a component body of the Natural Environment Research Council.

British Geological Survey offices

BGS Central Enquiries Desk

Tel 0115 936 3143 Fax 0115 936 3276

email enquiries@bgs.ac.uk

Environmental Science Centre, Keyworth, Nottingham NG12 5GG

Tel 0115 936 3241 Fax 0115 936 3488

email sales@bgs.ac.uk

Murchison House, West Mains Road, Edinburgh EH9 3LA

Tel 0131 667 1000 Fax 0131 668 2683

email scotsales@bgs.ac.uk

Natural History Museum, Cromwell Road, London SW7 5BD

Tel 020 7589 4090 Fax 020 7584 8270

Tel 020 7942 5344/45 email bgslondon@bgs.ac.uk

Columbus House, Greenmeadow Springs, Tongwynlais, Cardiff CF15 7NE

Tel 029 2052 1962 Fax 029 2052 1963

Maclean Building, Crowmarsh Gifford, Wallingford OX10 8BB

Tel 01491 838800 Fax 01491 692345

Geological Survey of Northern Ireland, Colby House, Stranmillis Court, Belfast BT9 5BF

Tel 028 9038 8462 Fax 028 9038 8461

www.bgs.ac.uk/gsni/

Parent Body

Natural Environment Research Council, Polaris House, North Star Avenue, Swindon SN2 1EU

Tel 01793 411500 Fax 01793 411501

www.nerc.ac.uk

Website www.bgs.ac.uk

Shop online at www.geologyshop.com

Foreword

This guide has evolved from the documentation for the Lowland Britain Quaternary Mapping Course that has been run since 2000. The training aims to provide geologists with the basic mapping skills needed to record and understand Quaternary successions and landforms, mainly related to the last glaciation (Devensian) in Lowland Britain. It considers glacial and periglacial processes and some geological hazards related to them.

Much of this guide concerning the glaciation of the Vale of York is based on a paper in the process of being completed for publication. The materials are copyright of BGS/NERC and must not be reproduced until they are formally published

Acknowledgements

This current guide builds on previous guides and contributions from many past and present colleagues, including Steve Booth, John Carney, Jon Ford, Simon Price, Jon Lee, Brian Moorlock, Tony Morigi, Adrian Humpage, Clive Auton, Jon Merritt and Jim Rose. We also extend our gratitude to Ann Evans and Jon Naden for their guidance and assistance in organising the course.

This course could not be run without the willing co-operation of the many landowners and farmers who continue to grant us unfettered access to their land; please keep in mind that it is the responsibility of everyone on the course to respect this privilege.

Contents

FIGURES

TABLES

Summary

This report was produced to describe the Quaternary geology of north-east England and how it can be interpreted and mapped. It is based on previous manuals for Quaternary geology mapping training produced by the British Geological Survey. It gives insight into the glacial and periglacial processes of the Yorkshire coast and the Vale of York.

Course objectives:

- To provide a hands-on opportunity to gain confidence in field mapping Quaternary deposits
- To familiarise individuals with some basic techniques to use when mapping the range of Quaternary and mass-movement deposits commonly encountered in lowland Britain within and next to the last glacial limit.
- To acquire an understanding of Quaternary depositional processes and landforms needed to develop 'landscape literacy' skills
- To understand the BGS standards for geological mapping
- To emphasise relevant Health and Safety issues, particularly in the use of augers and conduct both in the field and on mineral extraction sites

1 Introduction

1.1 COURSE SCHEDULE

1.1.1 Monday 20th October – Locality 1 - Leader Helen Burke

Keyworth depart 10am drive to coast (111 miles 2.5hrs) arrive about 12.30-1.00 lunch and coastal sections.

Lunch at caravan park cafe

Study coastal sections for up to 4 hours

Drive Barmston to Pocklington (28 miles 50mins-1hr)

1.1.2 Tuesday 21st October – Localities 2-8 Leaders Tony Cooper and Holger Kessler

Depart hotel 9.00am Drive Pocklington-Allerton Park (32 miles, 1 hour)

10.00-11.30 Locality 2 - Allerton Park, esker morphological features, soil types, augering, road section, and erratics

11.30-11.55 Drive to Farnham (6 miles, 15 mins) with brief stop to look at Allerton Park Folly and ridge +10 mins

11.55-12.10 Locality 3 - Look at abandoned pre-glacial valley at Farnham

12.10-12.25 Drive to Knaresborough and park (2 miles, 10 mins)

12.25-14.00 Locality 4 - Knaresborough Gorge glacial diversion; have lunch in Knaresborough

14.00-14.20 Drive from Knaresborough to Nidd flood plain on A59 layby (9 miles, 20 mins)

14.20-14.35 Locality 5 - 15 mins looking at flood plain and glacial lake bed features

14.35-15.00 Drive across flat glacial lake deposits (locality 6) to the rising ground of the York Moraine (locality 7) then on to Escrick Clay Pit pit 10 miles (13 mins) with brief stop at Escrick petrol station facilities

15.00-16.30 Locality 8 Escrick Clay pit

16.30 – 17.00 Locality 9 - If time permits, possible stop at Skipwith Common to auger the Breighton Sand Formation, Skipwith Sand Member and underlying peat

17.00-17.30 Drive to Church Hill, Holme on Spalding Moor (20 miles 30 mins)

17.30-18.15 Locality 10 – Church Hill, Holme on Spalding Moor. Consider the view across vale of York and the geography of the last glaciation, look at pre-Devensian deposits including ventifacts around church

18.15-18.30 Drive to Pocklington (9 miles 15 mins)

1.1.3 Wednesday 22nd October –Locality 9- Leaders Holger Kessler and Helen Burke

Locality 11 Mapping at Stillingfleet with travel at lunchtime by van to Eskrick Petrol Station for lunch and facilities

If Skipwith was not visited the previous day, stop at Skipwith Common on the way back to the hotel to auger the Breighton Sand Formation, Skipwith Sand Member and underlying peat

1.1.4 Thursday 23rd October – Locality 10 - Leaders Holger Kessler and Helen Burke with assistance from Steve Thorpe (drilling)

Locality 12 -Newton Clay Pit in the morning – logging glacial lake deposits, glacial till and cover sand sequence with glacio tectonics, depending on exposures

Stop at petrol station in Escrick to buy lunches and use facilities

Borehole logging at Stillingfleet drill site, plus time for some more ground truthing/mapping and consideration of geophysics obtained in the southern field

Evening - map compilation at hotel

1.1.5 Friday 24th October – Localtiy 13 - Leaders Jon Chambers and Tony Cooper

Depart 9.00 drive to Hollin Hill (45 mins 21 miles)

10.00-11.00 Locality 10 - Explanation by Tony Cooper of the local geology, Jurassic sequence, glacial deposits, glacial and periglacial geomorphology and setting of the local landslides

11.00-13.00 Explanation by Jon Chambers of the Hollin Hill landslide field laboratory and the various instrumentation and results

Lunch at The Art Café in the village of Terrington, possibly organised in advance http://www.yorkpress.co.uk/news/ryedale/11038253.Terrington_Village_Stores_caf___all_set_for_reopening/

14.00 latest depart for Keyworth; travel via York railway station and arrive in Keyworth 16.30ish (112 miles 2.5 hrs)

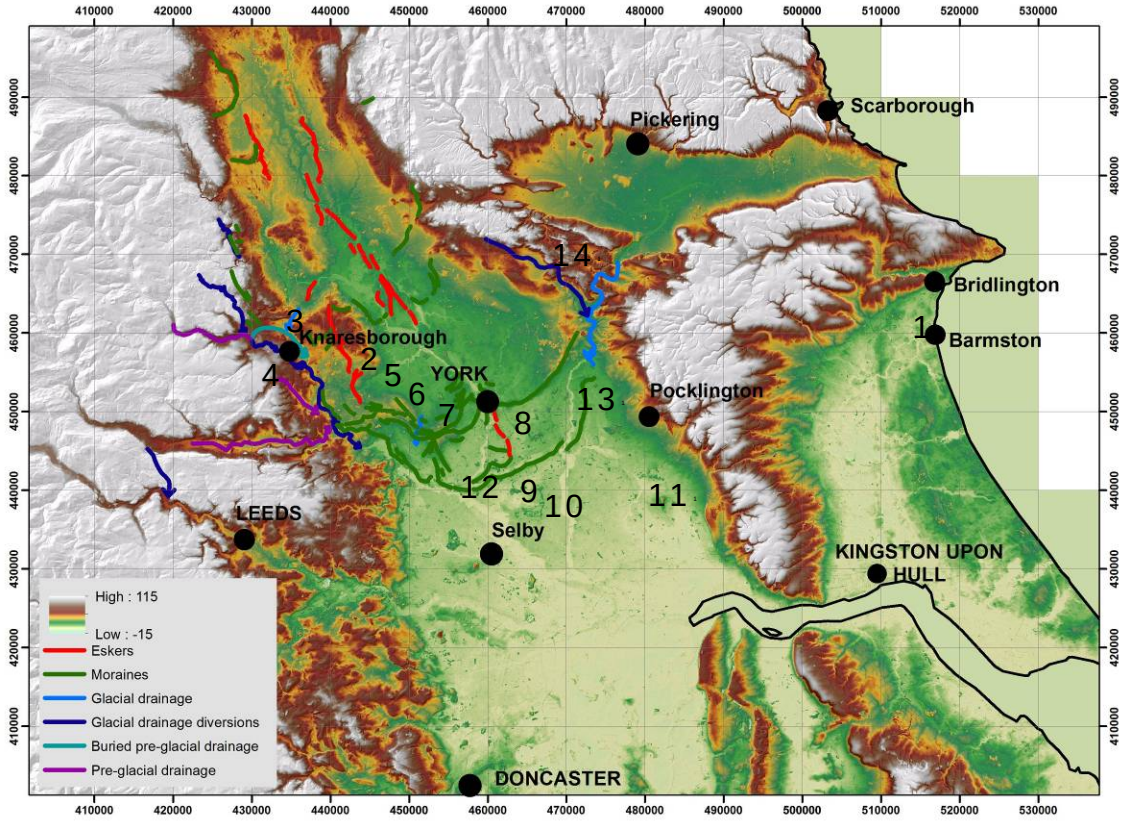

Figure 1-1 Elevation map (DTM) and localities to be visited

Figure 1-2 Topography and localities to be visited

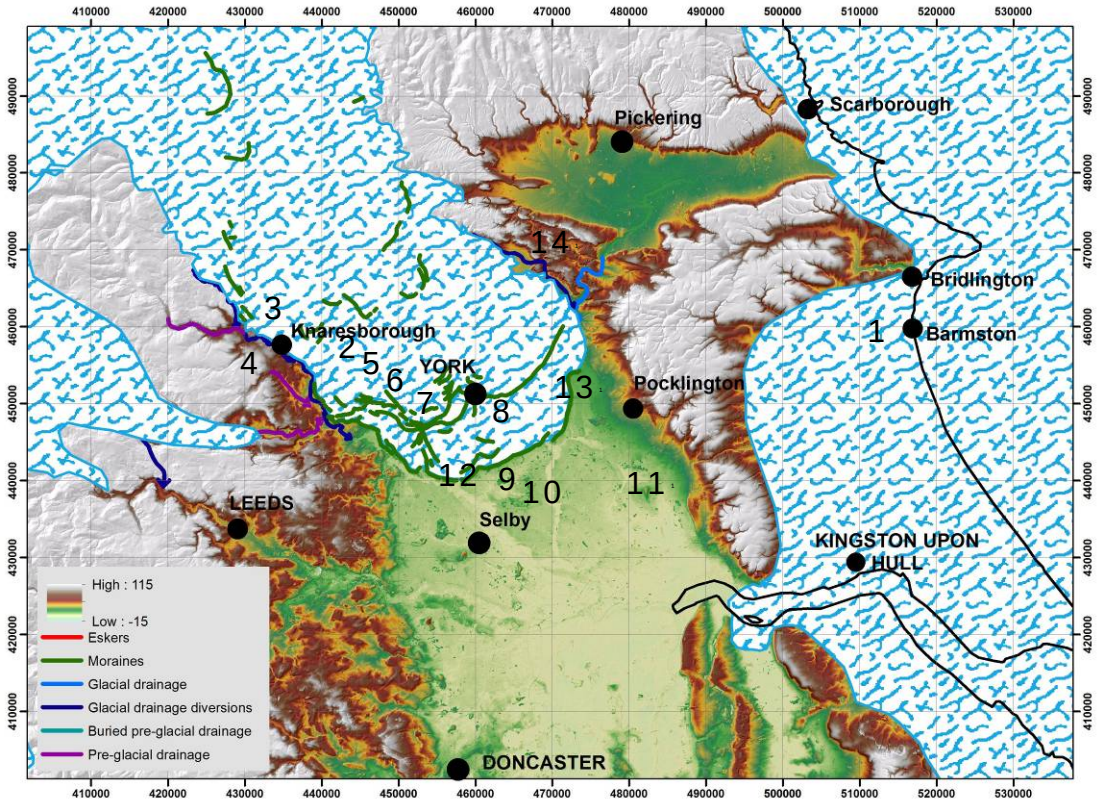

Figure 1-3 Last Glacial Maximum ice cover and localities to be visited

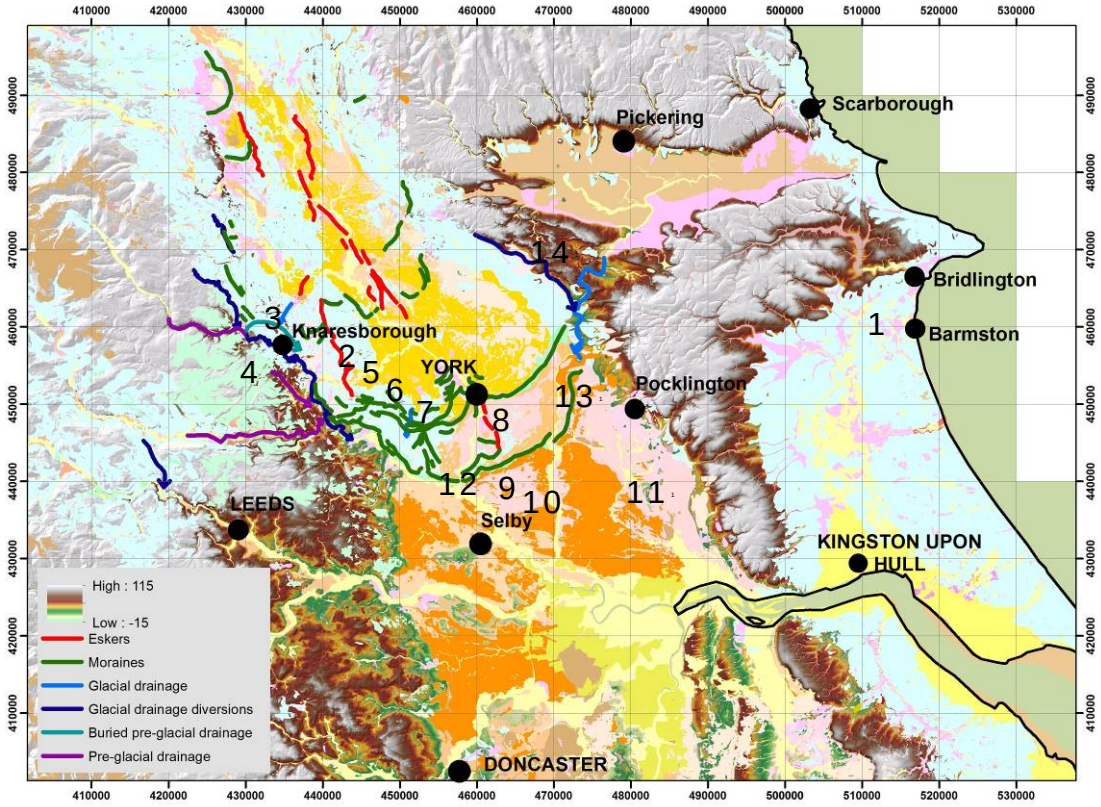

Figure 1-4 DTM for exposed rocks with superficial geology and localities to be visited

1.2 HEALTH AND SAFETY

Every person, in whatever job, has a legal responsibility for their own Health and Safety and for all those for whom they are responsible. This obligation is embedded in the NERC/BGS core responsibilities. Before any fieldwork is undertaken a full risk assessment must be carried out and signed off by a responsible officer/s. In the field it is the individual's responsibility at all times to watch out for themselves and their colleagues. Any concerns should immediately be raised with the person responsible for the trip.

This is not a Health and Safety manual; participants will have undertaken office-based risk assessments for the proposed work. They should be familiar with the risk assessment methodology and aware of the resources available to undertake this including:

NERC Risk Assessment Manual revised 2014:

http://www.nerc.ac.uk/about/policy/safety/procedures/procedure_riskassessment.pdf

NERC Safe System of Fieldwork 2007:

http://www.nerc.ac.uk/about/policy/safety/procedures/guidance_fieldwork.pdf

NERC Lone Working Policy:

http://www.nerc.ac.uk/about/policy/safety/procedures/guidance_lone_working.pdf

Other considerations include pesticide use on farms:
PSD www.pesticides.gov.uk/home.asp.

Note that it is easy to pick up diseases from animals and soil, the use of hand disinfectant gel or washing of hands before eating and drinking is essential:
http://www.hse.gov.uk/campaigns/farmsafe/ecoli.htm

1.3 ACCESS TO LAND AND PARKING OF VEHICLES

For the course module, land access has been negotiated and approved prior to your arrival. However, when undertaking mapping as part of your own project, it is important that you secure land access from the landowners *prior to* commencing mapping. Most farmers are very reasonable, but do keep in mind that the farmer(s) may be experiencing financial, crop or stock difficulties and may resent your presence on their land.

Experience has shown that it is best to call upon farmers at the time of fieldwork rather than to write to them in advance. Most geologists tend to visit the farms unannounced and simply ask for permission to carry out the survey, but some prefer to phone the farmers first to make an appointment – this is preferable on some of the larger farms and estates, which have managers. Always have your identification available.

Farmers often prove useful sources of information providing an insight on the local geology as they will be able to tell you where there are unusual conditions such as particularly heavy ground, springs, gravel pits, artificial ground etc. Many farmers have had boreholes drilled for irrigation purposes, and some have had surveys for aggregate conducted on their land. A few farmers may have commissioned soil surveys of their ground. If they are prepared to let you have sight of or to copy this information it is worth pursuing.

Whilst accessing the land, the farmer should be asked about dangerous farm animals, spraying of pesticides or any matter that relates to you safely conducting the survey. If such hazards are present, farmers may restrict your access or arrange for you to visit these areas at a more convenient date. Common reasons for this may include:

- land occupied by cows, pigs and poultry which can be particularly prone to disease such as TB, swine fever and avian flu, respectively.
- dangerous animals – cows after calving or bulls
- pheasant breeding and shooting
- fungal infections of root crops such as potatoes (*Phytophtora infestans*) and sugar beet (*Fusarim)* – this may result in affected fields being quarantined for several years
- spraying of pesticides or sulphuric acid on potato plants

Guidance on working around livestock and pesticides can be found on the web and within the BGS safe fieldworking procedures.

Please note that following DEFRA guidance, it is now necessary for visitors to record which farms (and fields) they have visited and when – just in case there is a further National emergency like Foot and Mouth. If farmers are concerned about hygiene they may insist that boots and vehicle wheels are disinfected before and after the farm visit has been made. The DEFRA guidance (summer 2003) puts the onus on farmers to provide disinfectant if they require visitors to use it, but some farmers may ask you to come equipped with wellingtons, a bucket, scrubbing brush, water and disinfectant.

With regards parking, it is best if vehicles are not parked in farmyards where they may come into close contact with farm animals or farm vehicles. Drivers should always ensure that their vehicles do not obstruct field access. When parking a vehicle, leave some form of identification on the dashboard. This will enable farmers, police, etc to realise that the vehicle has not been abandoned. If you are working in an area for a significant time, it is also recommended that you inform the local police of your presence and vehicle type/registration.

2 Preparation for fieldwork

2.1 THE MAPPING PROJECT

Prior to the commencement of fieldwork, there are several aspects of the project and fieldwork that need to be discussed and undertaken. These include:

- defining the mapping project objectives
- pre-fieldwork data acquisition

2.1.1 Defining the Mapping Project Objectives

Before any mapping project gets underway the following should be considered

- the purpose and objectives of this mapping project
- Health and Safety field-related issues and establishment of a project H&S file
- the domain characteristics of the mapped area – what are the known complexities of the Quaternary deposits?
- the extent/range/validity of previous work including mapping
- the availability of Remote Sensed imagery and Digital Terrain Models
- the mapping scale required by the project, normally 1:10,000 or 1:25,000
- the field methodologies to be employed in this instance
- the mapping intensity level needed to achieve the desired mapping resolution
- an assessment of a realistic timeframe for fieldwork and the anticipated delivery date

Conducting *preliminary research* into previous work should lead to a better understanding of the Quaternary depositional and/or mass-movement processes that may have been operating in the field area (e.g. ice directions and lithology/provenance of erratics; river terrace sequence and chronology). In addition to assisting with the field interpretation of the deposits, pre-field literature research lends scientific direction to a project and stimulates interest in the mapping task.

Assessing the *availability and potential usefulness of various techniques* (e.g. Remote Sensed data etc). The aim here is to focus on techniques that may increase the efficiency of field mapping. Table 2-1 provides a general overview of the range of techniques that can be employed within lowland Quaternary mapping, and their relative usefulness in (1) Devensian glacial terrains; (2) Middle Pleistocene glacial terrains; (3) modern floodplains.

The conclusions of *these deliberations should be documented* from the outset as part of the evolving and recorded *project strategy*. At this stage the anticipated *project outcomes* should be clearly defined, along with the working instructions to individual team members.

2.1.2 Pre-fieldwork data acquisition

There is a wide range of data sources available to the geologist that can be used to attain a good background understanding of the field area, as well as sources of information that can be used in the field. A significant part of the project time should be allocated to gathering this information. Much of the information is available to universities through EDINA http://digimap.edina.ac.uk/digimap/home# and other data is available from BGS and the Ordnance Survey as part of their Open Data http://www.bgs.ac.uk/opengeoscience/ . Potential sources include:

- ***Geological fieldslips, standards***

Available only directly from BGS. Any existing fieldslips/standards/published maps of the area should be examined. If you are making a revision survey, there should be 1:10,000 or 1:10,560 scale field slips and Standards available within the BGS archives. If you are making a primary survey there will be at best only one-inch to one-mile (1:63, 360) scale geological maps available. It is worthwhile incorporating these datasets in a GIS so that they can be displayed and printed on a modern 1:10,000 scale topographic base, which may highlight any obvious errors where the geology conflicts with the topography.

- ***Borehole logs and well records***

Available on the web via http://www.bgs.ac.uk/data/mapViewers/home.html Onshore GeoIndex and as a phone App via iGeology. Boreholes should always be examined prior to commencing any fieldwork (Figure 2-1). In general, site investigation boreholes will be more accurately logged than wells. Be aware that many wells were recorded relatively crudely, for example '100 feet of blue clay on 200 feet of brown sand', yet when metricated these figures can look very precise: '30.48 m of blue clay on 60.96 m of brown sand'. Similarly, heights of many of the older wells were estimated from the 100 ft contours on the maps – again these can look very precise when metricated.

- ***Aerial photographs***

BGS (and probably EDINA - OS MasterMap® Imagery Layer**)** has aerial photographs for the whole of England, Scotland and Wales. In BGS the images are stored digitally and georeferenced in 1 km squares so can be downloaded directly into a GIS layer, or opened simply in a photo software package. Note also that free aerial imagery is available on Google Maps, Google Earth and Bing Maps. Commonly different ages and sources of aerial photography are available through these sources and Google Earth has a date facility that allows different generations of images to be viewed on a slider. With a little extra work geological information can be imported into Google Earth and displayed along with their image information.

- ***Digital Terrain Models (DTM)***

The nationwide available Ordnance Survey DTMs (based on 10 or 5 metre contours) are useful to provide an overview of the morphology of the area and will pick up large features such as the Escrick moraine. They are, however, often unsuitable for detailed mapping as the data is often sparse in flat areas and spot heights on roads etc have been used to generate these datasets. The basic 1:50,000 scale dataset is available from the OS Open data as Land-Form PANORAMA http://www.ordnancesurvey.co.uk/business-and-government/products/land-form-panorama.html

Airborne radar derived DTMs such as NEXTMAP and LIDAR have proved very useful in delineating subdued features such as sand dunes and terraced topography (e.g. river terraces). These datasets may be available on EDINA. However, even very accurate DTM models will not reveal buried geological units with no topographical expression e.g. former glacial channels or help to determine what lithology comprises the feature.

Terrain type	Devensian glacial	Middle Pleistocene glacial	Floodplain
PRE FIELD			
Borehole data	●●●●	●●●●	●●●●
Soil maps	●●●	●●	●●●
Literature	●●●●	●●●●	●●●●
Historical records			●●
Flood data			●●●●●
DEM	●●●	●●●	●●●
REMOTE SENSING			
Aerial photos	●●●●●	●	●●●●
Satellite images	●●●		●●
Airborne radiometrics	●●	●	●●
LIDAR / SAR	●●●●	●	●●●●
FIELD METHODS			
Landform mapping	●●●●●	●●	●●●●●
Soil and brash type	●●●	●●●●	●●●
Standard augering	●	●●●●●	●
Altimetry (thalwegs)			●●●●
Section logging	●●●	●●●	●●●
Pitting	●	●●●	●
Shell & auger boreholes	●●●●	●●●●	●●●●
Flight auger boreholes	●●●	●●●	●●●
Hollow stem auger boreholes	●●●●●	●●●●●	●●●●●
Delft system drilling	●●●●●	●●●●●	●●●●●

Terrain type	Devensian glacial	Middle Pleistocene glacial	Floodplain
ANCILLIARY TECNIQUES			
Biostratigraphy	●●	●●	●●
Clast lithologies	●●●	●●●●●	●●●●●
Clay mineralogy	●●	●●	●●
Heavy mineral analysis	●●	●●●	
Particle size	●●●	●●●	●
Palaeoecology	●	●●	●
Radiometric dating	●●	●●●	●●●
EXPOSURE TECHNIQUES			
Sedimentary logging	●●●●●	●●●●●	●●●●●
Clast fabric	●●●	●●●	
Orientation of structures	●●●	●●●	●
Field sketches and photos	●●●●●	●●●●●	●●●●●
Lithological analysis	●●●	●●●	●
Collection of samples	●●●●	●●●●	●●
GEOPHYSICS			
EM Methods	●	●	●
High resolution seismic	●	●●	●
Ground penetrating radar	●	●	●
Resistivity	●	●●	●

Table 2-1. Suggested prioritising of mapping techniques for different types of drift deposits. The greater the number of dots, the higher the priority of the technique for use in a given type of Quaternary drift domain.

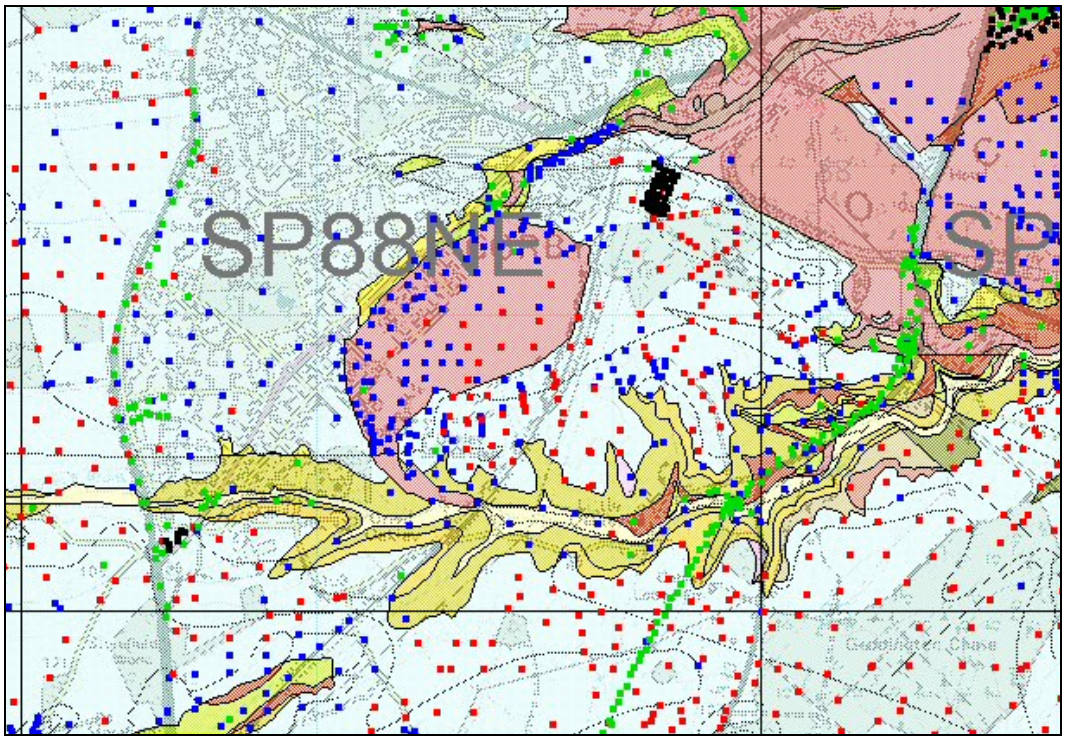

Figure 2-1. Map extract showing the distribution of boreholes around the town of Corby

- ***Soil Survey data***

It is always worth looking to see what Soil Survey data exists for the mapping area. This might only be 1:250,000 scale coverage but in a number of areas 1:25,000 scale maps are available; associated with these maps, grid surveyed soil sampling to one metre depth may be obtainable on request and at a price from the NGRS. Care should be exercised to ensure that Soil Survey linework is not replicated to produce a 'new' geological map. Aside from the important issue of Copyright Infringement, your lines should be based on geological observation and interpretation. Preliminary collaborative trials with the use of 're-classified' soil data as base data for geological mapping have proved reasonably successful in some parts of the Vale of York. The success was tempered by factors such as complexity of the underlying geology (especially the presence of thin "blanket deposits"), the classification scheme used by the soil surveyor and the subsequent translation of this soil schema into geological terminology.

- ***Old OS Maps***

Scans of these are available in BGS and also through EDINA. These may show evidence of former land use e.g. quarrying, mining, smelting, which may pose contaminated ground issues. They are also useful as they can show evidence of former hedges and ditches that have been removed or infilled (Figure 2-2).

- ***Other information***

The BGS National Geoscience Record Centre (NGRC) holds a series of files based on individual 1:50,000 sheets. These contain a miscellany of information – some of which might prove useful but it must be treated with considered caution! The NGRC also holds a collection of BGS field notebooks. These can provide much information, but it is not always easy to locate the geographical position of sections etc., in notebooks that pre-date the National Grid. However, where possible, these notebooks are indexed to their relevant 1:10,000 scale topographical maps.

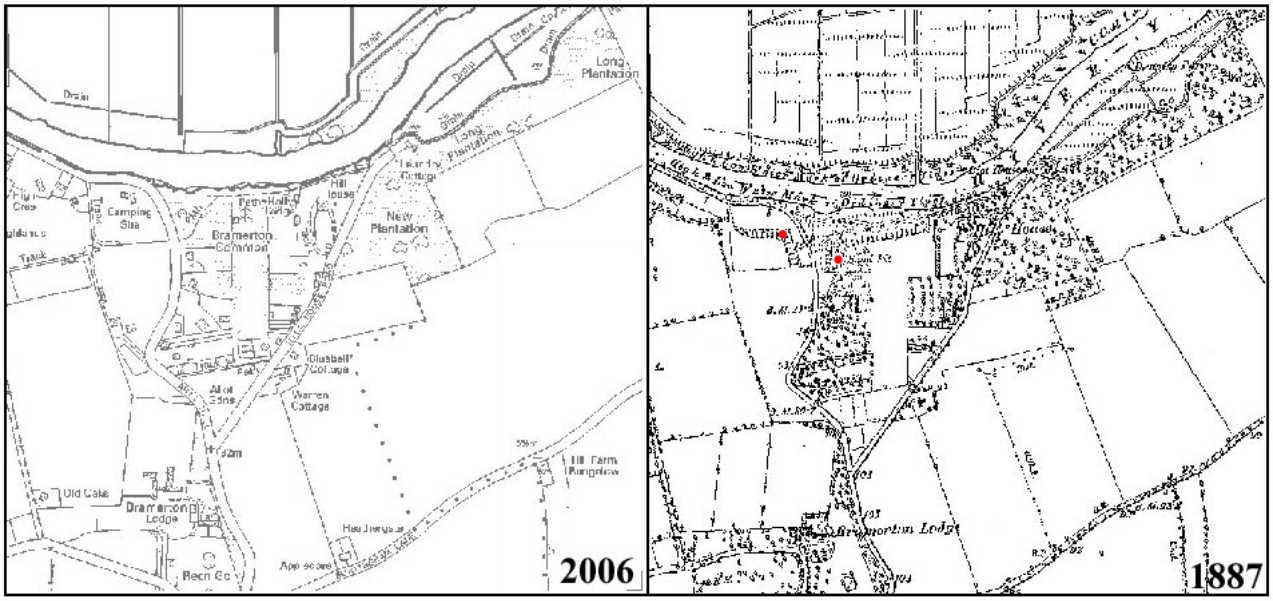

Figure 2-2. OS maps from 2006 and 1887 for the area near Bramerton, southeast of Norwich. The red dots on the 1887 map show sand pits that are no longer working and evident on the 2006 map. The old map also shows several field boundaries that have since been removed – a subtle crest line and area of worked ground may be found adjacent to these previous field boundaries.

2.2 SUMMARY

This chapter has covered several key elements that need to be addressed before field mapping can be started. These include:

- defining the mapping project objectives and methodologies, including personal deliverables
- the availability and appropriateness of different types of data to enhance geological mapping
- dealing with landowners and farmers, land access and parking of vehicles

3 Field observations and data recording

3.1 BASIC PRINCIPLES OF MAPPING QUATERNARY (SUPERFICIAL) DEPOSITS

Geological mapping inevitably involves many uncertainties, some of which will not be determined even after the completion of the map-making process. Starting from a base of information gathered during the project-planning phase, the proven methodology (not exclusive to Quaternary mapping) is to place reliance on what can be observed and recorded about **landform** and **lithology**.

Landform (morphology) simply relates to the shape of surface features (slopes, slope breaks) whilst lithology refers to the composition of a deposit and encompasses other elements such as colour, texture, sedimentology and fossil content.

An appreciation of both lithology and morphology helps the geologists to determine the basic building blocks of the geological map, the **geological units**.

Using the landform and lithology elements, a third element – **process** (the mode of origin) – may be inferred. An understanding of the process by which a geological unit was formed is in most instances *essential* to superficial mapping. If geological processes are known and understood, this insight enables the geologist to more confidently establish the spatial and temporal associations and complexities between individual sediments and their respective morphological elements.

In the early stages of mapping, the emphasis will be placed on observation:

- lithological descriptions at specific points (e.g. exposures, auger holes)
- recording landforms by means of form lines as interpretation of the process(es) responsible for lithology and landform evolves.

The combination of landform, lithology and process leads to *interpreted* **morpho-litho-genetic units**, - mappable units that provide the basis for establishing a **local stratigraphy**.

The local stratigraphy is the minimum benchmark that the geologist should be aiming for. Without this basic superposition understanding any map produced merely displays the spatial distribution of geological units present. As mapping progresses the surveyor will test and repeatedly revise this local stratigraphic sequence. Providing sufficient data exists, the next stage would be to incorporate this local stratigraphic model into its wider **regional stratigraphical** context, which in turn will involve **chronology** and **lithostratigraphy.** These elements contribute to the evolving conceptual model, towards the completed map and to a 3D (lithoframe) model.

A mapped geological unit must be defined in terms of its spatial extent enclosed by a boundary line, which defines a polygon in a digital geological map. Typically in BGS datasets each polygon is attributed with a code for lithology and a code for stratigraphy.

Lithological codes are available through the searchable BGS rock classification scheme http://bgs.ac.uk/bgsrcs/ - unfortunately, this includes both old and new codes. We recommend using codes from the "Unlithified deposits coding scheme" a hierarchical system that gives the components in descending amounts starting with the major component using the letters – B for boulder, V for gravel, S for sand, Z for silt, C for clay, P for peat. Sand is coded as S; a gravelly sand is SV; a diamicton/glacial till might be CSVB (a clay that is sandy with gravel and boulders); clayey peat would be PC.

Stratigraphical codes for existing named units are available through the Lexicon of Named Rock Units http://bgs.ac.uk/Lexicon/ Obviously, new unnamed units will not have a code; consequently, it is best to do a search and assign new codes that have not already been used.

3.2 WHAT DOES A LINE ON A GEOLOGICAL MAP IMPLY?

A geological line on any geological map principally demarks one **geological unit** from another – effectively that the deposit at the line edge thins to zero thickness. In reality, this definition is often let down by the geological practicalities of deciding upon the placement of the line, and cartographic limitations of drawing a line on a map since the visible representation will always appear to imply a degree of thickness. The scale of the map or section will of course determine this apparent thickness. There are several potential problems and issues that face the geologist regarding the positioning of lines, and these are outlined below:

What specifically can a geological line represent?

- a three dimensional geological boundary separating geological units.
- the 'top' and/or 'bottom' of a geological unit.
- the spatial extent of a deposit/unit = the locus of zero thickness
- a geological structure such as a fault.
- a time-related boundary – implying an event or a hiatus.

What other types of line are used in the mapping of Quaternary deposits?

Form lines may be used to define landforms as, for example, terrace outer edges and back features, landslide scars, glacial meltwater channel margins and centre lines, eskers, drumlins, kettle holes. Such lines are subject to the same degree of error in placement as geological boundaries.

What types of evidence are used to position lines?

- observation of features
- slope breaks associated with features
- DEM slope analysis (NextMap)
- stereo pair analysis of aerial photographs
- lithological observations derived from auger traverses and soil brash
- boreholes
- interpretation (best guess judgement)

How accurately are lines positioned?

Accuracy is a function of the scale of the map used, the thickness of the drawn line, the accurate drawing of the line, the accuracy of location in the field, the degree of interpolation between observations, the relative proportions of observation and inference used in determining the position of the line. For example, at 1:10,000 scale, the accumulated error will generally be ±15 m (empirically determined), occasionally better and sometimes worse. At 1:25,000 scale it's probably about ±40 m and at 1:50,000 scale ±75 m to 80 m.

Judgement

Judgement is an overriding factor when determining the existence and position of lines as, for example, in drawing a line representing gradational boundaries or uncertain boundaries, judgement is likely to improve with experience.

3.2.1 Morphological and geomorphological mapping

Morphological mapping is a classic method of landform mapping that lies upon the recognition and recording of observable changes in topography and surface form. Morphometric information, for instance, convex and concave changes of slope and the geometry of plateaux surfaces, gullies and ridges, is purely descriptive and based largely upon the judgemental recording of field and remote observations supplemented with occasional quantitative measurements (i.e. slope angle). The main morphological mapping symbols (form lines) used by BGS for this purpose are shown in Figure 3.1.

From a mapping perspective, it is perceived that morphometric changes may reflect changes in the underlying superficial geology - for example, a bed of sand sandwiched between two beds of more competent till, or a resistant bed of sand and gravel overlying a till. Consequently, lithological boundaries and geological lines may therefore correspond to changes in relief. Equally, it is possible that morphometric features may bear no resemblance to the underlying superficial geology and may instead relate to some form of post-depositional modification – this is especially the case in areas that have been subjected to periglacial processes.

Since morphological mapping is purely descriptive and not genetically interpretative, geological interpretations of morphological features will be based upon geological hypotheses developed by the geologist for an individual mapping area. It is critical therefore that these hypotheses and geological interpretations can evolve and are testable based upon field observations. As a consequence of this need for testing and re-evaluation, pure morphological mapping is perhaps best suited to areas where the relief and geology is not complex – for instance lowland areas.

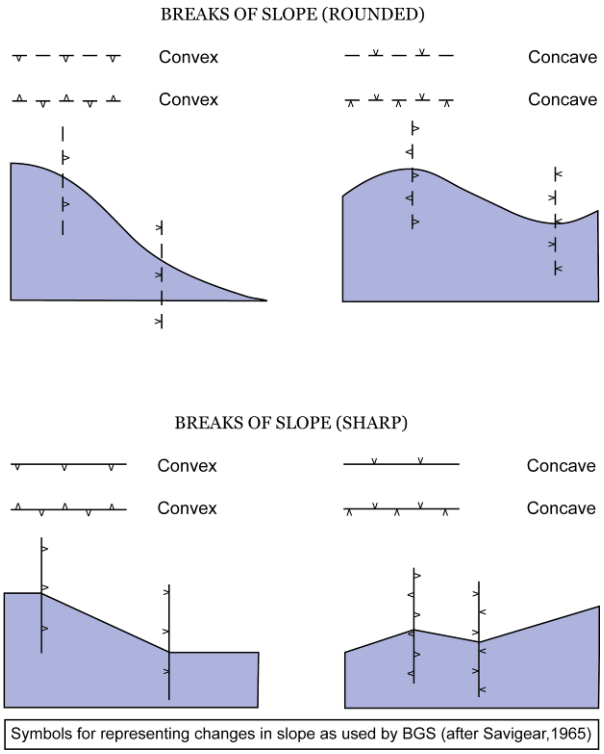

Figure 3-1. The primary morphological symbols for recording changes of slope

Geomorphological mapping enhances the purely morphological approach, as it also involves determining the genesis of the observed landforms, taking into account lithologies and their spatial geometry (including stratigraphy). As sound interpretation is the key to the success of this method, it requires a good understanding of landform assemblages and their genesis, together with an appreciation of other appropriate field and laboratory techniques that might assist in interpretation. Whatever other methods are brought into the geomorphological survey (e.g. if remotely sensed data are available, they can serve to increase the rate of ground coverage and reduce field time), ground-

truthing remains an essential element (e.g. to confirm remotely sensed interpretations, to observe sections and to record lithologies).

Augering. Two approaches to augering can be employed for boundary positioning (Figure 3-1). The initial approach is often to auger along a series of parallel traverses at intervals with auger holes separated by about 200m. If frequent variations in the geology are found or suspected it may be necessary to increase your frequency of augering. As boundaries between geological units are detected, the distance between auger holes should decrease so as to spatially constrain the boundary (i.e. boundary tracing). Geological boundaries can thus be interpolated between traverses, their positioning being guided by any other observations (e.g. slope changes) that have been made in the intervening ground and from contours on the base map. The often close link between slope changes and geological boundaries is particularly important for mapping once it has been recognised. Where the link is strong, walking along the feature whilst checking the relationship by judicious augering may be a preferable and time saving option to systematic traversing.

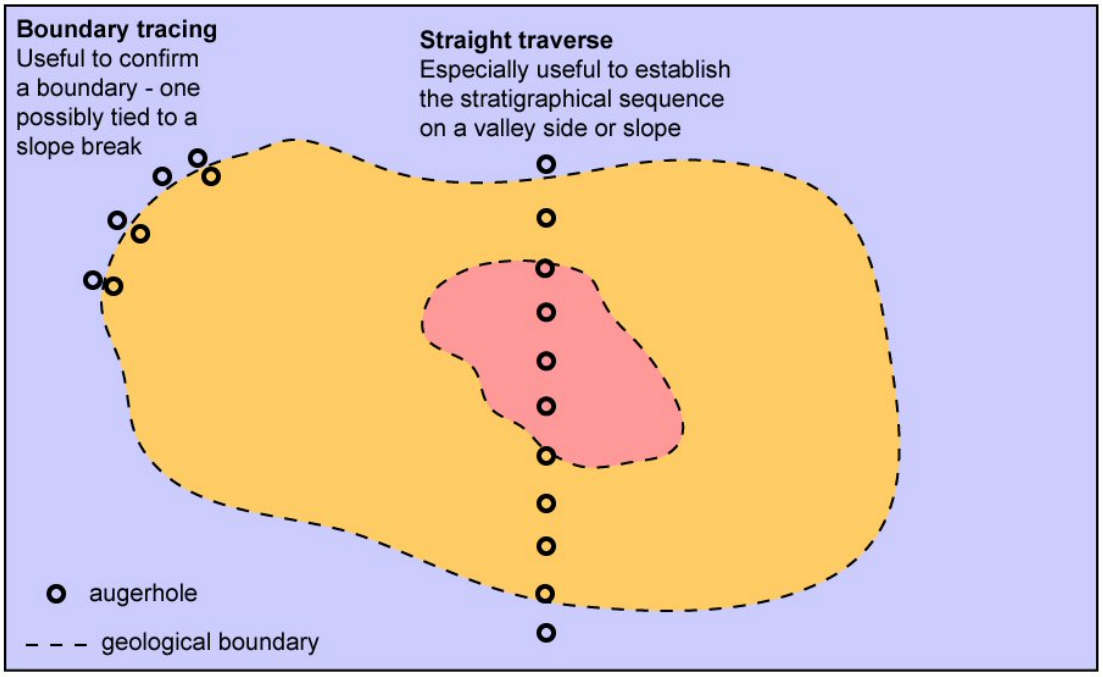

Figure 3-1. Two approaches to shallow augering and boundary positioning: (1) boundary tracing; (2) straight traverse

Auger locations are often marked on the base map by a dot or a cross with an abbreviated note alongside describing the lithologies encountered. BGS typically records *depth to* (from surface) in auger holes rather than the *thickness* of individual units, for instance silt to 0.5m, till to 0.9m, clay to 1.2m.

As familiarity with the terrain increases, geological and landscape subtleties often emerge and the significance of earlier observations becomes more apparent. This evolving understanding usually enables a reduction in augering frequency and leads to a more efficient mapping effort

3.2.2 Soil and spoil from animal burrows

Soil, especially over ploughed fields, and ‘spoil’ from animal burrows are often good indicators of the underlying geology. Although mapping of superficial deposits does not equate with formal soil mapping procedures, general observations on the textural properties of the soil should be made (e.g. whether sandy, clayey, peaty or stony). These observations may provide clues to the underlying ‘parent’ deposit and are thus a useful mapping aid.

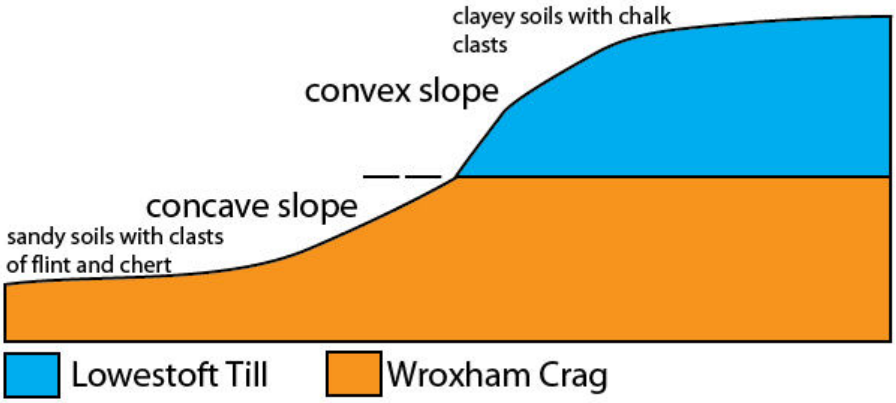

Figure 3-2. An example of soil texture and composition used in combination with slope breaks to determine the position of a geological boundary

Stones or fragments observed on the soil/ground surface are frequently referred to by the term ‘brash’; these fragments are often derived from the underlying parent material. Changes in soil texture, spoil or brash may provide a strong indication that a geological boundary has been crossed. The postulated presence of a boundary can be tested and constrained by augering and looking for possible related slope breaks. By way of an example, the transition from the Wroxham Crag to the Lowestoft Till in central East Anglia is marked by an abrupt change from light sandy soils with occasional flint and chert pebbles, to heavy clay-rich soils with abundant chalk. The sandy ground usually produces a concave slope whilst the till body tends to have a convex slope (Figure 3-2 and Figure 3-3).

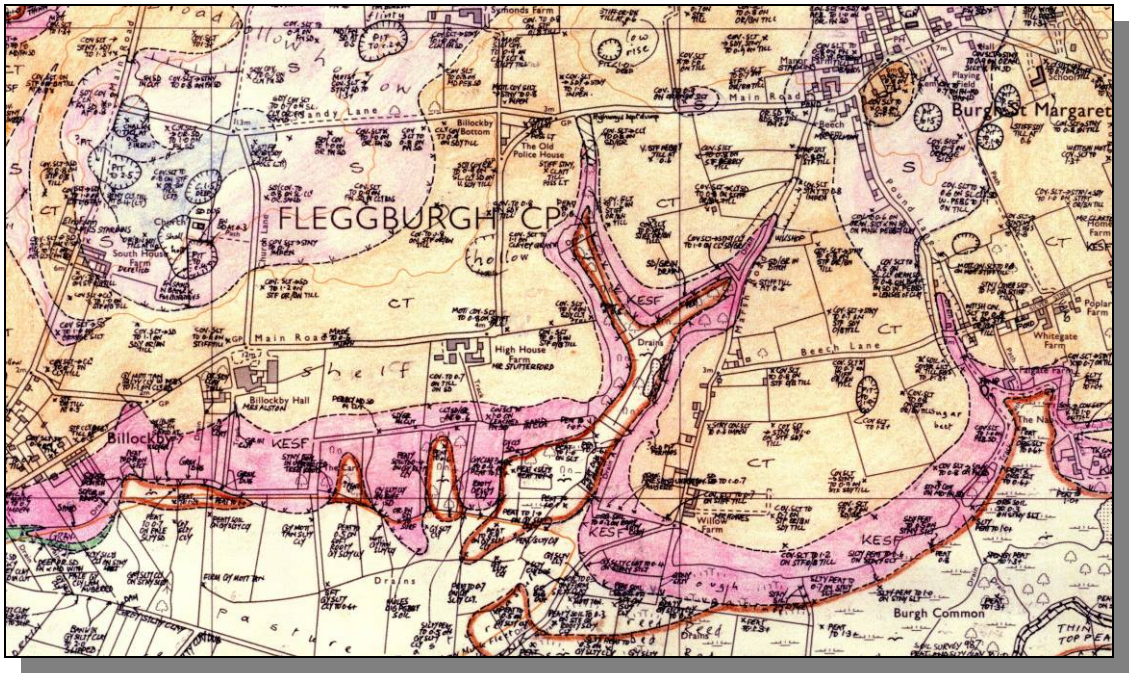

Figure 3-3. Map extract from a 1:10,000 scale fieldslip on the Great Yarmouth sheet. The fieldslip shows how slope breaks, auger holes and observations of soil brash have been used to constrain the geological boundaries

When fields were enclosed during the enclosure act, the hedge boundaries were commonly placed at lithological changes in soil type. This is commonly useful for mapping, but later modification and processes, as noted below, need to be considered. In recent times the removal of hedges and generation of large open fields can lead to features in the landscape that relate to previous hedge lines and hill-slope movements; historical maps can prove very helpful in determining the origin of some features.

Although soil, spoil and brash observations can be very useful, cultivation of the fields can in some cases produce some misleading results and a reasonable degree of caution needs to be exercised. Problems that may potentially be encountered include:

- ploughing or natural slope processes that may move material downslope over time causing build-ups on hedge lines and cutting away of downslope hill tops.
- soils may look especially stony in spring – the fine soil fraction having been washed away or mixed into the substrate by wind and rain over winter months
- landscaping and the application of lime and hardcore can modify the soil characteristics
- soils used to grow carrots and potatoes are often destoned by machinery, which sieves out the stones and redeposits them in rows alongside trenches.
- farmers tend to deposit stones and rubble in field entrances to make access easier, especially in clay areas. Never record the soil in a field entrance.
- farmers tend to clear large stones and deposit them in field corners or hedge bottoms, this is useful for recording erratics and ploughed up bedrock

3.2.3 Description of field sections

Recording and describing field sections (exposures) is an integral part of field observation. Sections can provide a wealth of lithological and stratigraphical information, as well as providing insights into the genesis and former dynamics of the geological sequence. Types of section that may be found include coastal cliffs and quarry faces, road and railway cuttings, ditches, trial pits and construction excavations. Sections may prove particularly hazardous; for example, the slopes may be unstable or have associated hazards, e.g. passing vehicles or trains. Health and safety considerations are therefore of paramount importance, and risk assessments for working on sections must be carried out during the project planning phase.

The examination and recording of your observations within exposed sections should follow a hierarchical approach. This will be based firstly upon simply recording your observations, and then interpreting these observations with respect to mechanism of deposition and finally environment of deposition.

Activity	Things to consider	Equipment
1. Record the OS grid reference	Proximity to exposure face; are there features obscuring the GPS instrument from the 'sky'	• GPS
2. Clean the section		• Spade, trenching tool or trowel
3. Make orientated and scaled sketches and photographs; draft sedimentary logs		• Field note book, data cards, pencil
4. Identify the principal geological units	• Visual breakdown of the sequence exposed	
5. Describe the section and the geological units	• Bed / unit geometry • Sediment texture • Structure • Lithology and composition • Colour • Palaeocurrents • Level of consolidation • Clast fabric • Organic content • Chemical content	• Tape measure • Grain size card • Hand lens, hammer • Compass clinometer • Munsell colour chart • Compass clinometer • Hand lens • Dilute HCl
6. Interpret the mechanism and dynamics of deposition, accretion / deformation	• Waterlain? • Windblown? • Sediment reworking	
7. Interpret the environment(s) of deposition / accretion / deformation	Are the sediments fluvial, shallow marine, subglacially derived?	

Table 3-1. Hierarchical approach to describing and interpreting sections

3.2.4 Other geological indicators within the field

Ditches

The presence of ditches usually indicates that the adjacent fields have poor natural drainage and are underlain by clay or silty or sandy clay. Ditches can be quite useful for augering in that they may give you a metre or so depth start. It is generally best to auger into the side of a ditch unless it has been very recently cleaned out. **Note**: beware of ditches polluted with slurry adjacent to farmyards and if in doubt avoid them! Ditches running down hillsides are a good place to determine the presence and thickness of any Head or hill-slope deposits.

Small pits in fields

In ploughed in pits, an examination of the rim will often reveal some evidence of what was originally dug. Many pits have been backfilled over the years. This may be evident from a change in the soil colour, the presence of brick, concrete, etc. Some may have been filled with the washings from sugar beet and these may not be obvious. Record the approximate depth of all pits as this may be important if the pits are later backfilled and development is planned. A check of the historical maps can also be useful in helping to define the exact sizes of former pits.

Crop marks

In hot dry summers, crops growing on well-drained deposits such as sand and gravel often become stressed and their growth is retarded. This characteristic provides an invaluable indication of small, isolated patches of sand and gravel on till plateaux, which otherwise probably would be missed. Similarly, the drying out of clay and presence of deep desiccation cracks can help define areas of clay.

Flora and fauna

The flora will often provide clues as to the nature of the underlying soils and superficial deposits. For example wild clematis (old man's beard) tends to occur on calcareous soils so may be an indicator of chalk-rich till (or Chalk bedrock!). Heather, gorse and bracken are typically found on the more acidic soils, so check for the presence of sand and gravel. Willows, sedges and mosses are generally associated with wet ground and commonly indicate the presence of alluvium and possibly spring lines. Mole hills, rabbit burrows and badger sets can be a very useful source of lithological information, though they tend to avoid waterlogged areas.

3.2.5 Supporting methods

Boreholes and trial pits provide invaluable lithological, stratigraphical and other property information supporting field mapping.

Boreholes

Boreholes are often the only way of obtaining information on the sediments at depths more than a few metres below the surface. A cable percussion 'shell and auger' rig is commonly used for most Quaternary sequences apart from where coarse gravels are prevalent. Lightweight rigs such as the BGS Dando drilling rig are particularly effective in deposits without large stones.

Trial pits

Trial pits dug with a JCB provide a quick and relatively inexpensive way of obtaining sub-surface information. However, *Health and Safety requirements* are making it increasingly difficult to excavate trial pits without placing shuttering within the excavations, which greatly increases the

costs and also minimises the faces that are available for study. It is essential to check with the Health and Safety Advisor before hiring any equipment or embarking on trenching operations.

Windpumps and handpumps

These may be associated with wells or former wells. It is worth checking with the farmer or landowner for information regarding why and how deep they were sunk; often there is an associated log, which may be made available for your purposes.

3.3 SUMMARY

This chapter provides the information on what data to collect, and how to record it within the field. You should now have a good general understanding of:

- the basic principles of mapping Quaternary (superficial) deposits
- representing geological units on a map
- what does the geological line on map imply?
- field techniques for mapping lowland Quaternary deposits.

4 Outline of the glacial geology of north and east Yorkshire

The pre-Devensian stages of glaciation, which probably affected the region, are hard to disentangle. Most of the pre-Devensian glacial deposits within the Vale of York probably date from the **Anglian** Stage, around 500 000 years BP when glacier ice reached southern England. Because of their considerable antiquity, the pre-Devensian deposits are now heavily dissected by erosion and only relics remain on the plateaux and elevated ground to the west, south and east of the Devensian ice-limit (Locality 10). These deposits vary considerably depending on the local bedrock, but generally include tills, sands and gravels plus valley fill deposits ranging from sandy clays to clays with local and exotic rock clasts. Many of the areas that were not glaciated are notable for the presence of gravel and boulder dreikanter or ventifacts. These are wind-worn faceted stones indicative of prolonged sand-laden wind erosion (possibly for just the Devensian at the margin of the ice or possibly for a longer period of time).

In the Wortley area of Leeds, [SE 2850 3310] ancient excavations in the Aire Valley yielded the remains of Hippopotamus preserved in clay dug from a terrace of the River Aire. This deposit has been inconclusively carbon dated, but suggests an **Ipswichian** age for its occurrence, indicating a warm temperate environment prior to the Devensian ice-age.

During the last, **Devensian** glaciation, ice covered most of northern Britain and occupied the North Sea and adjacent onshore areas, blocking the Humber gap and extending as far south as the Norfolk coast. The Pennines valleys were glaciated as far south as Leeds and a tongue of ice occupied the Vale of York. This ice appears to have been an amalgamation of North-Sea ice, ice from the Lake District that crossed the Pennines at Stainmore and Pennine valley glacier ice. The route of the ice movement is shown by the nature of the erratic clasts contained in the glacial till and the outwash deposits. In the west of the Vale of York these are dominated by Carboniferous sandstone and limestone. In the east more Jurassic and Chalk material is present. Within the Vale of York, the Devensian ice had retreated by about 14 000 years BP, leaving extensive glacial and pro-glacial deposits behind.

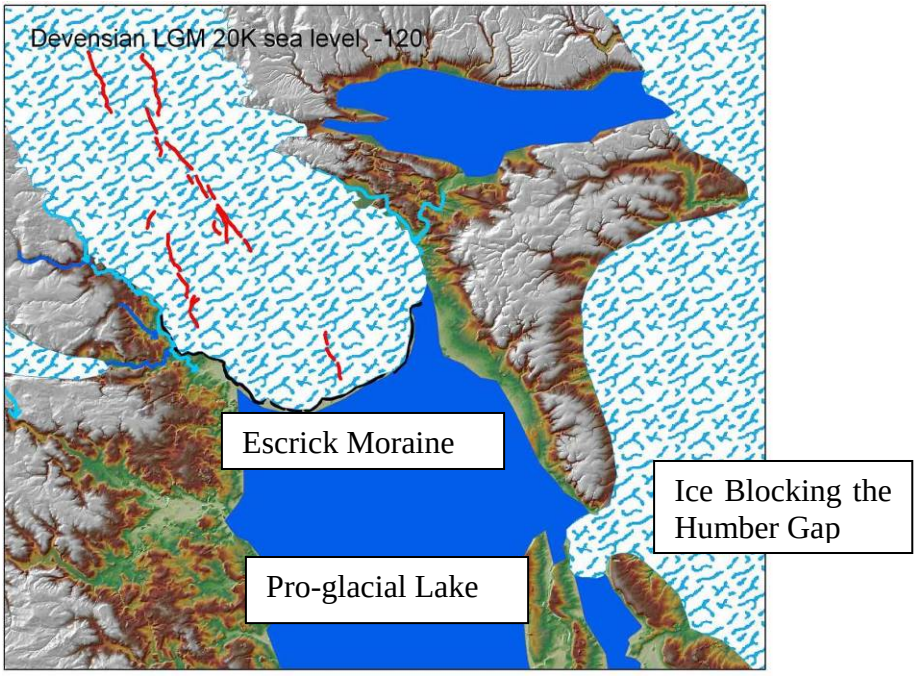

Figure 4-1. Approximate distribution of ice in the Vale of York at the Last Glacial Maximum (Escrick Moraine)

Within the Vale of York ice advanced as far south as the Escrick Moraine (Figure 4-1). At the same time, the North Sea ice advanced to Norfolk blocking the drainage out through the Humber gap. In front of the ice, glaciofluvial outwash deposits and pro-glacial lake deposits were formed in the dammed pre-glacial valley system. The large pro-glacial lake drained southwards down the Trent valley (in the opposite direction to the present drainage) and appears to have drained out through the Lincoln Gap.

The advance and retreat of the ice and the deposits associated with it in the North Sea coast area and the Vale of York have not been correlated. Several generations of glacial till are recognised in the coastal sequence (Catt, 2007). The oldest is the basement till of pre-Devensian age, this is overlain by the Skipsea Till followed by a sequence of sands and gravels capped by the Withernsea Till, the whole sequence representing two separate tills and fluctuations of the ice margin (Bateman et al., 2011). No correlation can be made with the Vale of York, but the presence of fluctuations of the ice margin on the coast may mirror that in the Vale of York.

In the Vale of York, as the ice built up towards to the Devensian maximum, it overrode many of the pro-glacial deposits. In the west, it built up a marginal belt of gravels and till, forming a lateral moraine. Subsequently, the ice margin then retreated progressively northwards with intervening readvances and still-stands depositing the lobate Escrick Moraine, the York Moraine and the Flaxby-Tollerton Moraine (Cooper and Burgess, 1993; Ford et al., 2008). These moraines represent still-stands in the ice margin where the supply of sediment-laden ice was in equilibrium with the degree of melting or wasting. In many places the ice-sheet and moraine were “bulldozed” into pre-existing glaciolacustrine deposits forming thrust surfaces with the essentially flat-lying laminated clays immediately in front of the moraine.

The advance of the ice down the Vale of York blocked the pre-existing Pennine drainage. Numerous rivers were blocked and pre-existing valleys filled with glacial deposits. The River Nidd used to flow to the east of Knaresborough, but it was diverted to cut its present gorge to the west of Knaresborough. It was then diverted to flow through what are now valleys with insignificant drainage, or which are dry, to join up with the River Wharfe just to the west of Wetherby. Here the drainage was also diverted around the south-west edge of the ice-sheet and Escrick Moraine incising the rock-cut gorge through Boston Spa (Cooper and Gibson, 2003). Upstream of this diversion the Wharfe valley is wide, downstream it is very narrow.

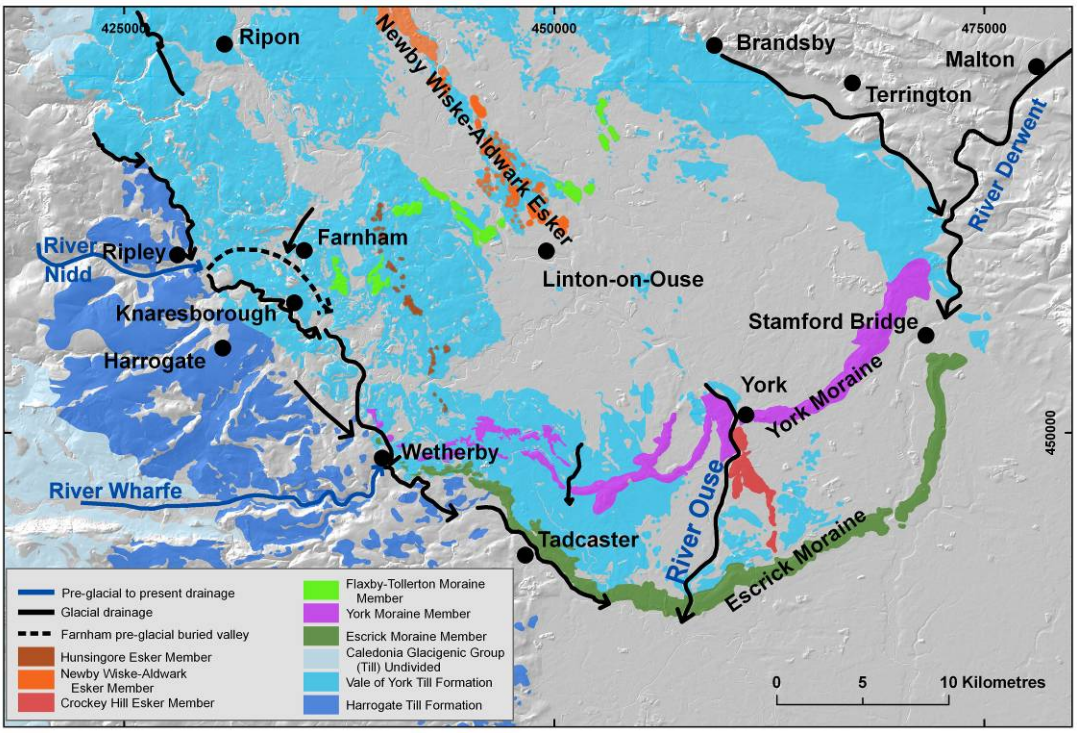

Figure 4-2. The Vale of York tills, moraines and glacial drainage diversions at the Last Glacial Maximum (LGM)

The vast amounts of meltwater draining from the ice-sheet formed en-glacial drainage systems that commonly became choked with sand and gravel (plus some laminated clay). Upon the ice-sheet melting, these choked drainage systems were left as ridges (eskers) of partially disturbed deposits. Where the drainage emerged from the ice-sheet (at the sides or in front, or was diverted around the edge of the ice) it commonly deposited terraces or fans of sand and gravel (such as at Pocklington and Linton upon Ouse). Where the drainage disgorged into glacial lakes these fans of sand and gravel formed with an upper surface approximating to the glacial lake water level. Glaciolacustrine deposits including laminated clay subsequently buried some of these fans.

The pro-glacial lake deposits mainly comprise laminated silts and clays with inter-bedded and overlying sands, especially where marginal or ice-sheet drainage entered the lake.

The ice-sheet of the Vale of York over-rode the early glacial lake so that laminated clay is found beneath the till in many areas (Figure 4-4). This early deposit of laminated clay is synchronous with deposits to the south, where the glacial lake was not overridden. The moraines separate at least three glacial lakes that formed as the ice-sheet waned. The glaciolacustrine deposits to the south of the Escrick Moraine are the Hemingbrough Formation. Between the Escrick and York moraines there is the Elvington Formation and to the north of the York Moraine the Alne Formation (Figure 4-3, Figure 4-4 and Figure 4-5).

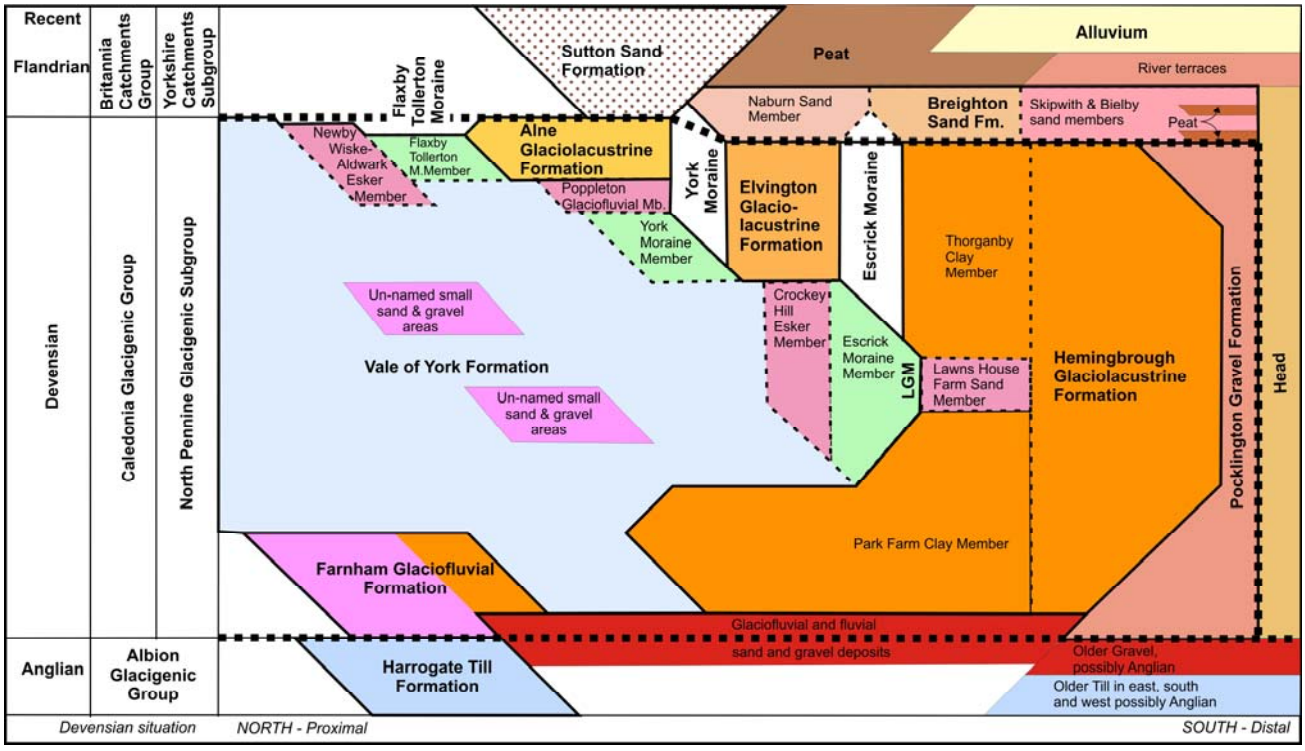

Figure 4-3. Stratigraphy and relationships of the Quaternary and Flandrian sequence of the Vale of York

Relative age	Event	Lithostratigraphy	Location
Youngest	Post glacial deposition of recent river deposits	Alluvium and peat	Askham Bogs
	Silting up of pro glacial lake, followed by removal of ice dam at Humber Gap and incision of fluvial drainage systems	Breighton Sand Formation, Naburn Sand Formation, Sutton Sand Formation, Alne Glaciolacustrine Formation, Elvington Glaciolacustrine Formation Hemingbrough Glaciolacustrine Formation	Tockwith Moor Skipwith Common Escrick Clay Pit Stillingfleet
	Melting and northward retreat of Vale of York ice and exposure of ice contact glaciofulvial sediments	York Till Formation including the Tollerton-Flaxby Moraine Member, Hunsingore Esker Member Poppleton Glaciofulvial Formation	Allerton Park
	Melting and northwards retreat of Vale of York ice-sheet and exposure of ice-contact deposits	Hemingbrough Fm -Lawns House Farm Sand Member Vale of York Formation including the York Moraine Member and Crockey Hill Esker	Skipwith Common
	Maximum southward advance of the Vale of York ice-sheet to the Escrick Moraine; glacial diversion of Pennine and Vale of Pickering drainage	Vale of York Till Formation including Escrick Moraine Member	Knaresborough Gorge Newton Clay Pit Stillingfleet
Oldest	Deposition of pro-glacial lacustrine sediments ahead of the advancing Vale of York ice	Deposition of sands and gravels in the buried valley system overlain by the Hemingbrough Formation (Park Farm Clay Member)	Escrick Clay Pit

Table 4-1. The Devensian and Holocene sequences in the Vale of York

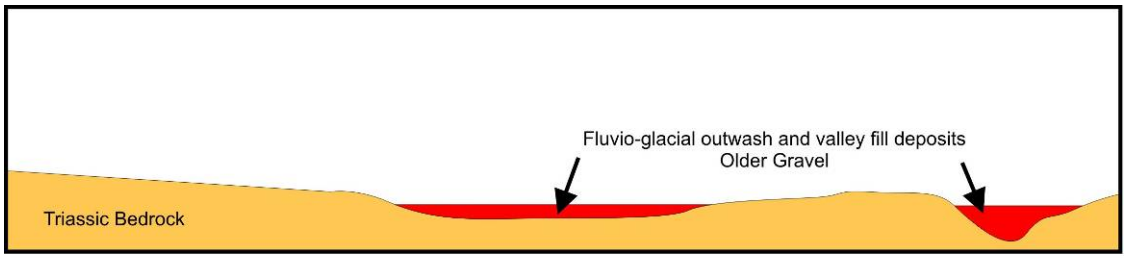

A. Pre-existing pre -Devensian topography and incision of drainage during the advance of the Devensian ice, deep weathering of the bedrock, topography partially filled in with fluvial and fluvio-glacial outwash and valley fill deposits.

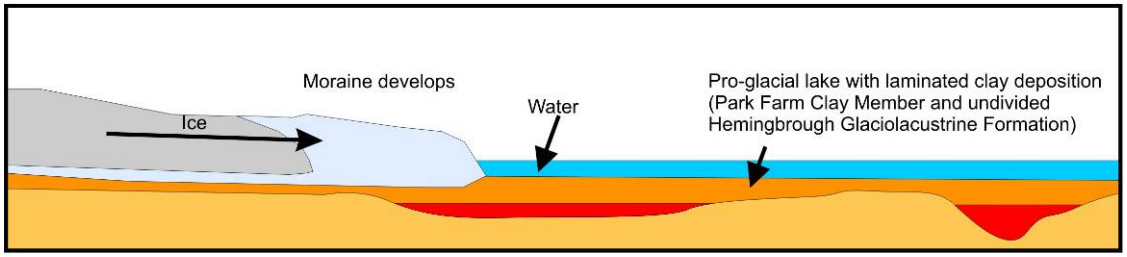

B. Ice advances over the pre-existing topography and valley fill deposits, moraine develops at still-stands with the, pro-glacial lake and laminated clay deposits of the Hemingbrough Glaciolacustrine Formation in front of ice sheet..

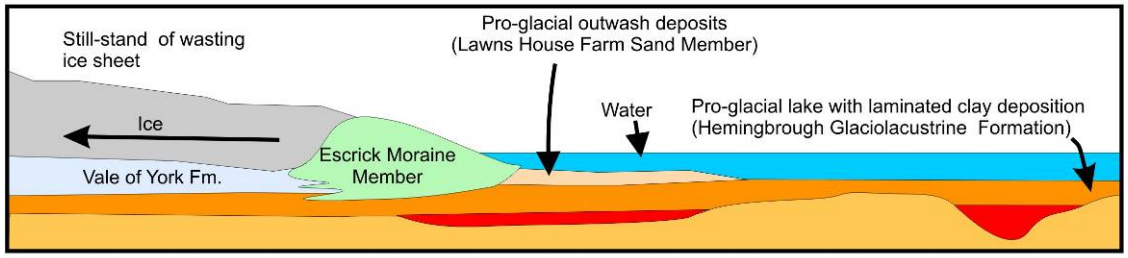

C. Ice retreats, and the pro-glacial lake continues in front of the developing Escrick Moraine. At the same time, Fluvio-glacial outwash and river terraces spill into lake depositing the sand of the Lawns House Farm Sand Member

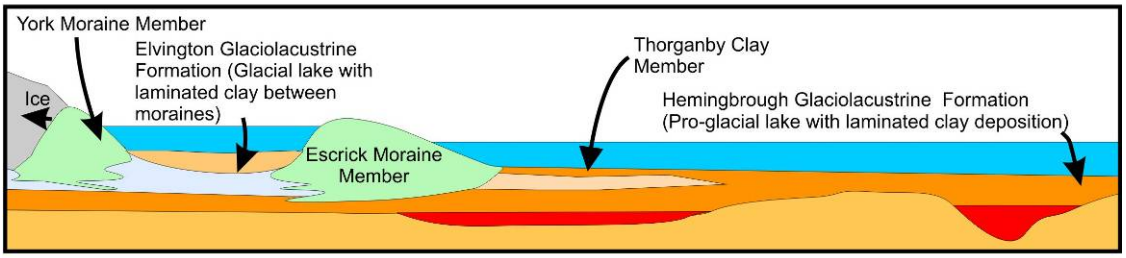

D. Ice retreats further north and a new pro-glacial lake develops between the Escrick Moraine and the new moraine formed at York. Laminated clay lake deposits (Elvington Glaciolacustrine Formation) develop between the moraines and the Hemingbrough Glaciolacustrine Formation (with Thorganby Clay Member) continues to be deposited in front of the Escrick Moraine Member.

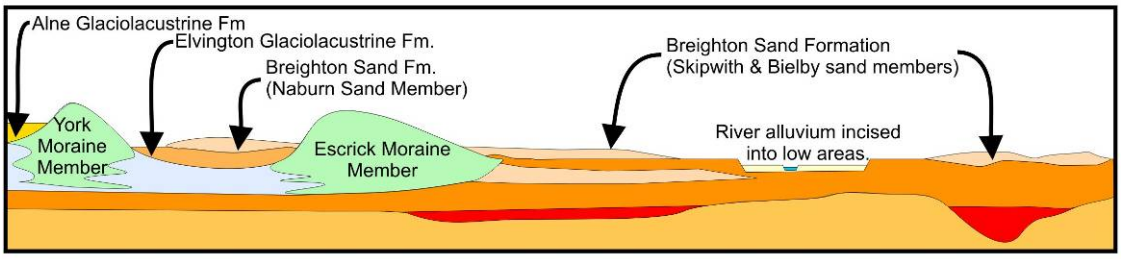

E. Ice retreats completely and the proglacial lake drains, fluvial and aeolian sedimentation and reworking of the sediments occurs and the rivers become incised.

Figure 4-4. Glacial evolution of the Vale of York ice sheet and related proglacial deposits

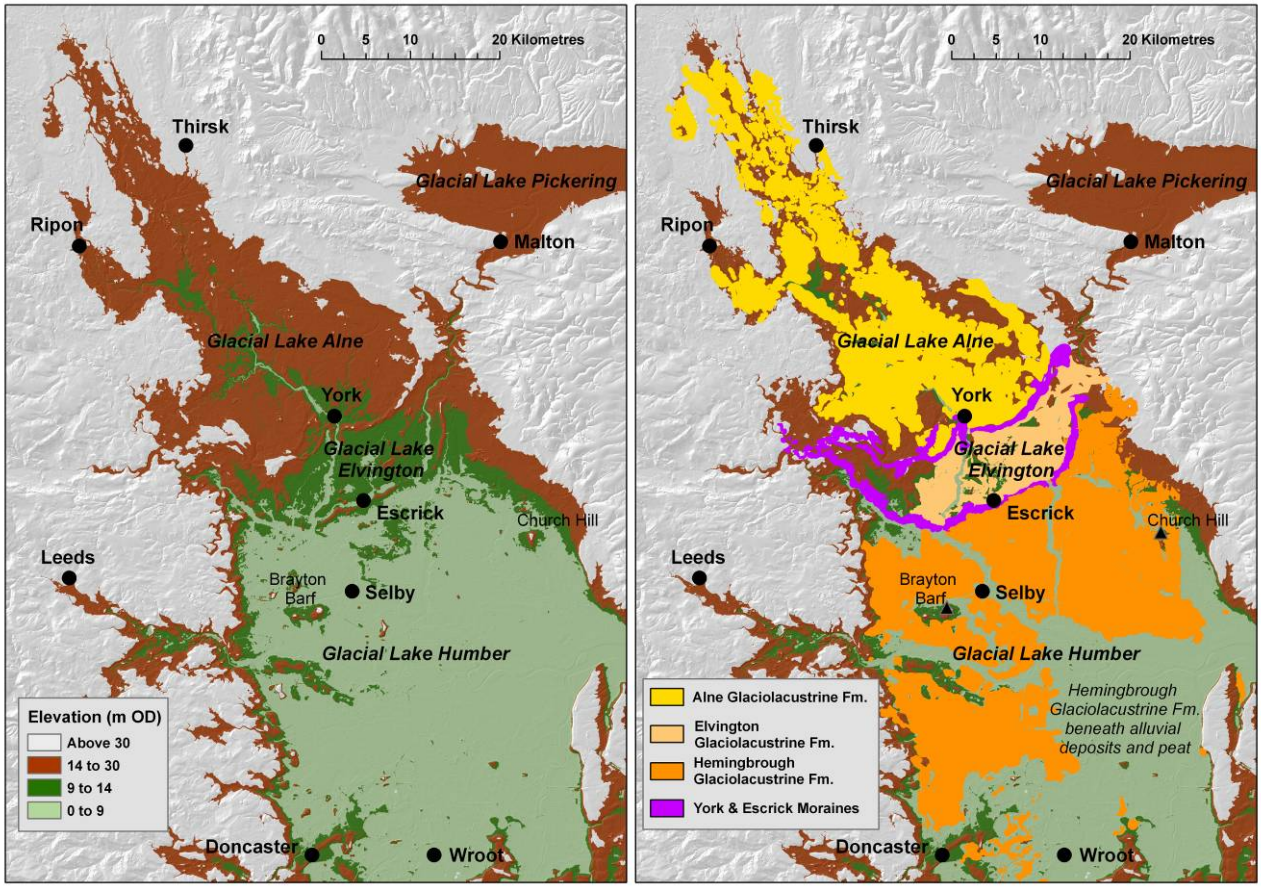

Figure 4-5. The main morphological features of the Vale of York and the 3 elevations of glacial lake deposits (note these are the bottoms of the drained lakes)

During deglaciation, the ice retreated from the Humber Gap and the pro-glacial lake of the Vale of York drained eastwards into the North Sea. Extensive sand deposits were washed out across the floor of the recently drained lake and spreads of sand with gravel were deposited. As these deposits dried and the drainage became established, aeolian sand deposits were blown around the newly emerged lake bed, forming subdued dunes of blown sand. Much of the drainage followed its previous course into the Vale such as around the front of the Escrick Moraine cutting into the glacial till, glaciofluvial outwash terraces and the associated glacial lake deposits. Other drainage followed its previous glacial course such as the River Ouse, which cuts through the York Moraine at a point near to where the glacial drainage used to emerge. The Rivers then incised their present flood plains with their flat alluvium and localised peat deposits in poorly drained areas.

5 Monday 20th October, Barmston, East Yorkshire Coast

Site information:

Parking and toilets at Barmston Beach Caravan Park. NGR: 517050 459340

1:50,000 maps sheet: Bridlington (65)

Access to the beach is via coastal footpath

High tide on October 20th: 14:31 (Bridlington)

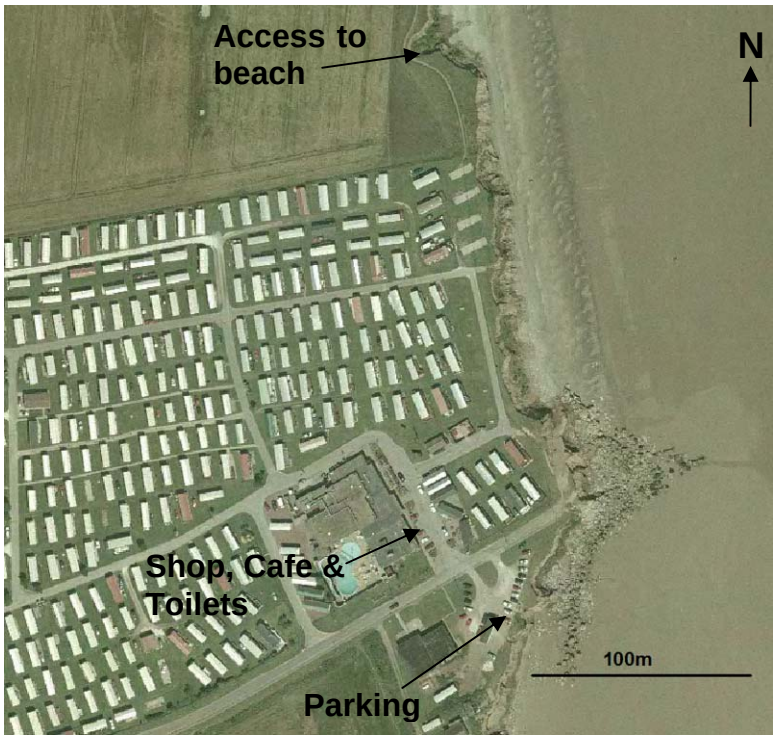

Figure 5-1. Aerial view of Barmston beach, parking and access

Geological Setting:

Barmston is located on the East Yorkshire coast, approximately 7.5km south of Bridlington. The coast in this area comprises a sandy beach, backed by cliffs. The coastline in this area is very dynamic, with an erosion rate of up to 8m/year, but can be more in some years. This stretch of coast gives the best exposure of the Late Devensian glacial succession in the region, and has been studied by several academics. BGS are also studying these cliffs, from Barmston to Hornsea, with a view to updating the geological maps of the area.

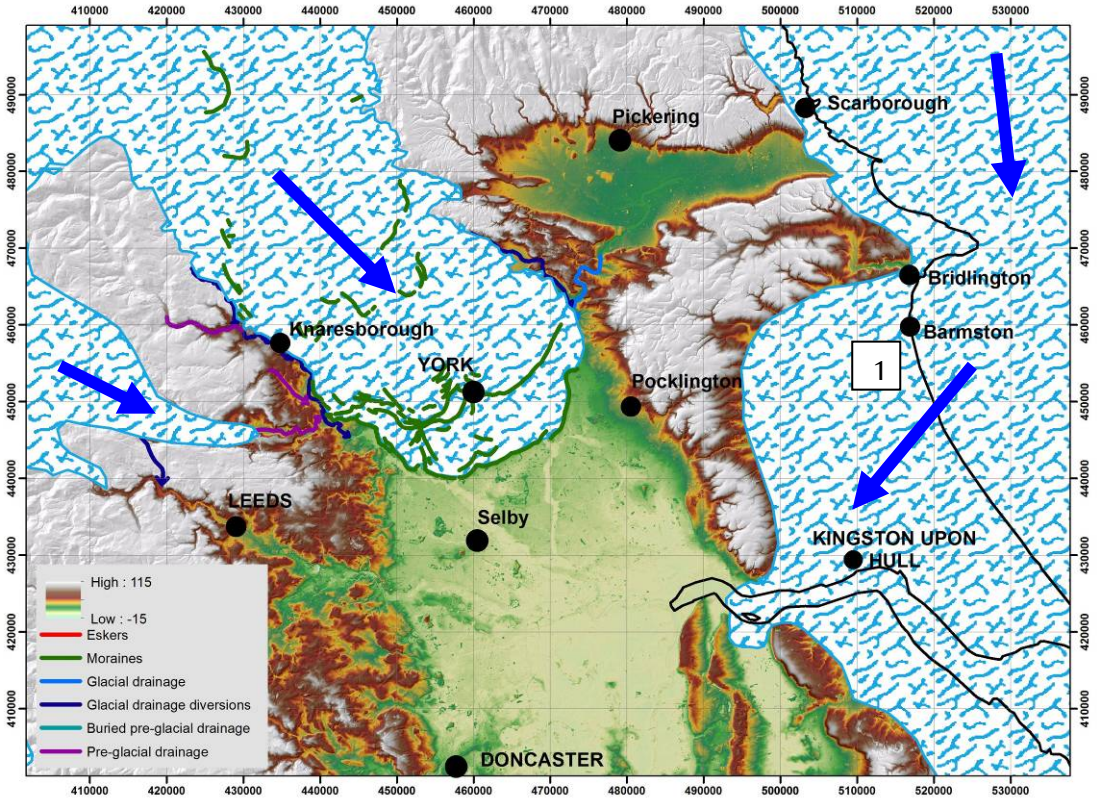

Figure 5-2. The Devensian ice sheet (at the Last Glacial Maximum (LGM)) and its relationship to Barmston and the Vale of York; approx ice movement directions shown by blue arrows

The late Devensian sediments on the East coast were laid down by the North Sea ice lobe, which stretched southwards as far as north Norfolk, with the ice flowing onshore from a north-easterly direction (Figure 1). The North Sea ice lobe was one of several ice streams that drained ice from the interior of the British-Irish ice sheet out towards its margins. The importance of this locality is that it reveals the geology deposited by an ice stream during retreat, and can provide clues as to the types of processes that happen beneath and in front of modern ice streams (e.g. Greenland and Antarctica). The cliffs at Barmston are composed of Late Devensian aged glacial deposits, and have been studied by Evans et al (1995) who recognise four distinct lithofacies, the basal till of the section being the Skipsea Till:

Lithofacies	
Gravel and coarse sand	Cross-bedded poorly sorted matrix supported gravels interbedded with sands and clays
Laminated sands, silts and clays	Upper part: climbing and ripple bedded sands with overlying clay drapes. Large scale convolutions are also present Lower part: laminated clays interbedded with sands and rare gravel;
Sands and gravels	Planar cross-bedded sands and gravels infilling depressions and scour fills in the basal till. Also forms veneers on the basal till surface
Basal till (Skipsea Till)	Matrix supported, over consolidated, sub-vertical joints, some lamination and shear zones

Top of cliff

Base of cliff

Table 5-1. Lithological sequence at Barmston (after Evans et al., 1995)

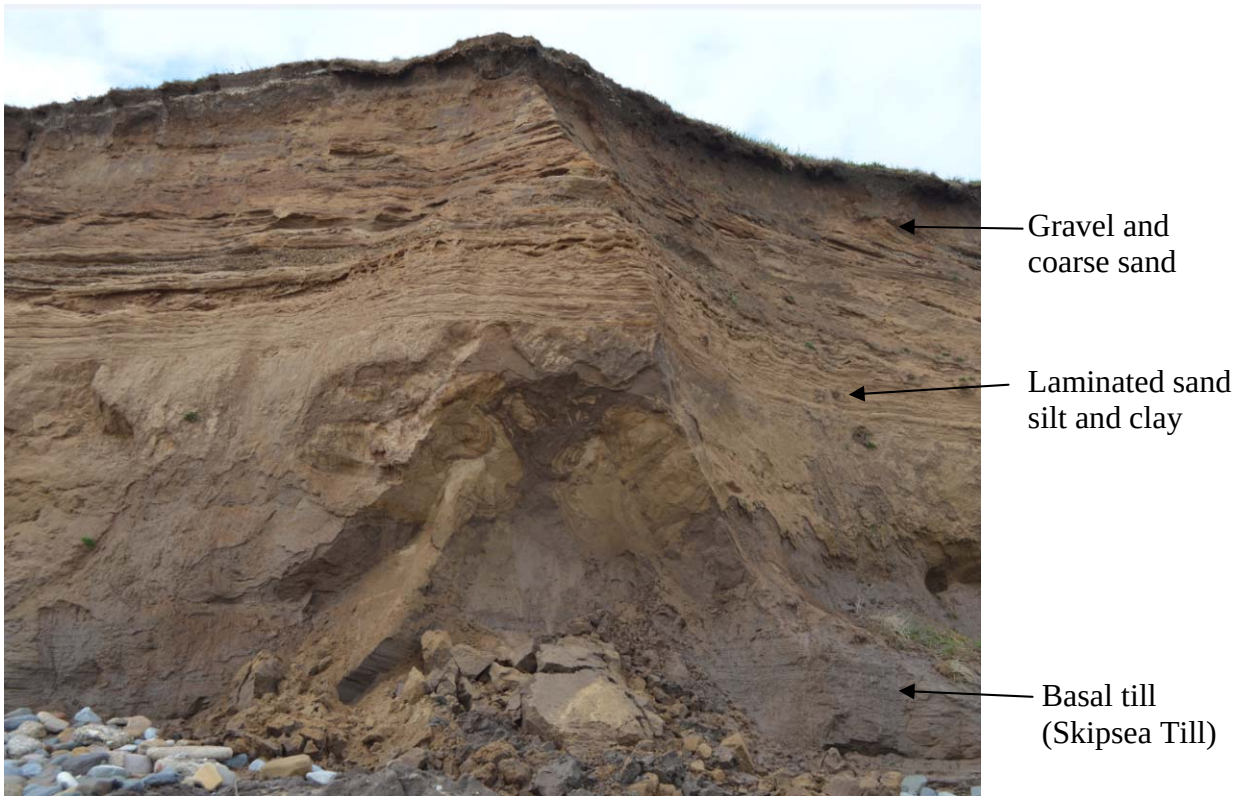

Figure 5-3. The geological sequence of the Barmston coast section

Aims for the day:

Divide into small groups to study sections of the cliff. Each group to record the different lithologies and sedimentary structures, think about the environment of deposition and note whether it changes and in what way. Each group to report back their observations.

6 Tuesday 21st October – Vale of York traverse and marginal channels

The aim of the day is to look at the geomorphology and lithology of depositional features of the Devensian ice sheet in the Vale of York. It will consider glacial esker deposits, moraines and pro-glacial lake deposits. It also aims to use augering, feature mapping and DTMs to show how a geological map is constructed. In addition, it will look at how the Devensian ice sheet affected the local drainage and formed glacial diversion channels around the edge of the ice.

6.1 LOCALITY 2 – ALLERTON PARK - HUNSINGORE ESKER [SE 418 572]

The Hunsingore Esker represents a former drainage route for water and sediment within, below or upon the ice-sheet in the Vale of York. It can be traced for approximately 13km and comprises mainly sand and gravel with a small amount of laminated clay. The morphology of the esker is that of a sinuous ridge that runs in a north-north-west direction parallel to the main flow-direction of the ice. At Allerton Park (2 on Figure 6-2 and **Error! Reference source not found.**) this ridge stands about 15 to 30m above the level of the Sherwood Sandstone Group bedrock. In the adjacent ground the glacial till is much thinner and more generally around 5-15m thick.

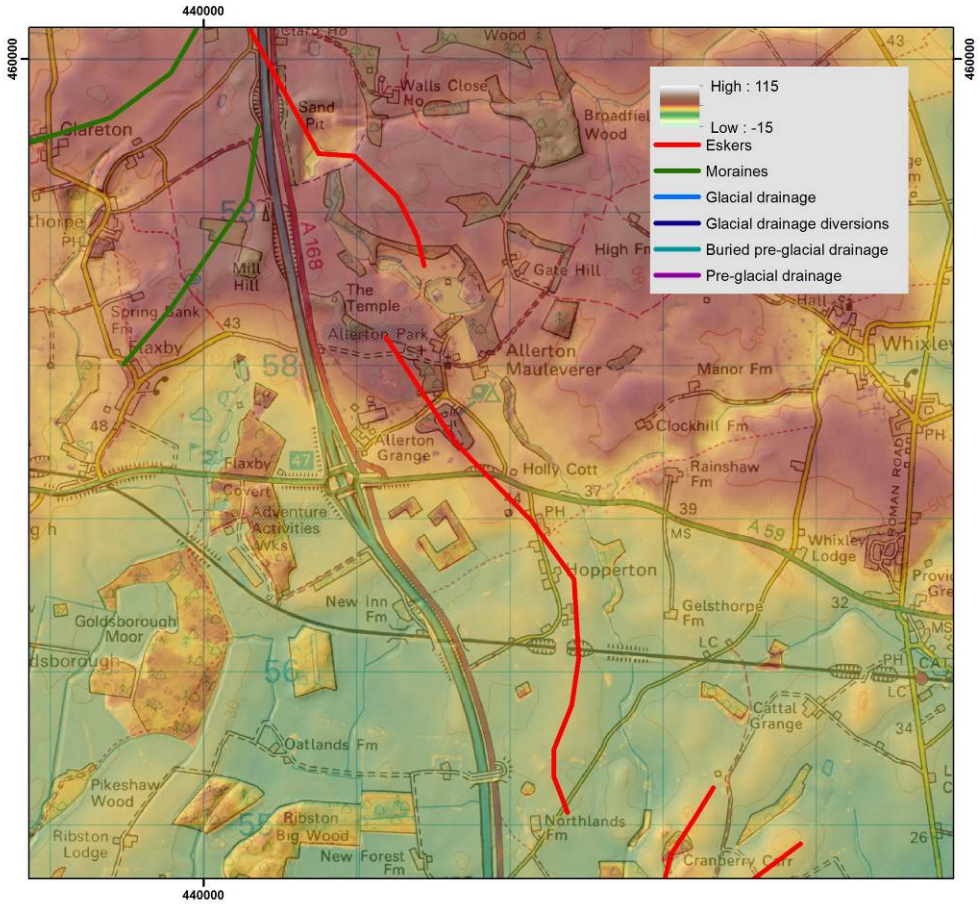

Figure 6-1 DTM and topographical map of the Allerton Park area Hunsingore Esker

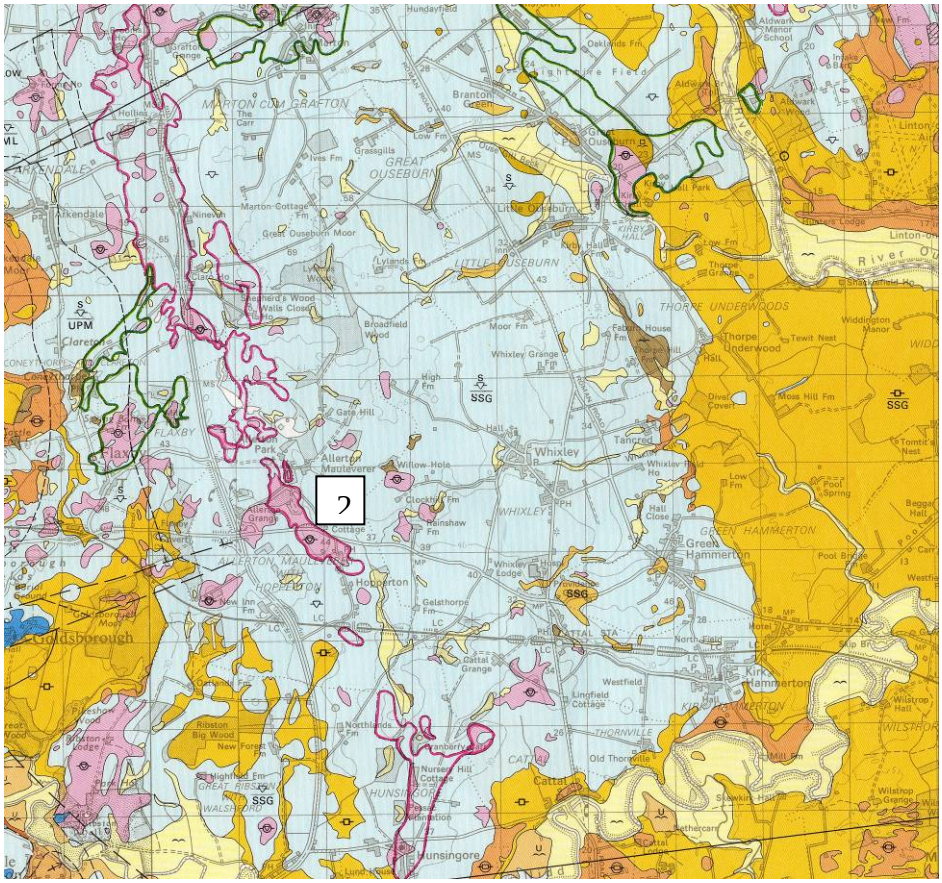

Figure 6-2. The geology of Hunsingore Esker

Extract from the Harrogate 1:50 000 scale map; pale blue - glacial till, pink – sand and gravel; esker edged in dark red; moraine edged in dark green; glacial lake deposits (Alne Formation) – orange; alluvium pale yellow.

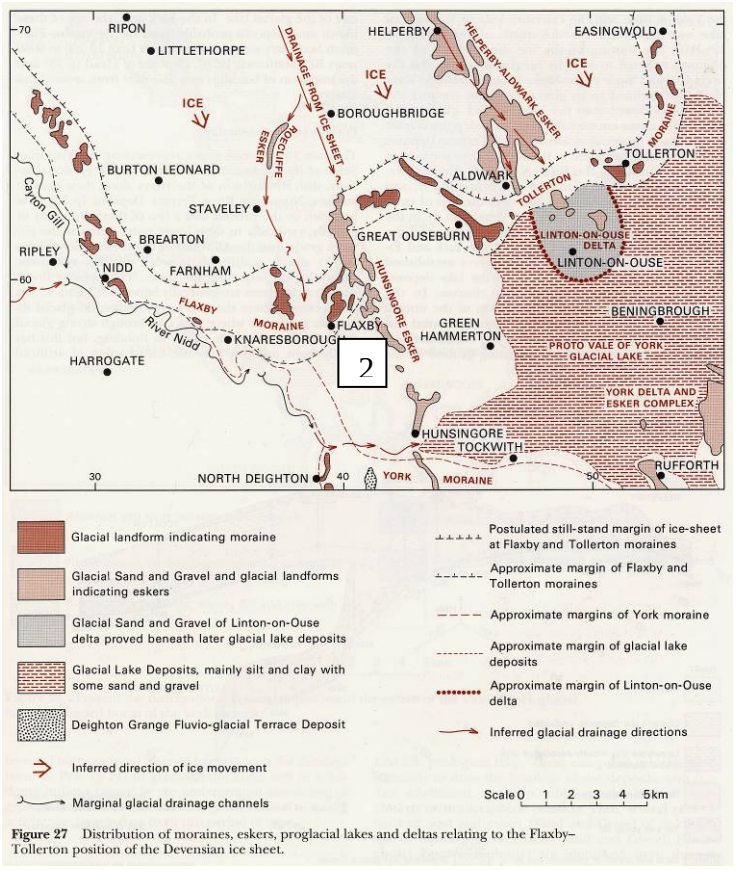

Figure 27 Distribution of moraines, eskers, proglacial lakes and deltas relating to the Flaxby–Tollerton position of the Devensian ice sheet.

Figure 6-3. The geology of the Hunsingore Esker. Extract from the Harrogate Memoir (Cooper and Burgess, 1993)

6.2 LOCALITY 3 – FARNHAM BURIED VALLEY AND OLD COURSE OF THE RIVER NIDD [SE 348 569]

At the start of the last ice-age (Devensian) the topography of the Knaresborough district was different to that seen today (Cooper and Burgess, 1993). The proto River Nidd ran to the north and east of the present town. It deviated from its present course at Nidd (SE 302 608), ran through Brearton and past Farnham (SE 345 605) to the northern outskirts of Knaresborough (SE 363 580) before heading eastwards (Figure 4-2, Figure 6-4 and Figure 6-5). During the advance of the Devensian ice-sheet a thick fan of sand and gravel was deposited in this valley emanating from the front of the ice-sheet via glacial channels around Farnham (SE 352 606) and Occaney (SE 352 619); this deposit is worked in the gravel pits north of Knaresborough (SE 356 587) (Figure 6-6).

If Knaresborough is approached from the north via the B6166 from Boroughbridge the extent of this buried valley and its associated sand and gravel deposits, can be appreciated from the road. As the ice advanced further to the south and west it overrode the sand and gravel completely blocking the proto-Nidd drainage and diverting the river westwards. Here the river exploited the lowest, softest rocks and incised the present Nidd Gorge. West of the Nidd Gorge the glacial deposits are generally thin and probably pre-Devensian in age; east of the gorge the Devensian deposits comprise thick hummocky glacial till with moraines, eskers and late glacial lake deposits (Figure 6-6).

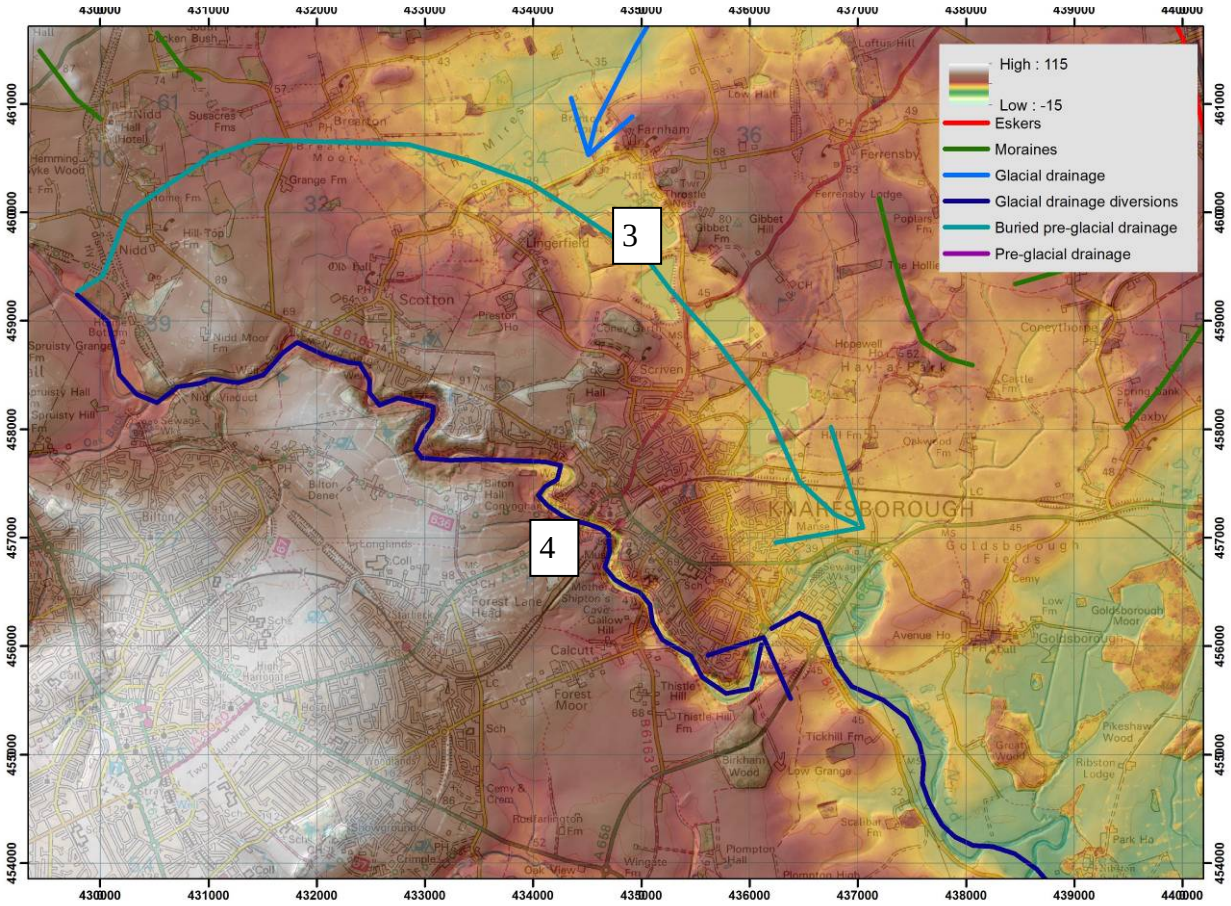

Figure 6-4. DTM of the Farnham and Knaresborough area showing the buried pre-Devensian drainage (3) and the glacial diversion of the River Nidd (4)

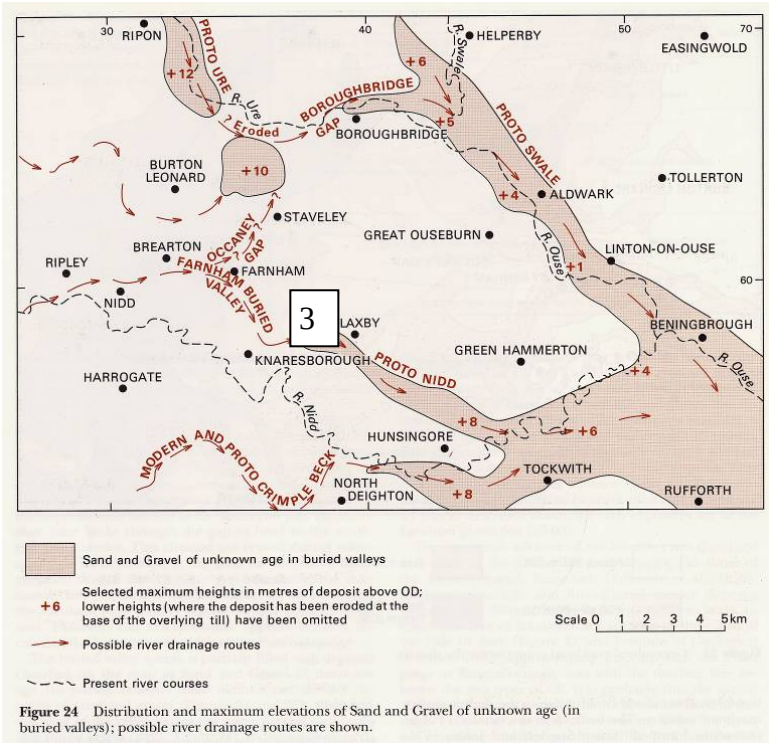

Figure 24 Distribution and maximum elevations of Sand and Gravel of unknown age (in buried valleys); possible river drainage routes are shown.

Figure 6-5. Pre-Devensian drainage and deposits in the Knaresborough area (from Cooper and Burgess, 1993)

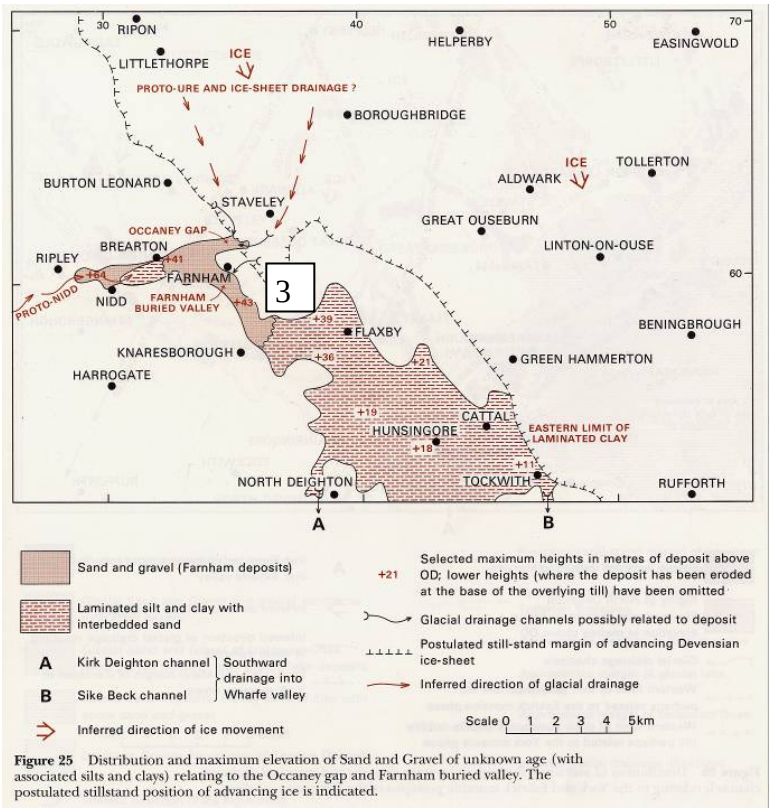

Figure 25 Distribution and maximum elevation of Sand and Gravel of unknown age (with associated silts and clays) relating to the Occaney gap and Farnham buried valley. The postulated stillstand position of advancing ice is indicated.

Figure 6-6. Diverted and blocked Devensian drainage, fluvio-glacial and glacio-lacustrine deposits in the Knaresborough area (from Cooper and Burgess, 1993)

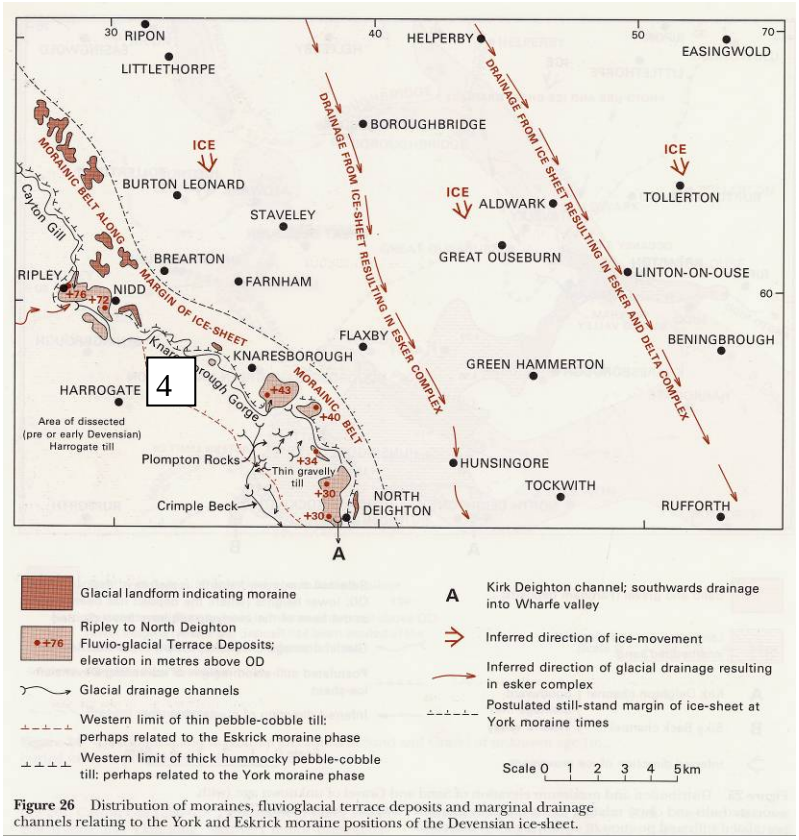

Figure 26 Distribution of moraines, fluvioglacial terrace deposits and marginal drainage channels relating to the York and Eskrick moraine positions of the Devensian ice-sheet.

Figure 6-7. Devensian marginal ice-sheet drainage and deposits in the Knaresborough area (from Cooper and Burgess, 1993)

6.3 LOCALITY 4 – KNARESBOROUGH GORGE GLACIAL DIVERSION [SE 348 569]

Before the Devensian Ice-age the River Nidd occupied a wide valley that came down from the Pennines and spilled into the Vale of York. As the ice advanced it interrupted all the drainage and diverted the river around the margin of the ice (Figure 4-2) causing it to cut a channel in the underlying Permian limestones and mudstones (Figure 6-4, Figure 6-8 and Figure 6-9). (A similar situation occurred with the River Wharfe between Wetherby and Boston Spa). Along the lateral margins of the ice sheet moraines developed and there are numerous overflow channels linking the rivers together. Drainage from the River Swale links with drainage from the Nidd, which in turn overflows along channels into the Wharfe before it enters the glacial diversion between Wetherby and Boston Spa. Note the wide flood plain (bottom right corner of Figure 6-8) to the east of Knaresborough, the narrow gorge flows into the wide flood plain with outwash gravel terraces as the drainage enters what was the pro-glacial lake.

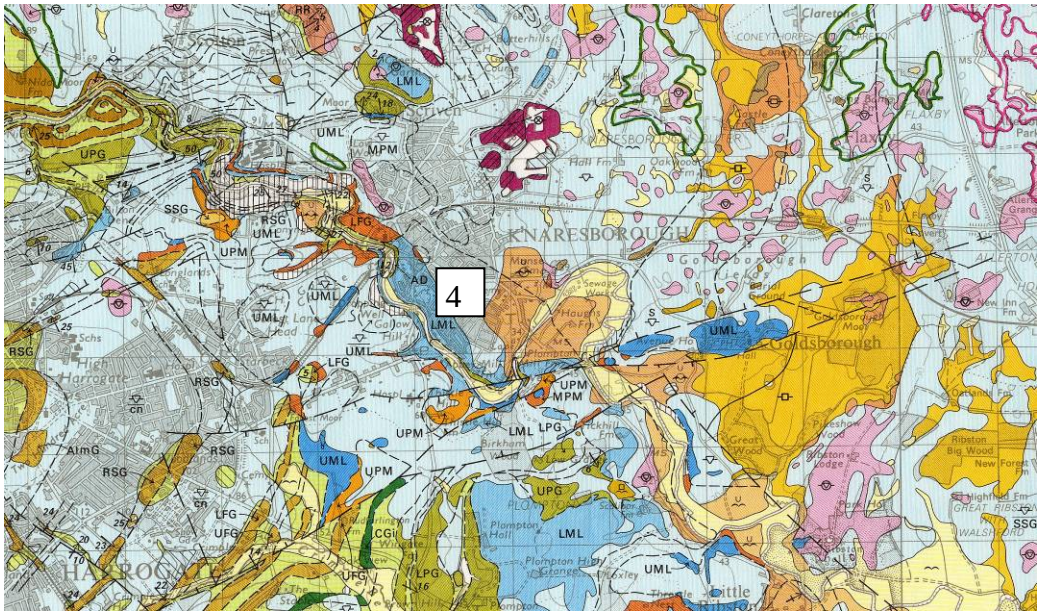

Figure 6-8. Extract from the Harrogate 1:50 000 scale map showing the diverted course of the River Nidd through Knaresborough and the relationship between the superficial and bedrock geology.

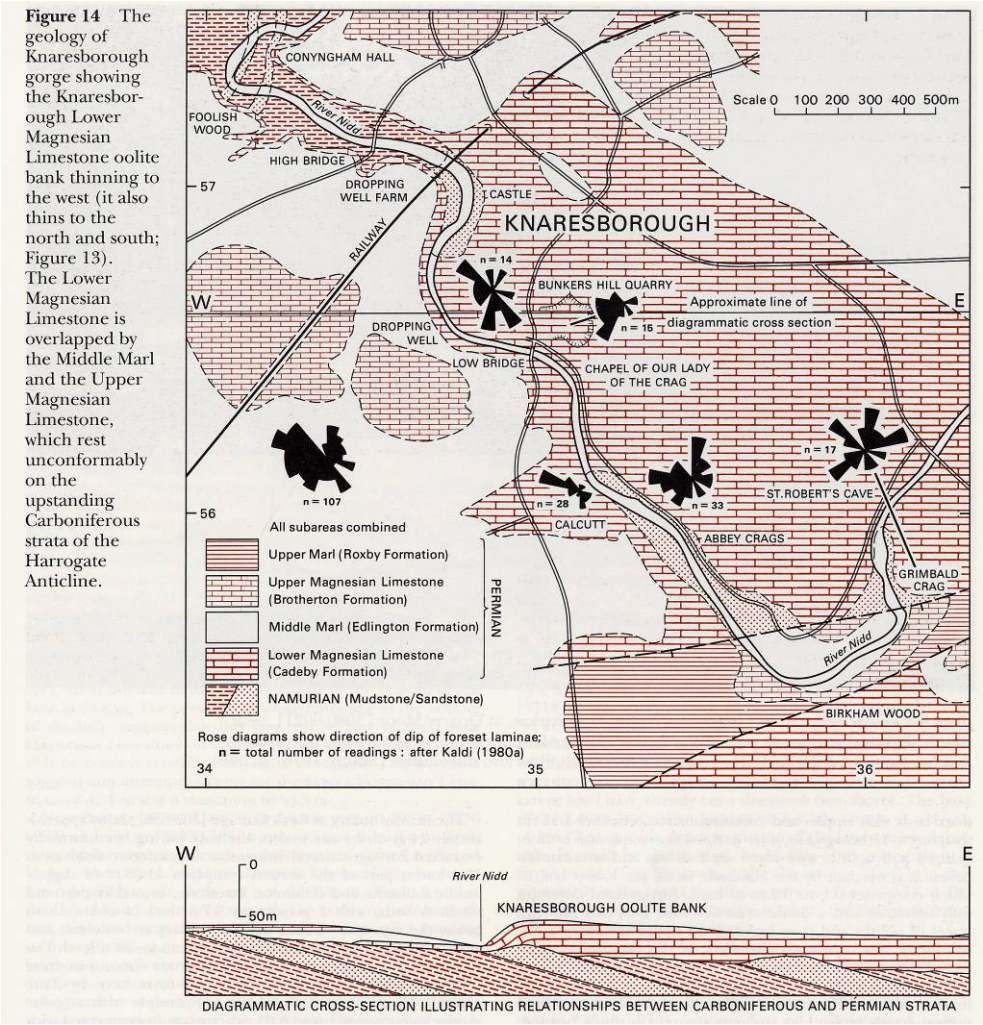

Figure 14 The geology of Knaresborough gorge showing the Knaresborough Lower Magnesian Limestone oolite bank thinning to the west (it also thins to the north and south; Figure 13). The Lower Magnesian Limestone is overlapped by the Middle Marl and the Upper Magnesian Limestone, which rest unconformably on the upstanding Carboniferous strata of the Harrogate Anticline.

Figure 6-9. Locality 4, the bedrock geology of Knaresborough Gorge. Extract from the Harrogate Memoir (Cooper and Burgess, 1993)

6.4 LOCALITY 5 – SKIP BRIDGE, ALLUVIUM AND GLACIOLACUSTRINE DEPOSITS [SE 4840 5600]

Driving back from Knaresborough past Allerton Park the route descends from the till-covered and sandstone-cored ridge of the Hunsingore esker and adjacent glacial till of the Vale of York Formation on to the low ground occupied by the glaciolacustrine lake flat of the Alne Glaciolacustrine Formation (Figure 4.4). The area of this glaciolacustrine deposit is essentially flat around 14m OD, but rising up to 21m at the margins. The present river drainage has incised into the flat lake deposits and the well-marked flood plain of the river is visible from the A59 layby at Skip Bridge (Figure 6-10 and Figure 6-11).

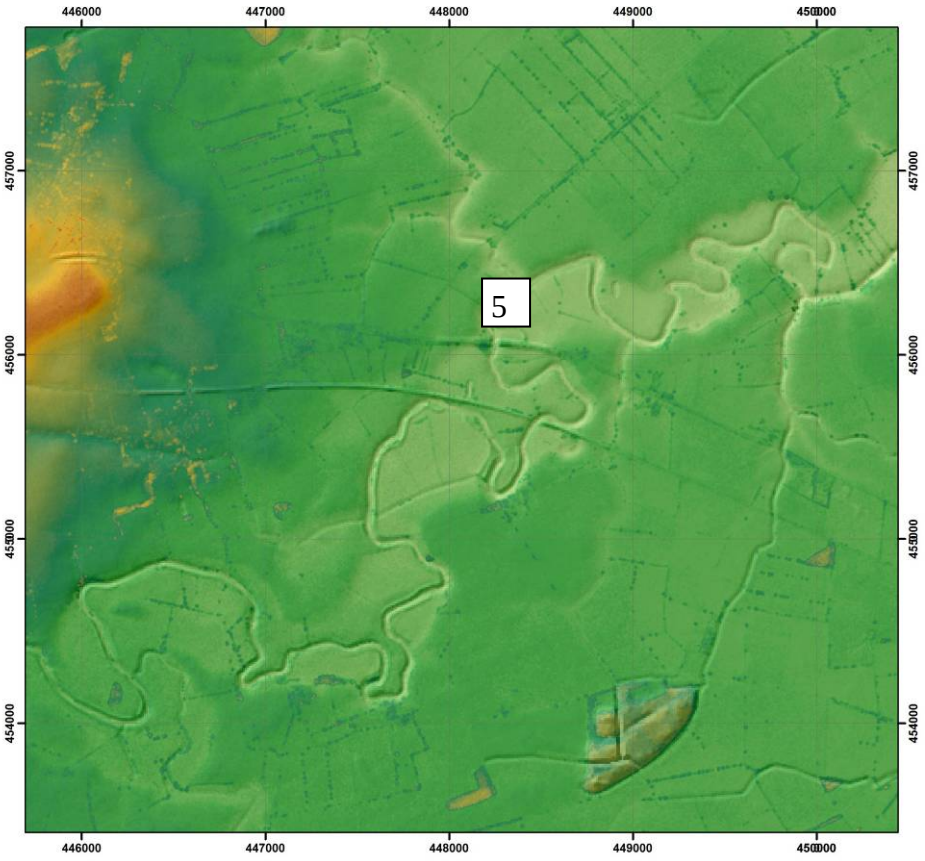

Figure 6-10. DTM for Skip Bridge area showing incised alluvium (pale green) surrounded by flat Alne Glaciolacustrine Formation lake bed deposits (medium green) with higher ground of till and bedrock to the west. Note the woods are also higher

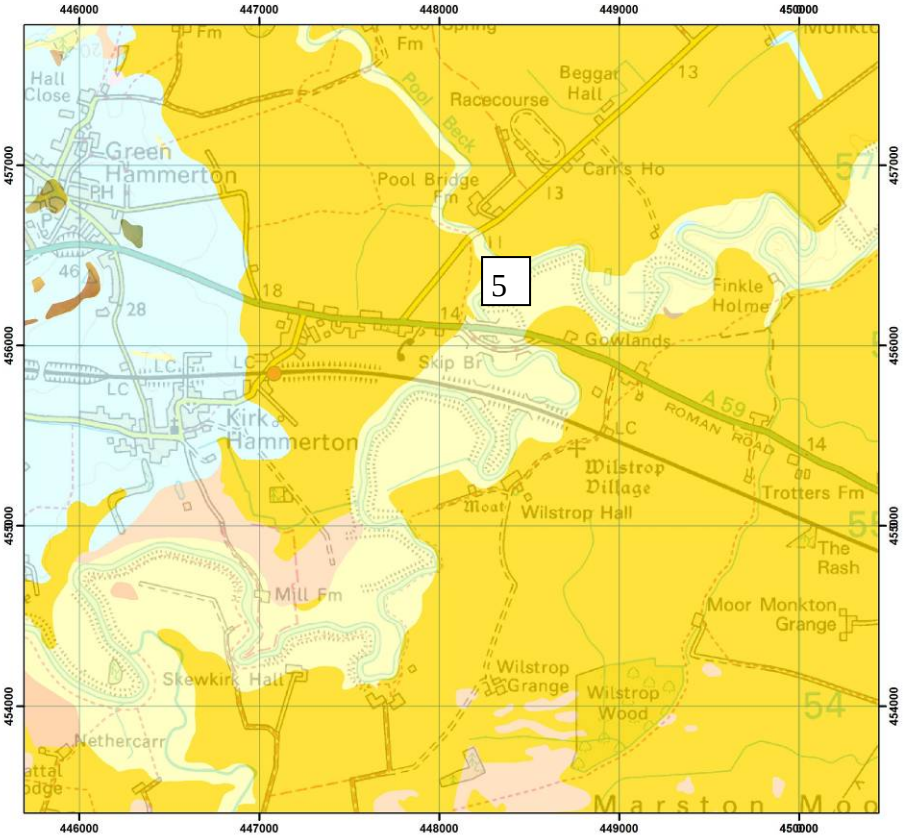

Figure 6-11. Geological map for the Skip Bridge area showing the alluvium of the River Nidd (pale yellow), Alne Glaciolacustrine Formation clays (dark yellow) with some outwash sands (pink) and glacial till (pale blue)

6.5 LOCALITY 6 - MOOR MONKTON [SE 5120 5460]

Time will probably not permit a stop here, but the journey takes us across essentially flat ground from Skip Bridge towards York. Maps and DTM are included to show the lack of relief of the Alne Glaciolacustrine Formation. Note that this is the bottom of the drained lake and that river terraces and marginal deposits extend up to about 21m, suggesting a depth of water of around 7-10m when the lake drained.

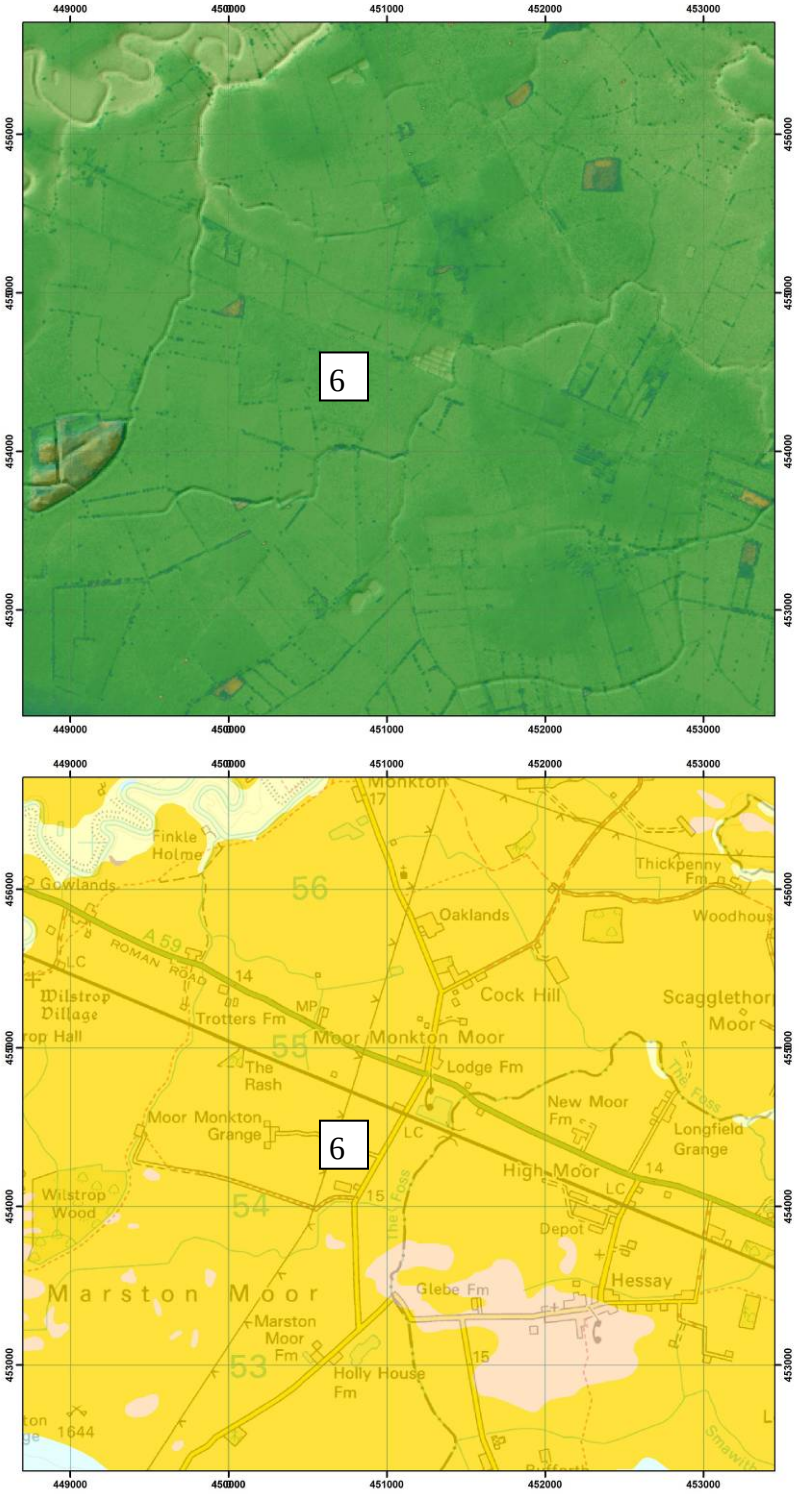

Figure 6-12 DTM and geology maps of the Moor Monkton area showing the flat Alne Glaciolacustrine Deposits (dark yellow) with some sand (pink)

6.6 LOCALITY 7 – ASKHAM BOGS AND YORK MORAINE [SE 5620 4790]

Time will probably not permit a stop here, but the topography even from a vehicle is very marked. At the end of the ice-age, the area to the north of the York Moraine was a low wet area with very poor drainage. Consequently, a peat bog developed which is now called Askham Bogs. To the south of the bog, the York Moraine rises to a height of about 20m compared with the elevation of about 12m for the bogs themselves (Figure 6-13

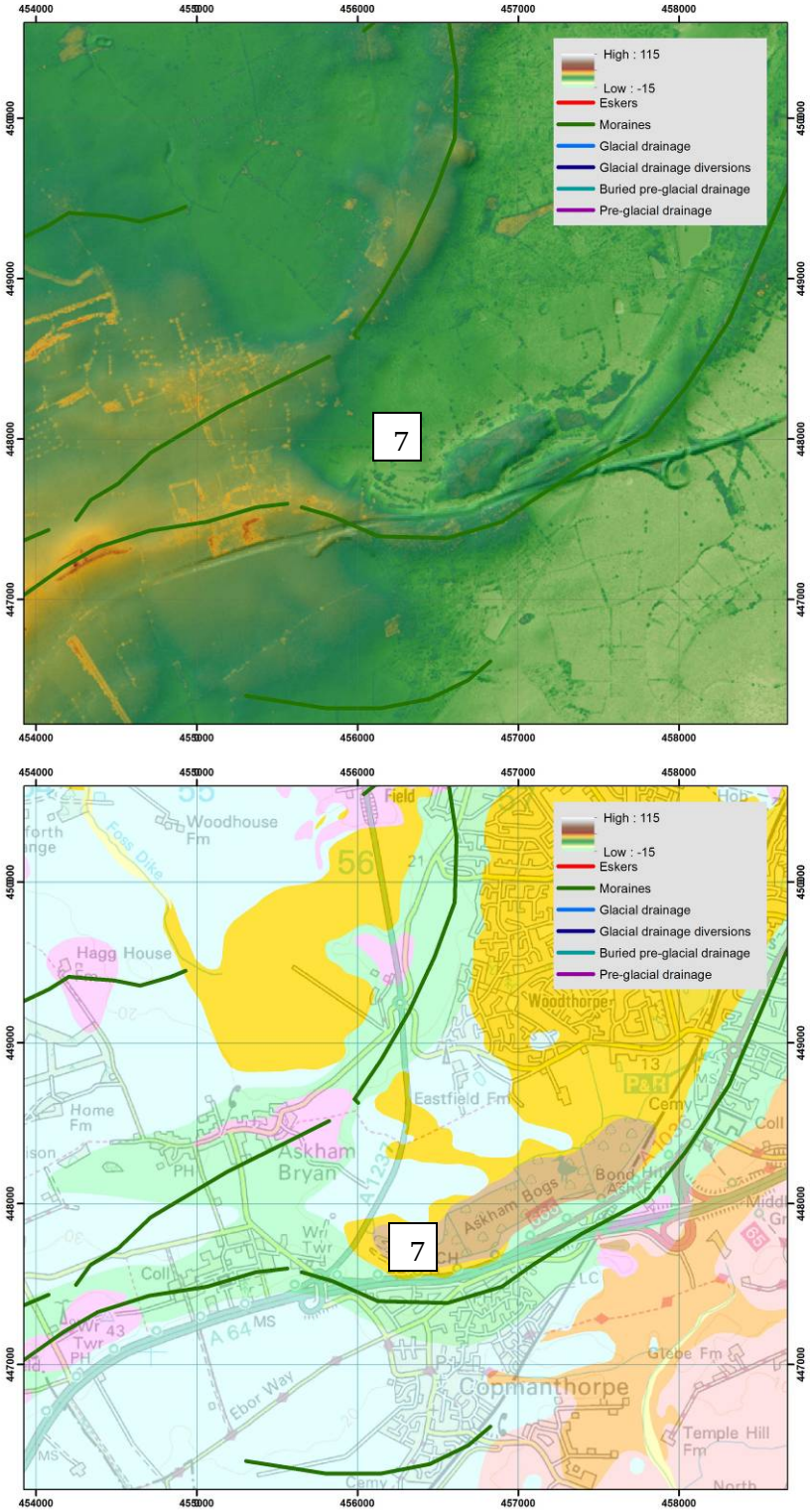

Figure 6-13. Extract from the Selby 1:50k map (Sheet 71) showing the position of Askham Bogs (peat – brown) to the north of the York Moraine (green). Note that the DTM shows a high area in part of the bog because there is a wood

6.7 LOCALITY 8 CROCKEY HILL ESKER AND BOREHOLE [SE 63621, 45504]

This locality will not be visited, but it will be passed en-route and is the location of the Crockey Hill Borehole that will have been examined in the laboratory at BGS. It lies north of the Escrick Moraine and has glacial till of the Vale of York Formation overlying laminated clays of the Park Farm Member of the Hemingbrough Formation. These clays will be examined at locality 9.

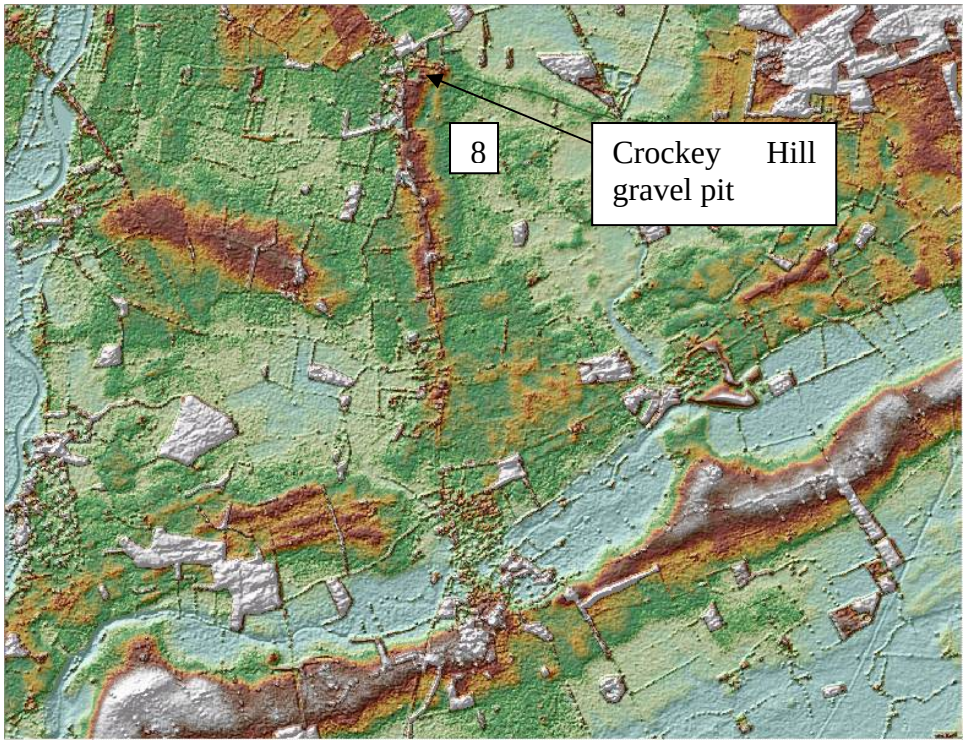

Figure 6-14. Till core from the Vale of York Formation from the Crockey Hill borehole (SE64NW293; [SE 63621, 45504])

Figure 6-15. Typical laminated clay and silt glacial lake deposits. In the Crockey Hill borehole (SE64NW293; [SE 63621, 45504] these underlie the till of the Vale of York Formation

6.8 LOCALITY 9 – ESCRICK CLAY PIT, GLACIOLACUSTRINE SEQUENCE [SE 6210 4030]

To examine typical laminated glaciolacustrine silts and clays of the Park Farm Member of the Hemingbrough Glaciolacustrine Formation (Figure 6-16 and 6-17), and to observe the contact with the overlying sands (Breighton Sand Formation) if exposures permit. The clay pit was initially dug for clay to manufacture drainage pipes, and some clay has also been used for engineering purposes, such as flood embankments. The quarry includes several cells of landfill with leachate collection facilities. The clays are similar to those seen beneath the Vale of York Till Formation in the Crockey Hill Borehole (locality 8) that lies north of here and the Escrick Moraine. Figures 6-16 and 6-17 also show locality 12 to indicate how it relates to locality 9.

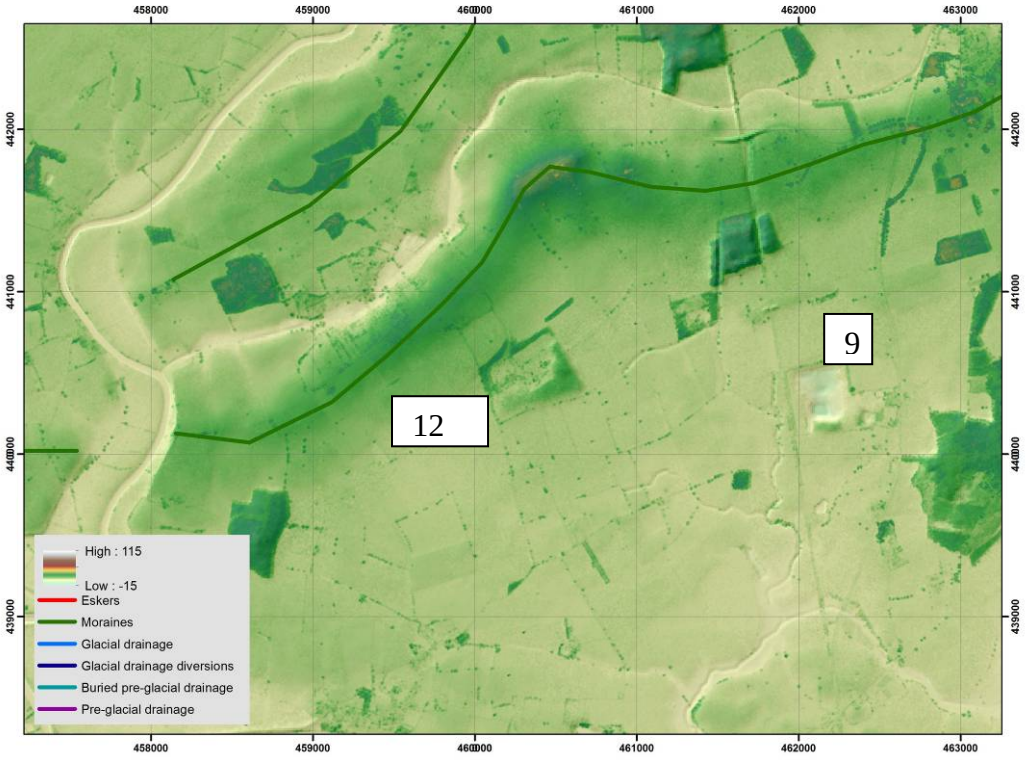

Figure 6-16. DTM showing Escrick Clay Pit (9) excavated through the Breighton Sand Formation into the underlying Park Farm Member of the Hemingbrough Formation the high ground to the north is the Escrick Moraine Member of the Vale of York Formation

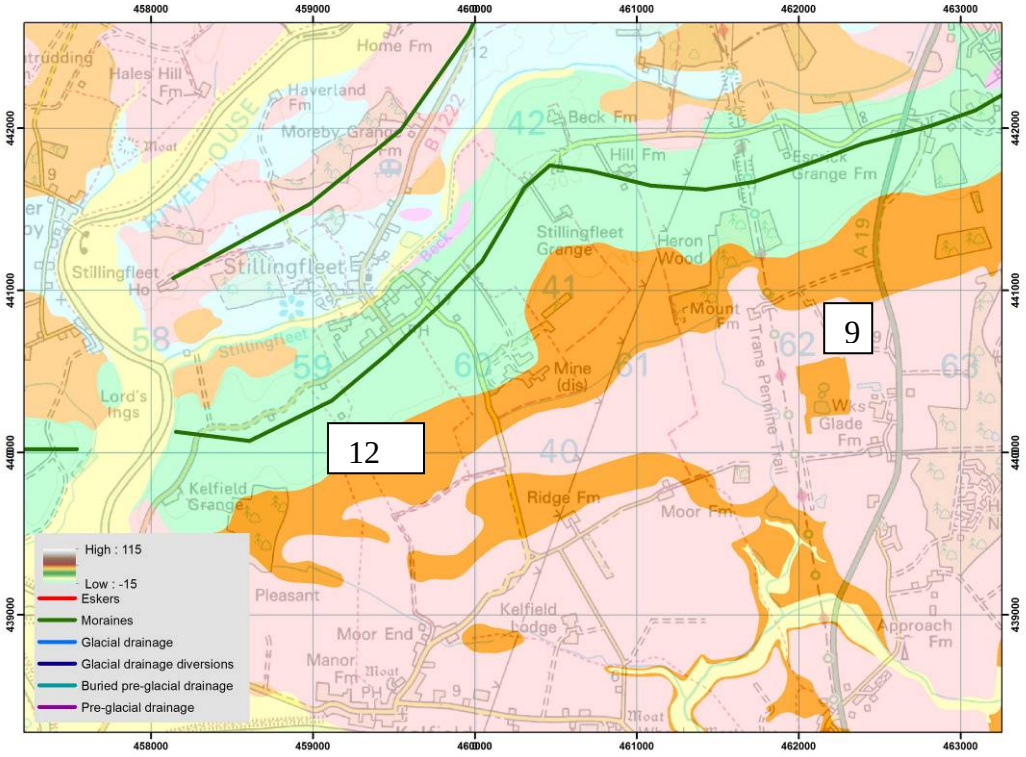

Figure 6-17. Escrick Clay Pit (9) excavated through the Breighton Sand Formation (pink) into the underlying Park Farm Member of the Hemingbrough Formation (orange) the ground (green) to the north is the Escrick Moraine Member of the Vale of York Formation

6.9 LOCALITY 10 - LITTLE SKIPWITH [SE 6690 3780]

To examine latest glacial and/or post-glacial fluvio-aeolian sand (Figure 6-20 including buried peat horizons (Breighton Sand Formation – Skipwith Sand Member) and evidence of former surface peat extraction. Deep augering and logging.

Figure 6-18. DTM and topography for Skipwith Common flattish Breighton Sand Formation over Hemingbrough Formation with alluvium in the low ground to the east

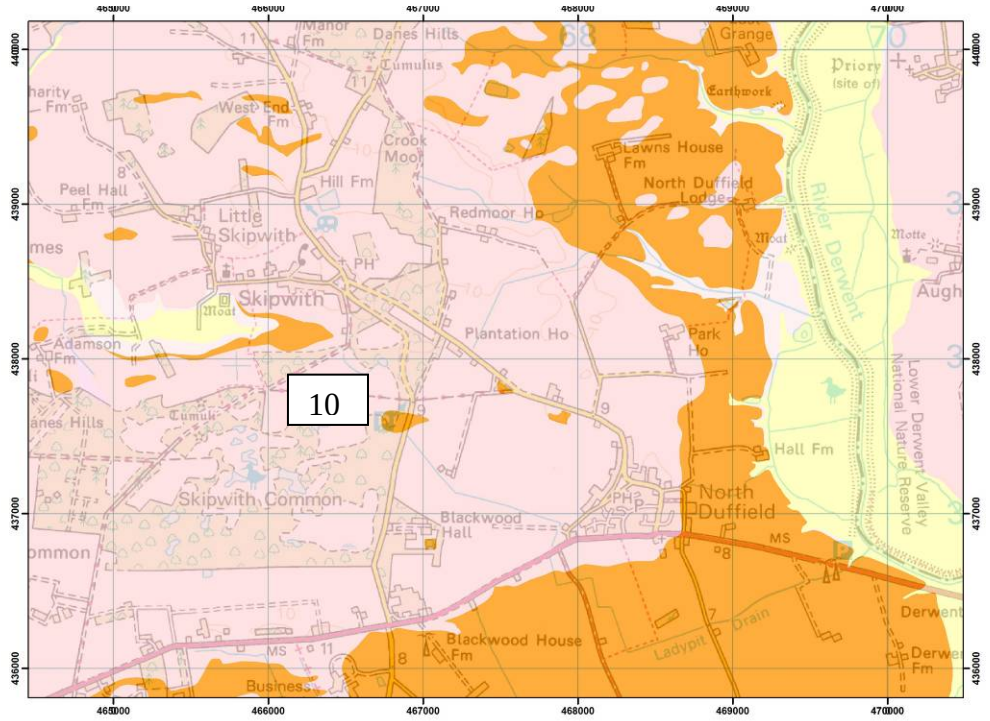

Figure 6-19. Skipwith Common Breighton Sand Formation (pink) over Hemingbrough Formation (orange) with alluvium in the low ground to the east (yellow)

Figure 6-20. The Skipwith sands exposed north of Skipwith [465150; 439400]

6.10 LOCALITY 11 – HOLME ON SPALDING MOOR, CHURCH HILL [SE 8205 3892]

The last stop of the day, if time permits is Church Hill, Holme on Spalding Moor. The hill is capped with a deposit of sand and gravel that contains numerous wind-eroded cobbles and boulders (Figure 6-21). These are indicative of erosion by wind and have the typical form of dreikanter or ventifacts, they are relics of the pre-Devensian deposits (possibly Anglian) that cap the hill. The hill below the sand and gravel is Triassic Mercia Mudstone, which weathers to a red soil. The flat low ground surrounding the hill is sand resting on glacial lake silts and clays of Devensian age. From Church Hill (if the weather is clear) there are good views over the Vale of York, which allow an appreciation of the extent and low relief of the glacial and pro-glacial deposits.

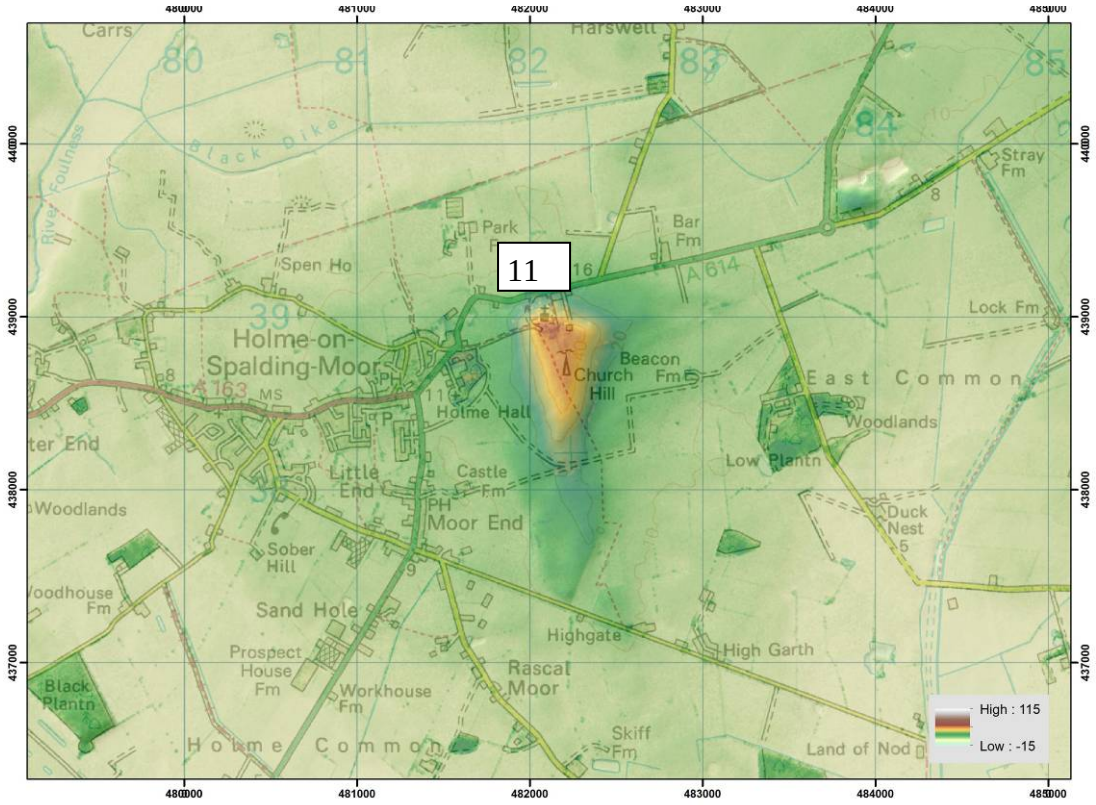

Figure 6-21. DTM of Church Hill south of the Escrick Moraine

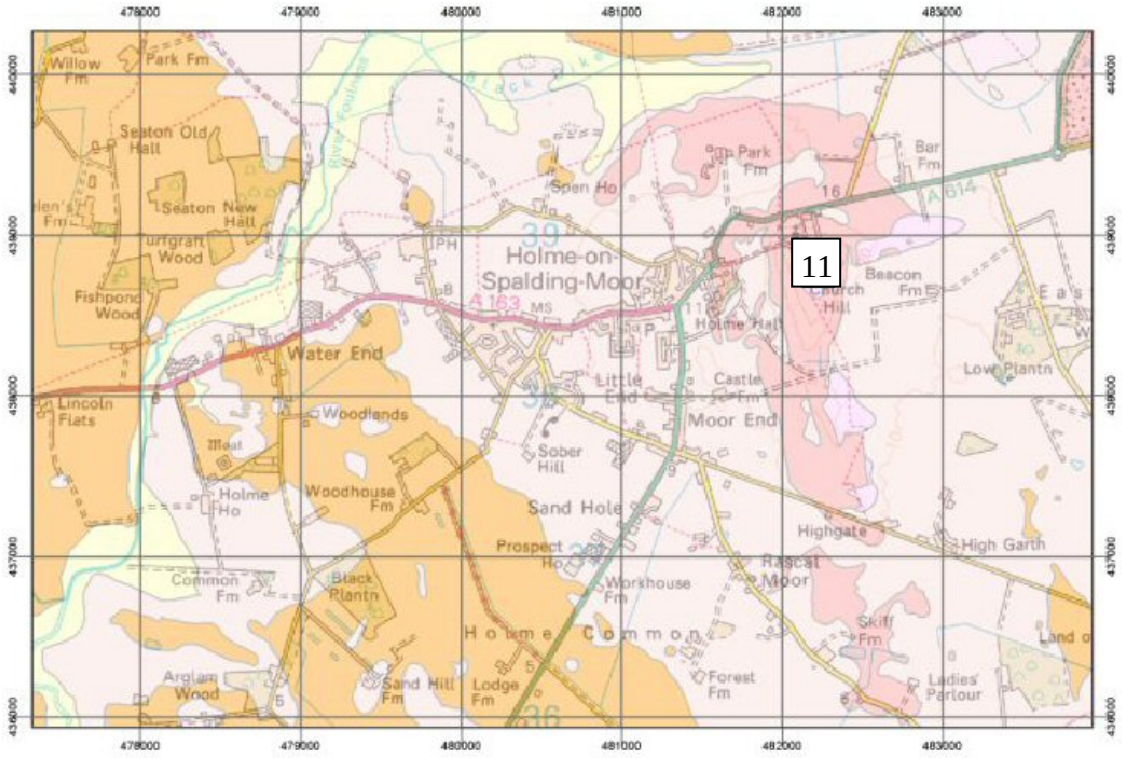

Figure 6-22. Geology of Church Hill (11) Mercia Mudstone Group bedrock (very dark pink), pre-Devensian sand and gravel (dark pink), Devensian Breighton Sand Fm (light pink), Hemingbrough Glaciolacustrine Formation (orange)

7 Wednesday 22nd October – Field mapping training

7.1 LOCALITY 12 – STILLINGFLEET, MAPPING EXERCISE [SE 5950 4450]

The purpose of this locality is to complete a small mapping exercise developing upon the geological information and knowledge that you have developed from the previous localities. The location for this exercise is the land between Stillingfleet and Kelfield (Figure 7-1). A cross-section (Figure 7-2), a NextMap DSM (Figure 7-3) and LIDAR image (Figure 7-4) of the mapping exercise area are provided.

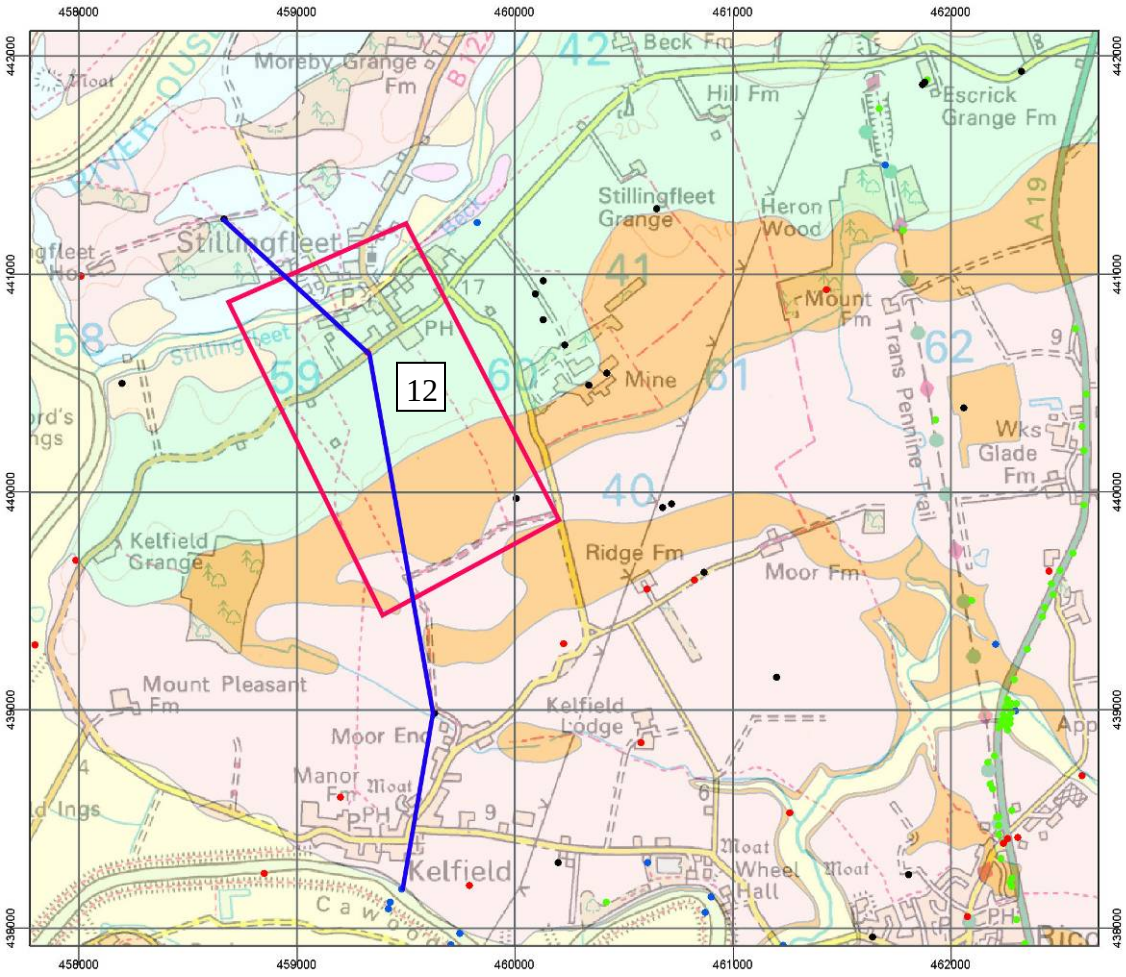

Figure 7-1. Map showing the geology and mapping exercise area (pink rectangle) near Stillingfleet to the south of York (1:50k Sheet 71 Selby; 1:10k Sheets SE54SE and SE53NE). The blue line follows a north-south section shown in Figure 7-2

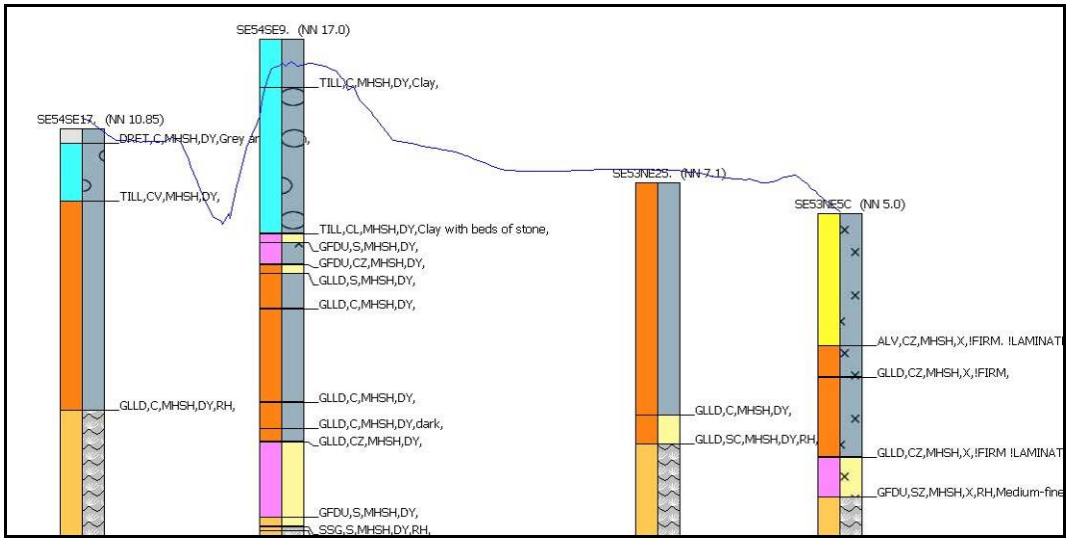

Figure 7-2. North-South cross-section across the mapping area using 4 existing boreholes. Till – blue; glaciolacustrine deposits (orange); basal glaciofluvial deposits (pink); Sherwood Sandstone (brown). The Blue Line Represents The DTM

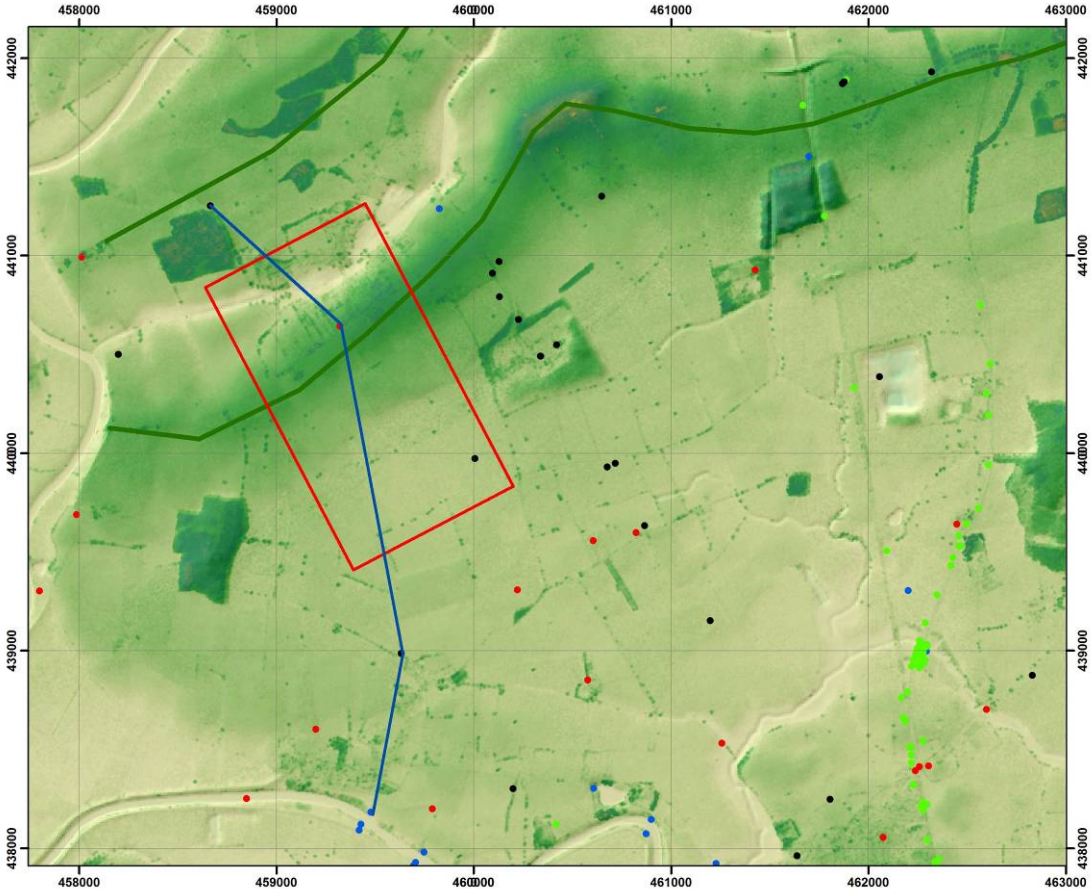

Figure 7-3. NextMap DSM 5m resolution dataset. Colour ramped -15 to + 115m and 40% transparency over 4 degree shaded 10m resolution hillshade derived from the same dataset. Area depicted is the same as Figure 7-1. Note the presence of woods and trees, also at this scale of colour ramping the height of the crops show in some of the fields

Figure 7-4. LIDAR images of training area to be used during mapping showing the moraine high in dark green and floodplains in brown (Licensed by EA for training purposes only)

8 Thursday 23rd October – Quarry section logging and borehole logging plus some field mapping

8.1 LOCALITY 13 - NEWTON CLAY PIT [SE 7240 5040]

To examine morainic tills, glaciotectonised lake sediments and fluvio-aeolian "cover" sands (Figure 8-3). Logging exercise of Breighton Sand Formation "cover sand" section.

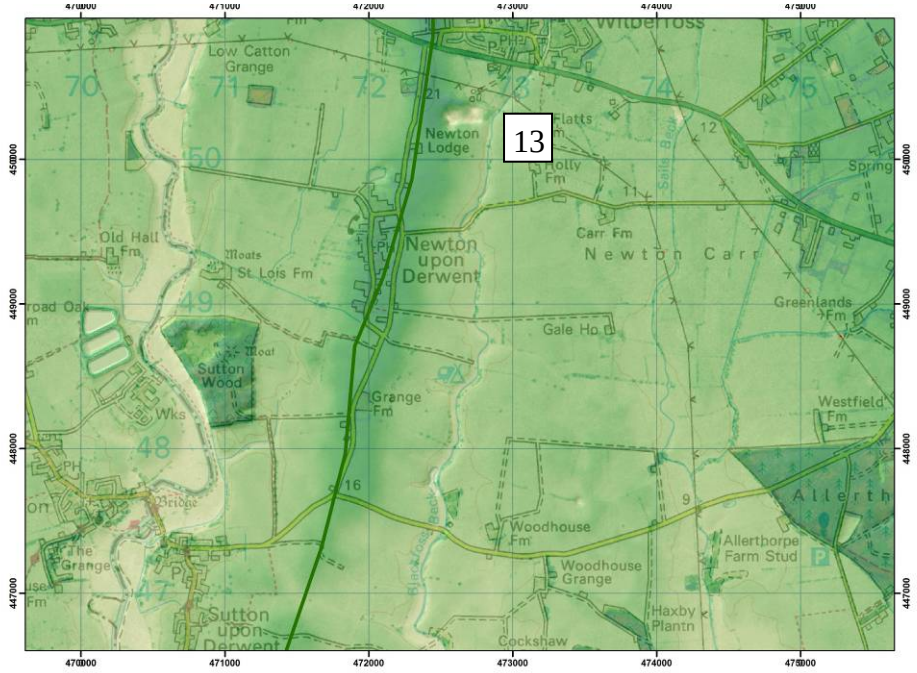

Figure 8-1. DTM showing the location of Newton Clay Pit on the east flank of the Escrick Moraine

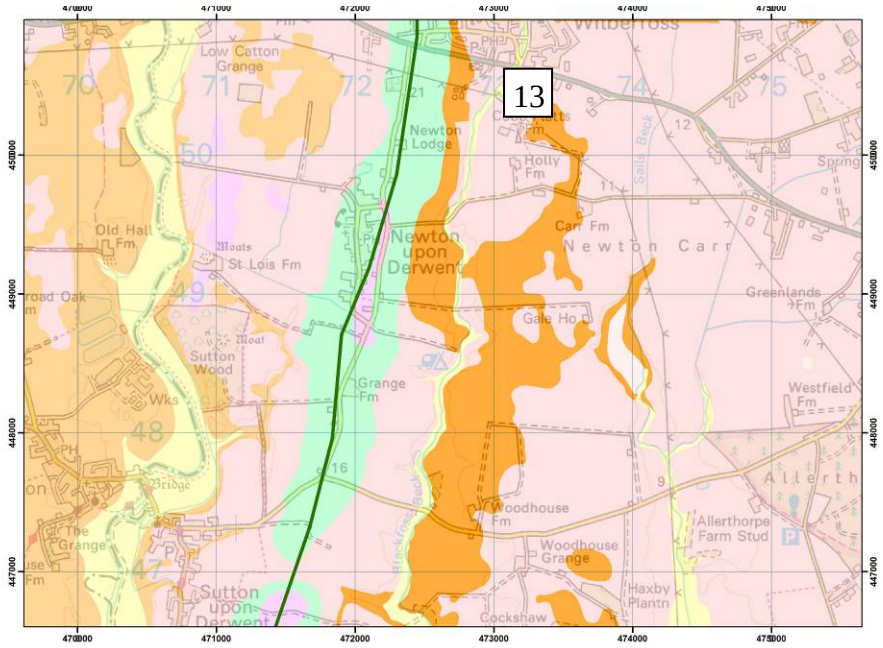

Figure 8-2. Geology map showing the location of the Newton Clay Pit on the east of the Escrick Moraine (green) overlying clay of the Hemingbrough Formation (orange) and partly covered by Breighton Formation (pink)

Figure 8-3. Newton Upon Derwent Clay pit [472700; 450300] showing glaciotectonics. The features in the face sloping gently to the left are thrust surfaces pushed through the glaciolacustrine lake clays in front of the Escrick Moraine.

9 Friday 24th October Geological hazards caused by landslides at Hollin Hill, Terrington

The eastern side of the Vale of York mirrors the western side in that there is glacial drainage along the former ice margin just outside of the marginal moraine (Figure 9-1 and Figure 9-2). This eastern area comprises Jurassic rocks of the Howardian Hills, which lay in a periglacial situation between the Vale of York glacier to the west and hills with Glacial Lake Pickering to the north-east. The erosion in the marginal channel location plus periglacial situation and the presence of the Whitby Mudstone Formation that is prone to landsliding mean that the geology here is prone to failure. Landslides were mapped here as part of the York area resurvey and they have been studied intensively for around 10 years. The hillside is failing and BGS has installed a landslide observatory using various geophysical techniques to monitor the ground conditions, triggering mechanisms and mode of failure. The landslide and surrounding geology will be examined along with the various geophysical monitoring techniques as described in Chambers et al., (2011) Gunn et al., (2013) and Merritt et al., (2014).

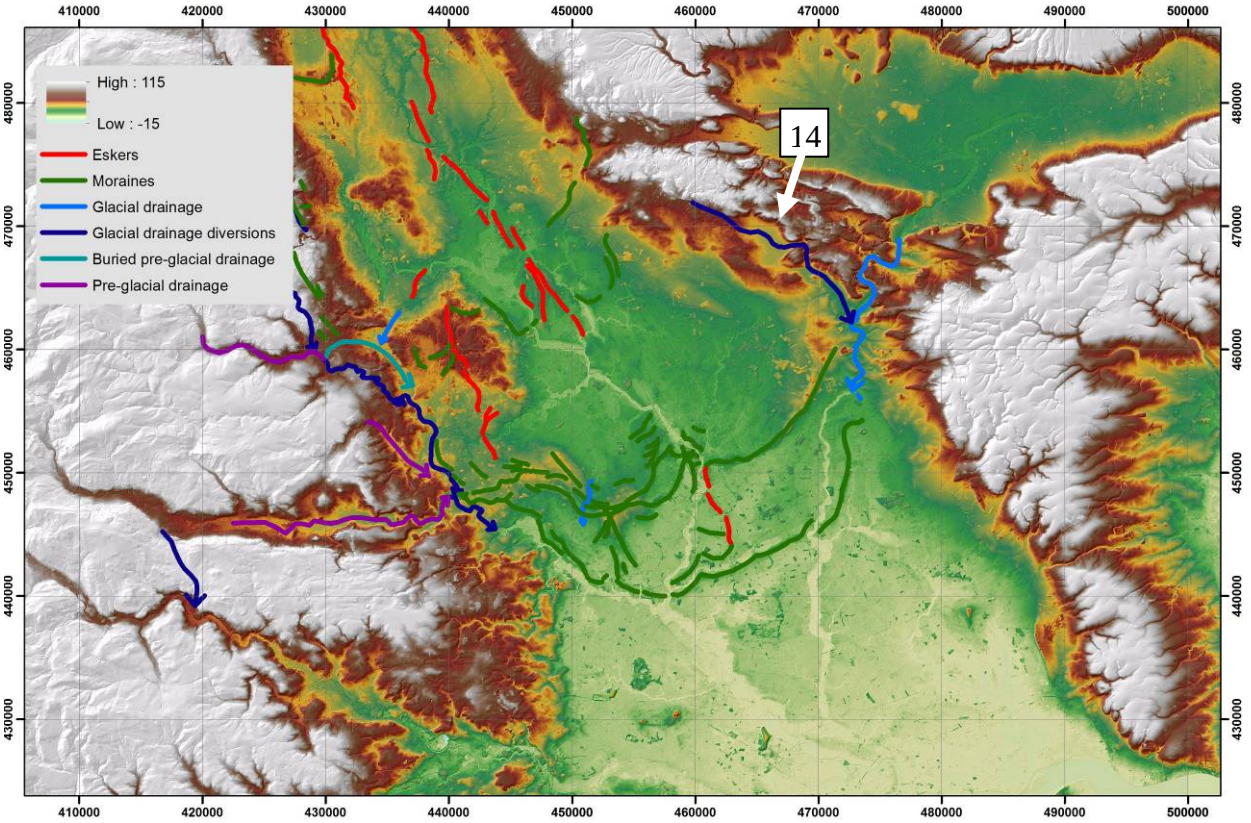

Figure 9-1. DTM showing the location of Hollin Hill (locality 14) and the marginal drainage

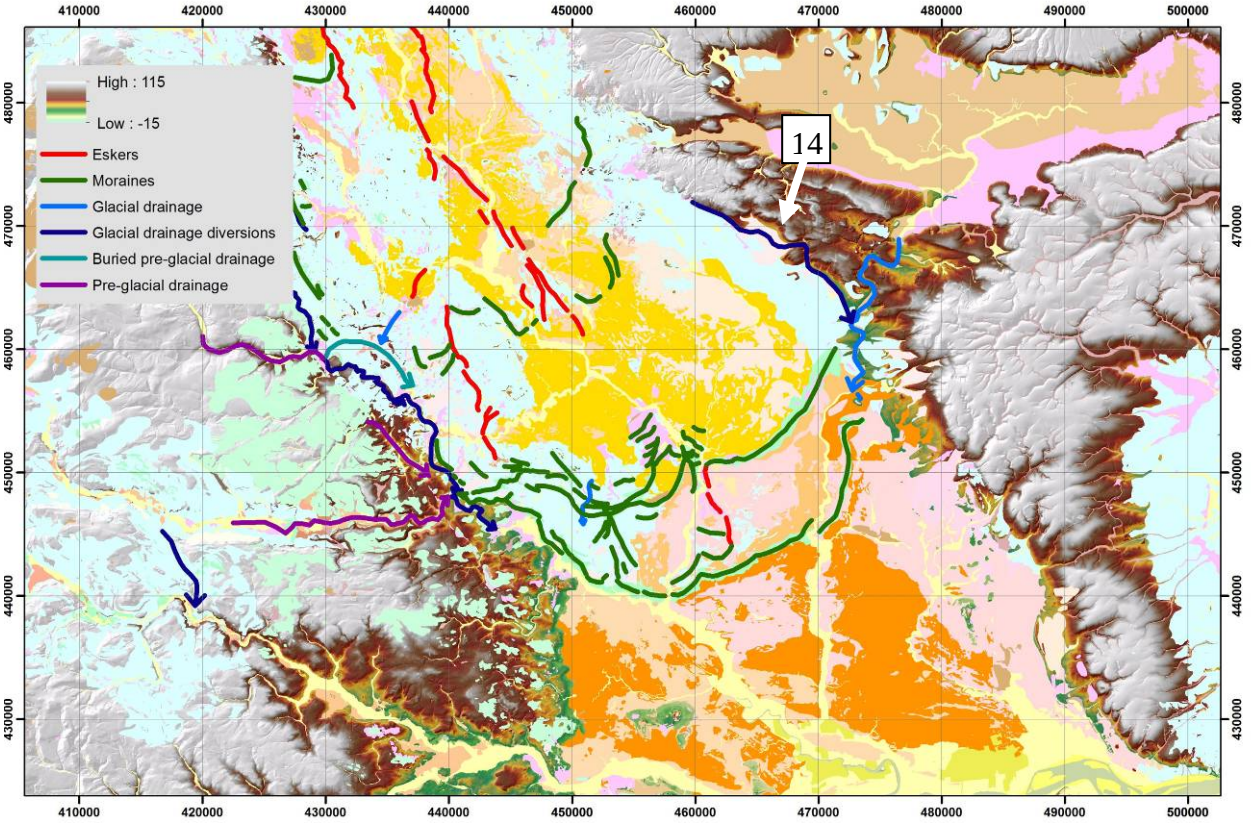

Figure 9-2. Superficial Geology and DTM for bare bedrock showing the location of Hollin Hill (locality 14)

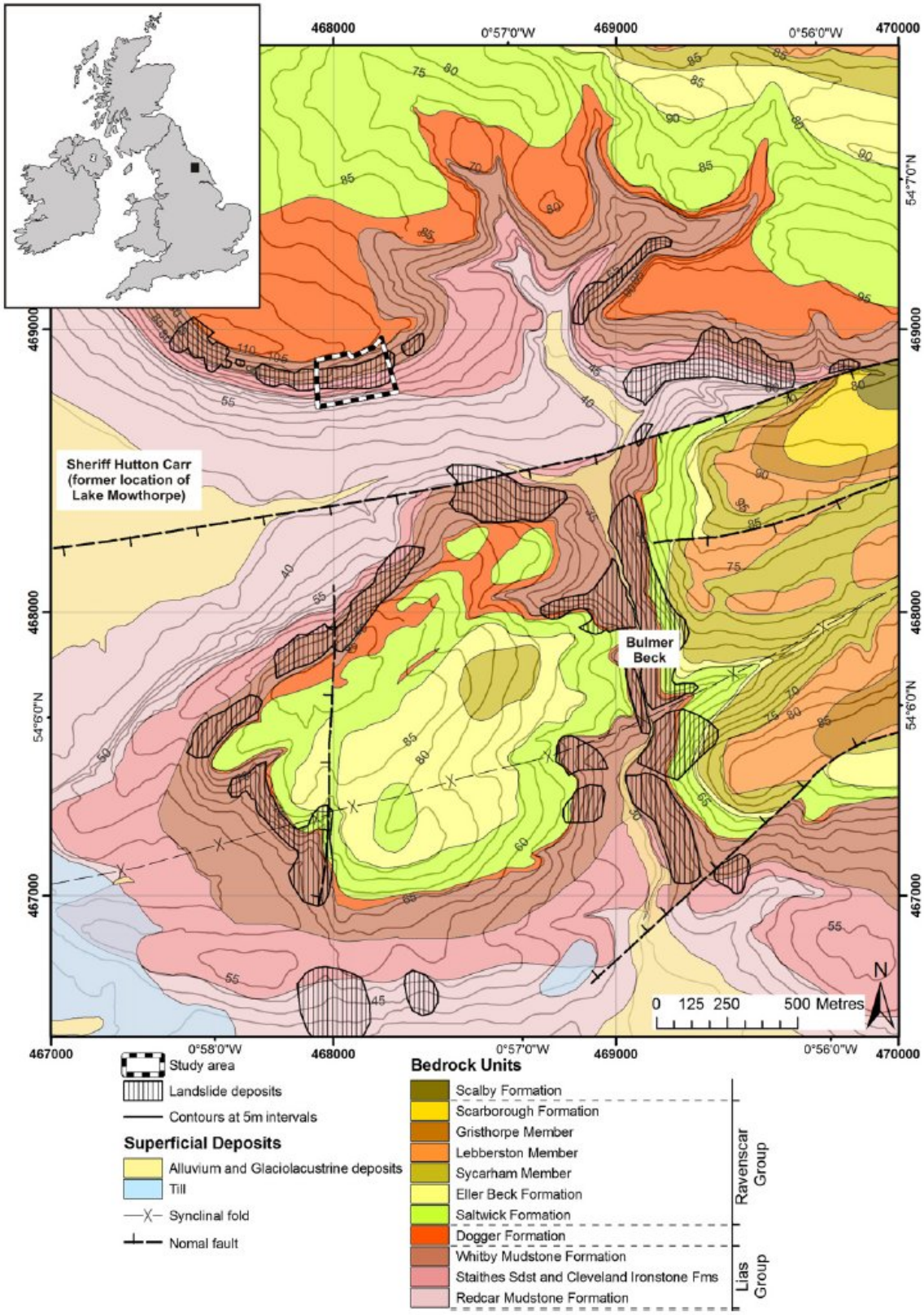

Figure 9-3. Geology of Hollin Hill and surrounding area from Chambers et al., 2011

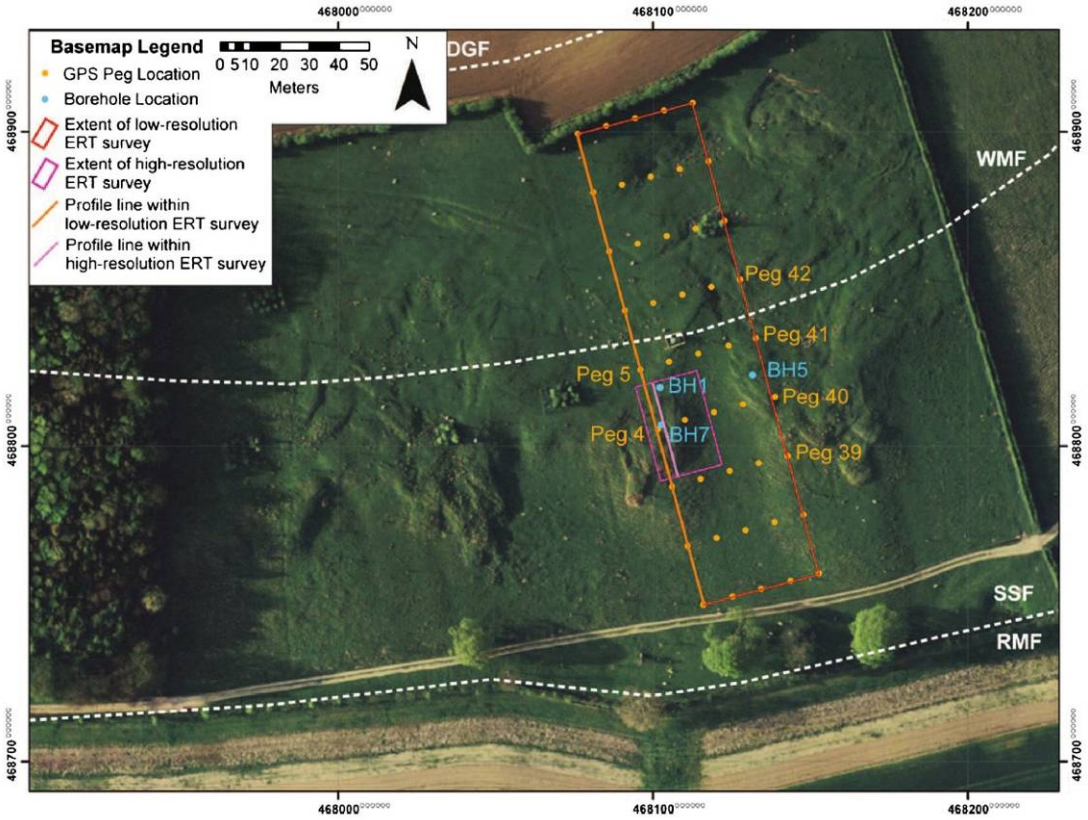

Plan view of study site, annotated with lithological boundaries (*dashed white lines*), positions of pegs (*yellow points*), borehole locations (*light blue points*) and areas of high- and low-resolution ERT surveys (low-res array: *red rectangle*, high-res array: *purple rectangle*). *Orange* and *lilac lines* indicate positions of interpreted profiles presented as Figs. 9 and 11, respectively. *Inset left* shows the position and number reference of GPS pegs. Coordinate system is British National Grid (BNG). Illustration of study site based upon an aerial photograph © UKP/Getmapping Licence No. UKP2006/01

Figure 9-4. Hollin Hill, aerial topography and geophysical installations from Merritt et al., 2014

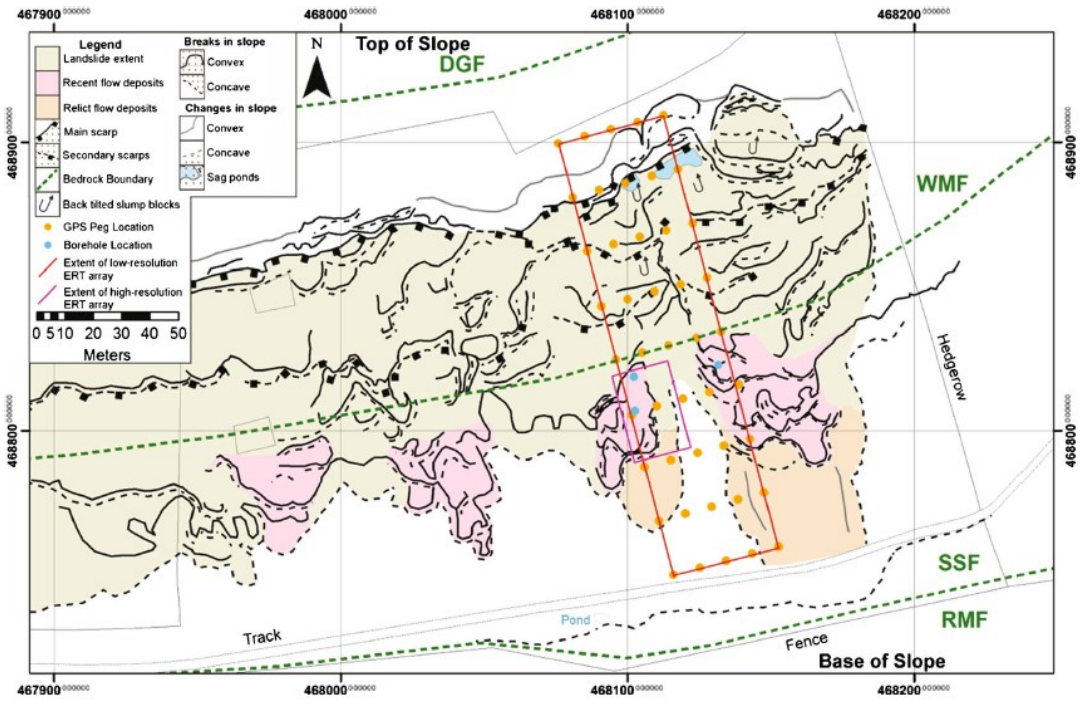

Geomorphology map of the field site produced from an airborne LiDAR dataset, visualised using GeoVisionary software and presented using ArcGIS10. The top of the slope is towards the north of the map, with the base towards the south; coordinate system used is BNG

Figure 9-5. Hollin Hill morphology mapped from airborne LiDAR from Merritt et al., 2014

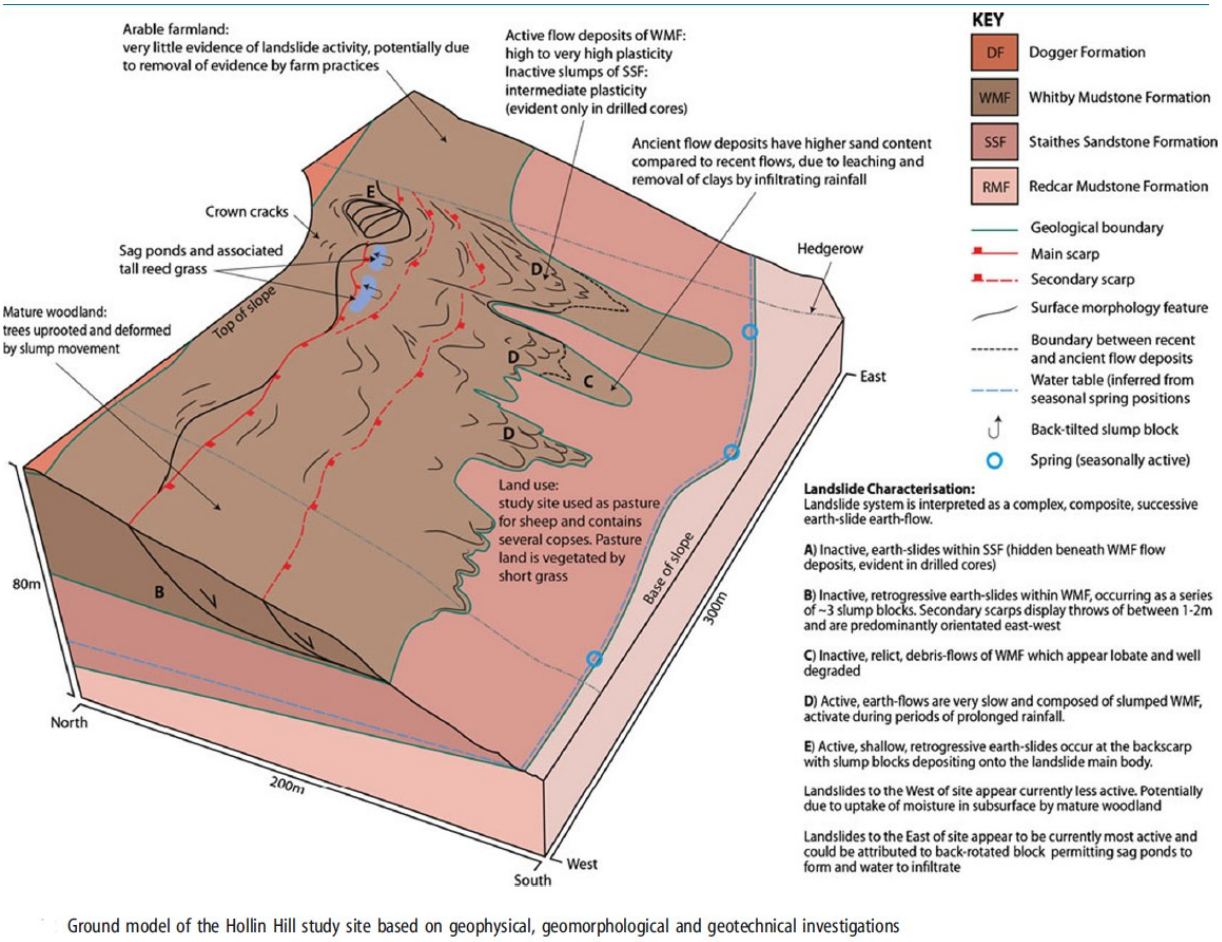

Ground model of the Hollin Hill study site based on geophysical, geomorphological and geotechnical investigations

Figure 9-6. Hollin Hill, 3D ground model from Merritt et al., 2014

References

British Geological Survey holds most of the references listed below, and copies may be obtained via the library service subject to copyright legislation (contact libuser@bgs.ac.uk for details). The library catalogue is available at: http://geolib.bgs.ac.uk.

BATEMAN, M D, BUCKLAND, P C, WHYTE, M A, ASHURST, R A, BOULTER, C, and PANAGIOTAKOPULU, E. 2011. Re-evaluation of the Last Glacial Maximum typesite at Dimlington, UK. *Boreas*, Vol. 40, 573-584.

CATT, J A. 2007. The Pleistocene Glaciations of Eastern Yorkshire: a review. *Proceedings of the Yorkshire Geological Society*, Vol. 56, 177-207.

CHAMBERS, J E, WILKINSON, P B, KURAS, O, FORD, J R, GUNN, D A, MELDRUM, P I, PENNINGTON, C V L, WELLER, A L, HOBBS, P R N, and OGILVY, R D. 2011. Three-dimensional geophysical anatomy of an active landslide in Lias Group mudrocks, Cleveland Basin, UK. *Geomorphology*, Vol. 125, 472-484.

COOPER, A H, and BURGESS, I C. 1993. Geology of the country around Harrogate; Sheet 62 (England and Wales). *Memoir of the British Geological Survey*.

COOPER, A H, and GIBSON, A D. 2003. *Geology of the Leeds District.* Sheet Explanation of the British Geological Survey, 1:50 000 Sheet 70 (England and Wales).

EVANS, D J A, OWEN, L A, and ROBERTS, D. 1995. Stratigraphy and sedimentology of Devensian (Dimlington Stadial) glacial deposits, east Yorkshire, England. *Journal of Quaternary Science*, Vol. 10, 241-265.

FORD, J R, COOPER, A H, PRICE, S J, GIBSON, A D, PHARAOH, T C, and KESSLER, H. 2008. *Geology of the Selby district : a brief explanation of the geological map Sheet 71 Selby*. Explanation (England and Wales Sheet). No. 71. (Nottingham, UK: British Geological Survey.)

GUNN, D A, CHAMBERS, J E, HOBBS, P R N, FORD, J R, WILKINSON, P B, JENKINS, G O, and MERRITT, A. 2013. Rapid observations to guide the design of systems for long-term monitoring of a complex landslide in the Upper Lias clays of North Yorkshire, UK. *Quarterly Journal of Engineering Geology and Hydrogeology*, Vol. 46, 323-336.

MERRITT, A J, CHAMBERS, J E, MURPHY, W, WILKINSON, P B, WEST, L J, GUNN, D A, MELDRUM, P I, KIRKHAM, M, and DIXON, N. 2014. 3D ground model development for an active landslide in Lias mudrocks using geophysical, remote sensing and geotechnical methods. *Landslides*, Vol. 11, 537-550.

Landslides (2014) 11:537–550
DOI 10.1007/s10346-013-0409-1
Received: 19 December 2012
Accepted: 29 April 2013
Published online: 21 May 2013

A. J. Merritt · J. E. Chambers · W. Murphy · P. B. Wilkinson · L. J. West · D. A. Gunn · P. I. Meldrum · M. Kirkham · N. Dixon

3D ground model development for an active landslide in Lias mudrocks using geophysical, remote sensing and geotechnical methods

Abstract A ground model of an active and complex landslide system in instability prone Lias mudrocks of North Yorkshire, UK is developed through an integrated approach, utilising geophysical, geotechnical and remote sensing investigative methods. Surface geomorphology is mapped and interpreted using immersive 3D visualisation software to interpret airborne light detection and ranging data and aerial photographs. Subsurface structure is determined by core logging and 3D electrical resistivity tomography (ERT), which is deployed at two scales of resolution to provide a means of volumetrically characterising the subsurface expression of both site scale (tens of metres) geological structure, and finer (metre to sub-metre) scale earth-flow related structures. Petrophysical analysis of the borehole core samples is used to develop relationships between the electrical and physical formation properties, to aid calibration and interpretation of 3D ERT images. Results of the landslide investigation reveal that an integrated approach centred on volumetric geophysical imaging successfully achieves a detailed understanding of structure and lithology of a complex landslide system, which cannot be achieved through the use of remotely sensed data or discrete intrusive sampling alone.

Keywords Lias mudrocks · 3D ERT · Landslides

Introduction

Nature of the problem/motivation

Landslides are complex, strongly heterogeneous natural phenomena. A considerable number of landslide types exist, exhibiting varying states, distributions and styles of activity (Cruden and Varnes 1996). If a better understanding of landslide internal processes is to be achieved, firstly, an understanding of landslide internal structure is required. Detailed information regarding landslide internal structure, lithological properties and relationships can be displayed in the form of a ground model. The principal use of a ground model is to inform about the range of possible subsurface conditions that exist at the site, knowing the geological processes that formed the ground beneath the site (McDowell et al. 2002; Fookes 1997; Griffiths et al. 2012) and are commonly presented as a 3D block model. Ground model development pulls data together from many information streams: from surface characterisation methods, such as geomorphological mapping using light detection and ranging (LiDAR), to subsurface characterisation methods, including borehole logging and geophysical surveys.

Much research is concerned with rapid characterisation of landslides using aerial photography or remote sensing methods, such as digital photogrammetry, LiDAR and InSAR (de Bari et al. 2011; Perrone et al. 2006; Jaboyedoff et al. 2012; Colesanti and Wasowski 2006; Baldo et al. 2009; Dewitte et al. 2008). These methods rely on surface expression—such as slope angle or morphology—to ascertain the spatial extent and type of landslide. However, they provide very little or no information about internal landslide structure. Conversely, conventional intrusive investigations, such as sampling and borehole inclinometers, offer ground-truth data at high resolution, but implementing such methods over a large, inherently unstable feature such as a landslide is both costly and labour intensive. Geophysical methods are therefore being increasingly applied (Jongmans and Garambois 2007) as a means of producing high-resolution volumetric information, which can be sensitive to both subsurface structure and lithology, making full 3D characterisation of the subsurface possible and permitting 3D ground model development.

Geoelectrics are a class of geophysical methods that can bridge the gap between intrusive subsurface investigative methods and remote sensing for ground surface characterisation in the context of landsliding. The main benefits of geoelectrical imaging methods are two-fold. Firstly, they employ lightweight equipment (relative to drill rigs) and are minimally invasive and result in little ground disturbance. Secondly, they provide spatial and volumetric subsurface information, as opposed to conventional intrusive ground investigative techniques, such as core sampling, which provide discrete, 1D information for a given location.

In the last decade, electrical resistivity tomography (ERT) has become a standard geophysical imaging technique for environmental and engineering investigations (Reynolds 2011) and is routinely implemented to locate the failure surfaces within landslide systems (Jongmans and Garambois 2007). The method can be effectively applied to ground investigation due to its sensitivity to lithological variation, principally, quartz and clay content, but also water content and pore-fluid conductivity (Telford et al. 1990). When applied to landslides, ERT is implemented to highlight lithological variations and boundaries, as well as geological discontinuities such as faults, drainage channel systems and other structural features (Lebourg et al. 2005). Because ERT provide indirect subsurface information, it is most appropriately applied alongside other techniques for calibration and validation.

2D electrical resistivity tomography is extensively applied to landslide investigation due to its capacity to model landslide geometries such as body thickness, lateral extent and position of slip surfaces in a number of varying geological settings (Perrone et al. 2004; Lapenna et al. 2003; Godio et al. 2006; Jomard et al. 2007; Sass et al. 2008; Schmutz et al. 2009; Colangelo et al. 2008; Bichler et al. 2004). In contrast, 3D ERT is rarely implemented to investigate landslide systems; this could be attributed to several factors, principally the additional field and processing effort that is required relative to 2D ERT. However, for complex 3D structures, which landslides typically are, a fully volumetric 3D approach is

more appropriate. A number of examples of 3D landslide studies exist in the literature; a brief summary of the most relevant is provided below.

A 3D resistivity survey was performed at a coastal setting by Udphuay et al. (2011). They implemented 3D ERT to assess the vulnerability of a cliff section in Normandy to cliff collapse. The various formations present—identified based on variable resistivity response—were assigned different mass movement potentials, despite the presence of extreme topography and cultural signals.

Heincke et al. (2010) studied the Åknes rockslide in western Norway using a combined 3D geoelectrical and seismic tomographic approach. Seismic low velocity zones coincident with low resistivity anomalies were associated with drained (air-filled) and water-filled parts of tension cracks. Low-velocity and low-resistivity anomalies are explained by elongated tension cracks that are dry close to the surface and water-saturated at greater depths and correspond to tension cracks previously located and mapped in the region.

Pyroclastic cover material subject to debris-flow processes were investigated through high-resolution 3D resistivity surveys by Di Maio and Piegari (2011) in the Sarno Mountains of Campania Region, southern Italy. These landslides are periodically triggered by critical rainfall events; hence, subsurface water content distribution is a key factor influencing the stability of the investigated lithologies. Laboratory-determined petrophysical relationships were used to determine subsurface soil moisture content from ERT images.

A semi-empirical approach to slope stability analysis of pyroclastic cover material was proposed by Di Maio and Piegari (2012). They introduced a geophysical factor of safety in terms of in situ electrical resistivity and slope angle. They outlined the benefits of applying 3D ERT, a volumetric geophysical technique to assess slope stability as opposed to conventional physical analyses whose input parameters are determined through point-sample testing and laboratory tests performed on small volume soil samples, which are unrepresentative of the wider slope.

The La Clapiere landslide in the South East French Alps is responsible for large-volume mass movement of metamorphic bedrock. Lebourg et al. (2005) applied 2D, 3D and 4D ERT to investigate the rupture processes taking place within deep seated landslides. The investigation successfully located the principal slipping surface of La Clapiere landslide as well as the draining system in terms of identifying vertical draining structures and perched water table in superficial moraine deposits.

Aims and objectives

This paper aims to develop a detailed landslide ground model using an integrated 3D geophysical and geotechnical approach for a landslide in Lias mudrocks. The landslide is located within the Whitby Mudstone Formation (WMF) on a valley side and is typical of many inland slope failures in Lias mudrock.

Our study site has the advantage of being the focus of previous geophysical investigation (Chambers et al. 2011), in which multiple geophysical reconnaissance methods were applied and assessed. Here we focus on the most effective geophysical methodology considered in the previous study, 3D ERT, to develop a detailed ground model based on additional high-resolution volumetric resistivity imaging work, detailed core logging and testing, direct calibration of ERT data through laboratory analysis and remote sensing visualisation techniques. We outline the methodology for ground model development and critically assess the benefits of incorporating 3D ERT into landslide investigation at different image resolutions and regions of the landslide. There is no other example of ground model development in the Whitby Mudstone Formation in the literature, and very few examples of integrated ground investigations centred on the use of 3D ERT.

Site background

Geology and geomorphology

The research area is located 4 miles west of the market town of Malton, North Yorkshire, UK. The field site itself is located on a south-facing hill slope used as pasture land. It is bounded to the north, south and east by hedged arable land—mostly wheat and rape—and by mature woodland to the west. Figure 1 provides an overview map, which shows the geology of the field site and surrounding area.

Beyond the base of the field site hill slope is a wide topographic embayment called Sheriff Hutton Carr, to the south of which is a ridge composed of Lower Jurassic formations. During the Devensian, much of Northern Britain was covered in a thick ice sheet. Sheriff Hutton Carr was the site of an ice-marginal lake, responsible for depositing lacustrine-derived material in the lowland between Hollin Hill slope and the ridge (Ford 2013).

The hill slope is composed of four geological formations of Lower and Middle Jurassic Age. The base of the Hollin Hill slope comprises Redcar Mudstone Formation (RMF) and marks the oldest formation at the field site and is overlain by Staithes Sandstone Formation (SSF) which gives way to WMF, with Dogger Formation capping the hill slope. Dogger Formation is the lowermost formation of the Ravenscar Group of the Middle Jurassic and has an erosional base over most of the Yorkshire Basin (Powell 1984; Rawson and Wright 1995).

Lias Group formations—in particular WMF—are prone to slope instability. The study site covers an area of roughly 450× 200 m and a change in elevation of ~50 m from the base to the top of the slope and contains a complex landslide system that exhibits a variety of landslide types and activity. The landslide system extends many hundreds of metres along the hill slope beyond the limits of the study site and has been previously described as a slow to very slow moving multiple earth slide—earth flow (Chambers et al. 2011). A site plan and aerial photograph of the field site is presented as Fig. 2 and shows the locations of installed monitoring equipment, drilled boreholes and of the major geological formation boundaries which outcrop at the site.

Previous investigations

The landslide at Hollin Hill has been previously reconnoitred using several geoelectrical geophysical methods including electrical resistivity tomography (2D and 3D), self-potential profiling, mapping and tomography and mobile resistivity mapping (Chambers et al. 2011). A 3D ERT was performed at the site of an area which extends from the back scarp to the toe of the landslide and encompassed the most active areas of the landslide system. The results of 3D ERT model show that the succession from low resistivity RMF to more resistive SSF through to less resistive Whitby Mudstone Formation is clearly displayed, as is the general 5° North dip trend of the surveyed formations. Mobile resistivity mapping was undertaken using the

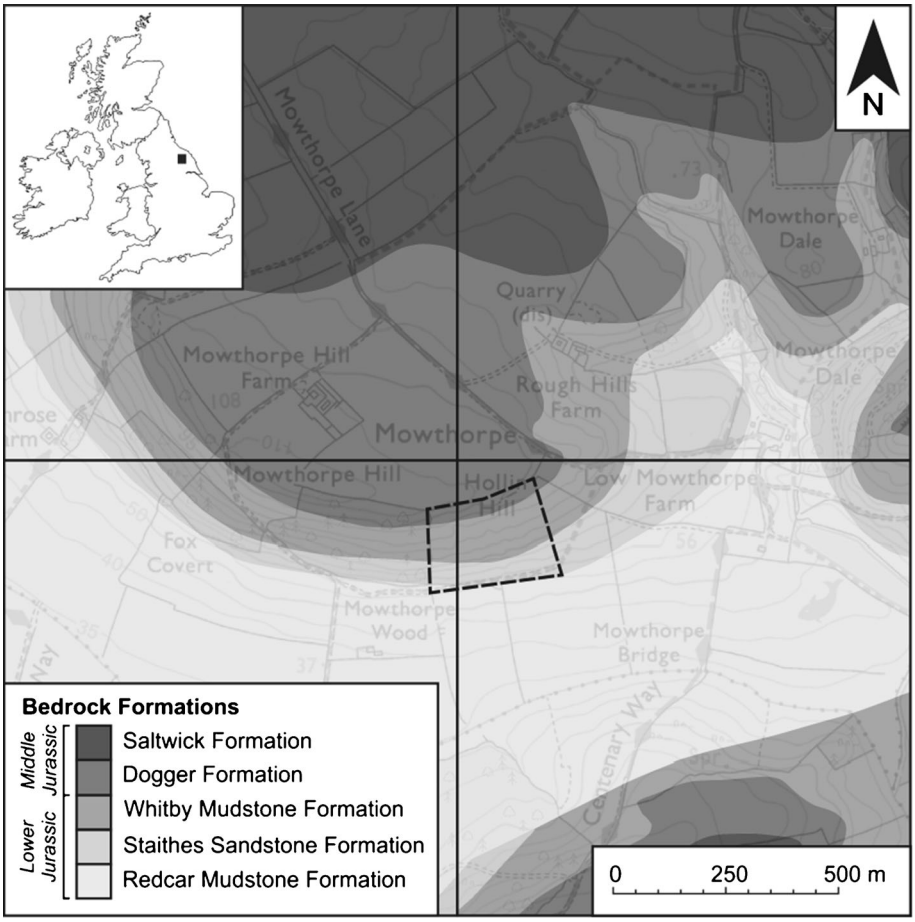

Fig. 1 Geological map of the study area and *inset* large-scale map. Geological mapping, BGS © NERC. Contains Ordnance Survey data © Crown Copyright and database rights 2013

automated profiling technique—developed by Geocarta SA, France—with the aim of producing very near surface property maps. This technique produced a map of apparent resistivity and informs about soil spatial property variation attributed to texture, clay content, stoniness and depth to substratum. Groundwater movement was investigated through the identification of streaming potentials in the subsurface using self-potential profiling, mapping and tomography. 3D self-potential tomography reveals the nature of drainage and surface run-off on the slope. Interpretation of 3D SP tomograms reveals that infiltration and drainage into SSF is occurring. The lack of strong positive charge occurrence probability in the WMF suggests that rainfall runs off the relatively impermeable formation and infiltrates SSF further downslope.

Methodology

This paper builds on previous investigations at the research site in several key areas. ERT surveys are presented at different resolutions to display the internal structure of the landslide system and display improved detail afforded by higher-resolution imaging. New high-resolution ERT images of the most active area of the landslide are interpreted using detailed core logs and laboratory sample analysis; in particular, laboratory analyses are used to establish relationships between resistivity and lithologies of the key formations (i.e. WMF and SSF). Surface and subsurface observations of movement are used to indicate the distribution and rate of slope movements and the location of slip surfaces. The latest Digital Terrain Model (DTM) data generated from airborne LiDAR is analysed alongside aerial photographs using GeoVisionary, an immersive 3D graphical visualisation software package, designed to allow the user to undertake virtual fieldwork in which even subtle geomorphologic features can be identified (Jordan et al. 2009). This combination of high-resolution surface and subsurface data is used here to develop a site-specific ground model.

Surface characterisation

Aerial LiDAR/GeoVisionary

LiDAR optical remote sensing methods are implemented to produce high-resolution Digital Elevation Models. An airborne LiDAR survey of Hollin Hill was performed January 2011, and GeoVisionary 3D Stereographic Software System was used to visualise the resulting survey dataset. GeoVisionary is a software package developed specifically for virtual field reconnaissance (Jordan et al. 2009). The software is capable of visualising high-resolution spatial data containing geomorphologic features, such as changes and breaks in slope, which can be digitised directly onto the 3D digital elevation model. The geomorphological map produced at Hollin Hill shows the distribution of landslide features, breaks in slope and other landforms throughout the field site.

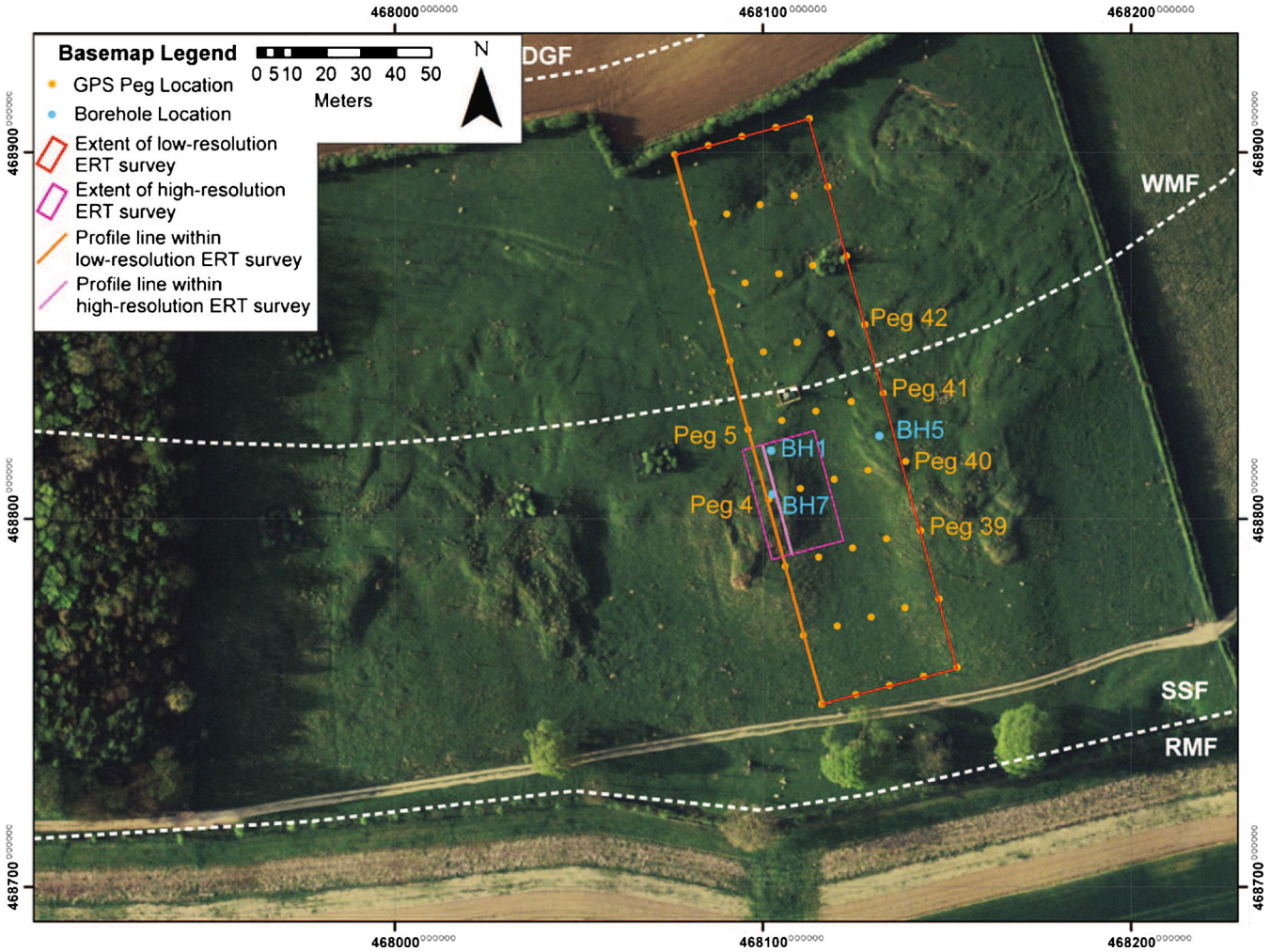

Fig. 2 Plan view of study site, annotated with lithological boundaries (*dashed white lines*), positions of pegs (*yellow points*), borehole locations (*light blue points*) and areas of high- and low-resolution ERT surveys (low-res array: *red rectangle*, high-res array: *purple rectangle*). *Orange* and *lilac lines* indicate positions of interpreted profiles presented as Figs. 9 and 11, respectively. *Inset left* shows the position and number reference of GPS pegs. Coordinate system is British National Grid (BNG). Illustration of study site based upon an aerial photograph © UKP/Getmapping Licence No. UKP2006/01

GPS survey of peg positions

A series of 45 surveying pegs were inserted approximately 0.3 m into the top soil at the field site in a rectangular-shaped grid as shown on the base map (Fig. 2). By repeatedly surveying the position of each peg periodically over a number of years, it has been possible to determine both the landslides rate of movement, its most active regions and its movement history since monitoring began in March 2008. The Leica System 1200 Real-Time Kinematic-Global Positioning System (RTK-GPS) is used to make repeat measurements of pegs installed at the field site. Accuracy of the system in kinematic mode (receiving real-time position corrections) is up to 10 mm (rms) horizontally and 20 mm vertically (Fig. 3).

Subsurface characterisation

3D electrical resistivity tomography

Electrical resistivity tomography was performed on the landslide at two scales. The large-scale survey covered a region of the landslide system from the crown to beyond the landslide foot and toe and is represented by the red rectangular area on the base map (Fig. 2). Electrode spacing was 4.75 m along-line and 9.5 m between lines, covering an area of 38×147.25 m. Data were acquired using the AGI Supersting R8 electrical resistivity survey system. Measurements of potential were made using a dipole–dipole configuration, with dipole sizes of 4.75, 9.5, 14.25 and 19 m (a=1–4) and dipole sizes (n) of 1 to 8a. A complete set of reciprocal measurements was utilised for data quality assessment and editing (Dahlin and Zhou 2004; Wilkinson et al. 2012).

The higher-resolution ERT survey imaged an active flow lobe at a level of resolution closer to that of deposit heterogeneity (i.e. sub-metre rather than metre scale). A similar measurement configuration was employed, dipole–dipole, with dipole sizes of 1.0, 2.0, 3.0 and 4.0 m (a=1–4) and n of 1 to 8 a. Higher resolution was achieved for the second survey by decreasing the electrode spacing of the second ERT survey by a factor of 5 to 1 m along-line spacing and 2 m between survey lines. A total 28 lines were performed, 11 31-m-length surveys parallel to y-axis and 17 20-m surveys

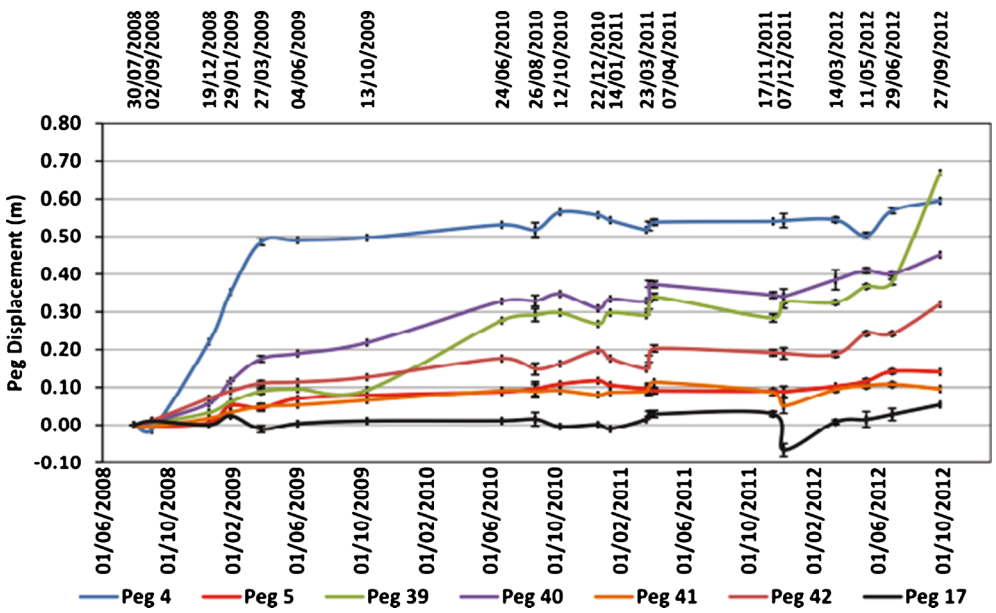

Fig. 3 Displacements of seven pegs at field site by repeat measurement by RTK-GPS

perpendicular to the *y*-axis which were combined to produce a fully 3D resistivity dataset. The high-resolution survey covered an area of 31×20 m using a grid of 32×21 electrodes.

Dipole–dipole measurements of resistance are made by four-point measurement, with two current and two potential electrodes. The reciprocal measurement (ρ_r) of the transfer resistance (ρ_r) is made by interchanging the current and potential dipoles. The reciprocal error for a given four-point measurement of resistance is defined as the percentage standard error in the average resistance measurement (average of transfer and reciprocal measurements) and is calculated:

$$|e| = 100 \times \left|\rho_n - \rho_r\right| \Big/ (\rho_n + \rho_r)$$

Chambers et al. (2011) report the error handling method and values utilised for the large-scale ERT survey. The higher-resolution ERT survey of the flow region 92.9 % of measurements had a reciprocal error of less than 1 %, and so, all data points greater than 1 % reciprocal error were removed before inversion. After editing a total of more than 8,700 transfer resistance data, points were inverted and an acceptable model convergence was achieved within four iterations of 1.83 % mean absolute misfit error.

Boreholes and geotechnical testing

During October 2009, a drilling campaign was undertaken using the Dando Terrier geotechnical percussion drilling rig and a total of nine boreholes performed, each to a depth of between 5 and 7 m. The decision was made to focus attention on the most active part of the landslide system within the field site, which exhibited the freshest landslide features (a sharp crown and main scarp and lightly vegetated flow deposits).

Three of the eight boreholes performed during the drilling campaign at Hollin Hill were logged to BS5930 (British Standards Institution 1999) and index tested to BS1377 (British Standards Institution 1990). Cores selected for logging and geotechnical index testing were subjected to the following: particle size distribution (fines content by X-ray sedigraph), moisture content and shear strength by hand vane. Also, a series of Atterberg Limit tests were performed, to give an insight into the consistency and behaviour of the WMF and SSF at various moisture contents (Head 2006), and X-ray diffraction (XRD) analysis was used to investigate clay mineralogy. Particle size distribution analyses were performed every 0.5 m until a lithology change was reached, in that case a PSD was performed either side of the lithological boundary. The positions of boreholes selected for logging and geotechnical index testing are shown on the field site base map (Fig. 2), with boreholes 1 (BH1) and 7 (BH7) located on the western lobe and borehole 5 (BH5) on the eastern lobe. Boreholes were interpreted based on the results of detailed core logging, high-resolution core photographs and index testing into landslide deposit type and stable, in situ material. Therefore, the 1D structure of the landslide system is known at three discrete regions, these interpreted core logs. Four divisions were used to classify the core in terms of lithology and internal structure: top soil, flow deposits, rotational slump deposits and in situ Staithes Sandstone Formation.

Borehole inclinometer

Periodically, borehole inclinometer measurements were made using an ITMSOIL vertical inclinometer system at boreholes BH1, BH5 and BH7, during 2009. Displacement readings were taken every 0.5 m within the casing to determine the depth, direction and magnitude of slip surface displacement over time.

Core resistivity and cation exchange capacity

Laboratory measurements of soil resistivity were made on core from BH5 and BH7, with the aim of aiding the differentiation between units and formations. The cores were halved—using a purpose-made rock core cutting saw—by making an axial cut, along the full length of each 1-m core run. At 0.1 m spacing, a Decagon 5TE (Topp et al. 1980) soil moisture and bulk electrical conductivity (EC) probe was

inserted into the half core and bulk EC measured for the whole length of cores BH5 and BH7. The results of core resistivity measurements are presented along with the interpreted borehole logs in order to show the variation in electrical resistivity between soil units at Hollin Hill.

Electrical conductivity of soils is a function of several physical factors pertaining to the soil's mineralogy and structure. In a sand-rich soil, the main physical factors affecting conductivity are the bulk conductivity of pore fluid, soil saturation, porosity and pore tortuosity. However, when dealing with clayey soils and rocks, there is an additional factor, which is the propensity of the surface of clay minerals to conduct and therefore contribute to the bulk electrical conductivity of the soil (Revil and Glover 1998). Surface electrical conductivity is related to the cation exchange capacity (CEC) of the clay minerals present in soil, and therefore, the greater number of cation exchangeable sites within the sand-clay soil mixture, the higher the bulk conductivity of the soil. A series of 32 soil core samples from BH5 and BH7 were tested for CEC and a plot of core resistivity—measured using Decagon 5TE soil moisture sensor (described above)—versus CEC produced. These tests were used to differentiate between the major soil types on the basis of lithological properties (i.e. CEC) and resistivity, thereby establishing petrophysical relationships to aid the interpretation of the 3D resistivity images.

Results and discussion

Surface expression

The geomorphology map of Hollin Hill is shown in Fig. 4. To the north of the site, an abrupt decrease in slope angle—highlighted by positive and negative break in slope—indicates the presence of the main scarp along with associated crown cracks as the landslide continues to retrogress northward. The back tilted nature of the head of the landslide is suggestive of rotational slumping. The main scarp can be traced east–west across the site; however, it is the northeast region that appears to be currently most active. The existence of fresh, very shallow rotational slumps to the northeast is evidence that shallow slumping is taking place alongside less active and more extensive, deeper-seated slumping. Traversing south from the main scarp and beyond the fresh, shallow rotational slumps are a series of five or six subtle pairs of positive and negative breaks in slope. Each pair is separated by near-horizontal or slightly back tilted ground surface and is indicative of rotated slump blocks. The number of rotational slumps present across the landslide system appears to vary in the mid-hill slope region of the system. The eastern region of the site has more visible fresh slumps than the west suggesting that the eastern has recently experienced more slumping events compared to the west of the site.

The geomorphologic nature of the site transforms further south as approximately parallel breaks in slope give way to curved breaks

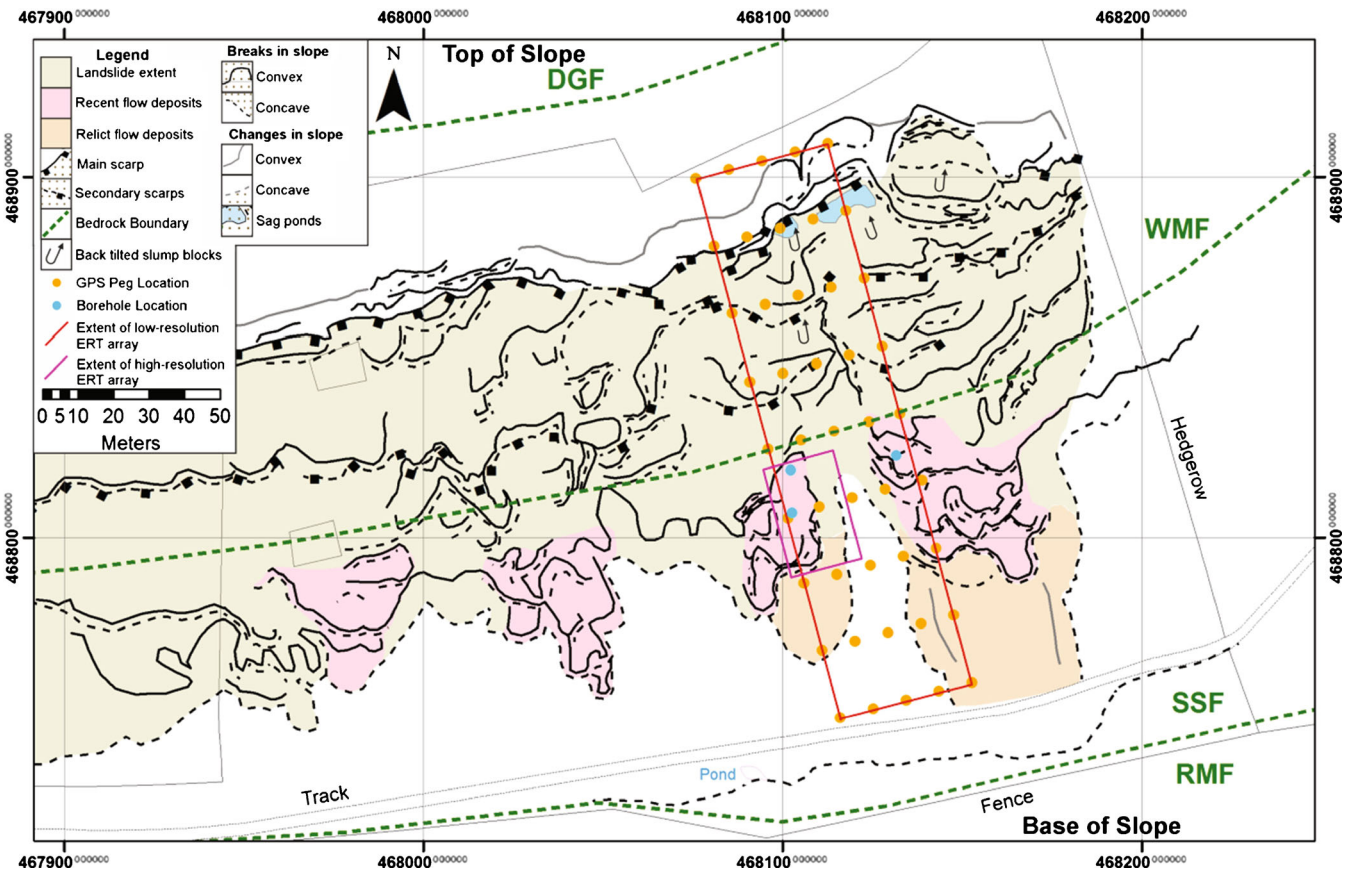

Fig. 4 Geomorphology map of the field site produced from an airborne LiDAR dataset, visualised using GeoVisionary software and presented using ArcGIS10. The top of the slope is towards the north of the map, with the base towards the south; coordinate system used is BNG

in slope. The change in surface expression is attributed to a change in landslide type as rotational slumping seen in the mid- to upper regions of the slope gives way to flowing, with several flows being active simultaneously. There are four regions of the landslide system where flows have developed and overridden slumped material. Each lobe of flow deposits is composed of previously slumped material and is comprised of several smaller flows—moving on multiple shear planes—which together form four distinct zones of accumulation throughout the field site. The zone of depletion of the landslide system lies between the main scarp to the north and the flow deposits further to the south. Above the two most easterly flow deposit lobes exists an area of relatively flattened and smoothed hill slope; this area is supplying displaced material to the currently active flow lobes.

Rates and distribution of movement

The results of the GPS survey are presented in Fig. 3, which shows marker peg movement during the monitoring period. Typical rates of movement are in the order of a few tens of centimetres per year and are restricted to small areas towards the front of the earth flow lobes, with most of the marker pegs remaining static.

Inclinometer data (Fig. 5) produced over a period of 2 months in 2009 (Oct–Dec 2009) at BH7 and a period of 12 months (Jan–Dec 2009) at BH1 show that the active slip surface of the flow lobes is at between 1.0 and 1.5 m depth, indicating that the same flow lobe is moving at the two locations. Maximum shear surface displacements during the period of investigation by inclinometer at BH1 and BH7 are 25 and 15 mm, respectively. BH5 inclinometer records show that a small amount of movement within the slumped deposits took place (2 mm of displacement), along with movement between 0.5 and 1.0 m depth during the 2009 period of monitoring.

Soil structure and types

The results of core logging, index, resistivity and CEC testing from BH1, BH7 and BH5 are shown in Fig. 5. These indicate that below the top soil layer are three principal soil units.

The uppermost layer is composed of several flow deposits, each separated by narrow slip surfaces. BH7 and BH1 are both interpreted as comprising six flow deposits, in which inclinometer data indicate that movement is occurring along shear planes between 1.0 and 1.5 m (see "Rates and distribution of movement" section). Flow shear planes were identifiable by core logging due to the existence of thin yellowish-brown clay layers, often found in conjunction with organic-rich horizons, decayed rootlets underlain by mottled grey, gleyed clay zones. Flow deposits of BH1 and BH7 show similarities in their particle size distributions as their upper 0.7 m is dominated by clay- and silt-sized material, below this depth—until the contact with slump deposits is reached at 3.1 m—sand-sized material dominates.

With increased depth, the clay-dominated and sand-dominated flow deposits give way to a series of rotational slump deposits. Slump deposits at BH1 and BH7 are distinctly heterogeneous, gravelly silty clay and clayey sandy silt being the most common soil types. Three slip surfaces are present in all three boreholes and are identifiable in soil core due to the existence of gravel-sized rip-up clasts, mostly composed of sub-angular, iron-stained clasts of sandstone. Where the formation is silt-dominated, shear surfaces exist as thin silt/clay-rich layers, 10 cm in thickness. At greater depths, at 5.20 and 4.90 m in BH7 and BH1, respectively, the base of the slump deposits exists and the top of in situ Staithes Sandstone Formation is reached. In the core, SSF is a firm to hard light olive grey to yellowish brown micaceous sandy clayey silt with occasional nodules of ironstone and siltstone. Inclinometer records show that no movement within slumped material took place within BH1 and BH7 during the period of monitoring.

The lithologies present within BH5, located on the eastern most flow lobe, follow a similar sequence to boreholes 1 and 7: a thin layer of top soil, followed by a series of clay-dominated flow deposits, three rotational slump deposits and in situ Staithes Sandstone Formation. Flow deposit thickness is 1 m thicker in borehole 5 than boreholes 1 and 7 located on the other investigated lobe, the second lobe to the east. Inclinometer records show two active shear planes, between 0.5 and 1.0 m—within flowed material—and between 4.0 and 4.5 m within slump deposits.

Soil properties

Clay content and mineralogy

The plasticity index and liquid limit of the unstable formations were determined and results presented in a plasticity plot (Fig. 6). The results show that WMF consistently has a high to very high plasticity with all points plotting below the a-line indicating that the formation behaves in a silt-like manner, whereas SSF has a lower liquid limit, plasticity index and plasticity compared to WMF and is attributed to SSF having a higher silt and/or sand content.

Clay mineralogy, determined from XRD analysis of material recovered from BH7, is summarised in Table 1. Clay contents vary from more than 50 % to less than 6 %, with illite-smectite and kaolinite represented. The sample of the slip surface within SSF—at 5.2 m—has a higher illite–smectite content (26.6 %) compared to other SSF-derived samples. Samples from 4.35, 5.2 and 5.7 m have a chlorite content of between 3.7 and 7.4 %, which could be a result of the slip surface acting as a conduit for clay minerals, transported by groundwater flow or rainfall infiltration. Comparison of the XRD and CEC results (i.e. Fig. 5 and Table 1) shows a consistent correspondence between high clay contents and CECs, demonstrating that CEC is a good indicator of clay content at this site.

Soil cation exchange capacity–resistivity relationships

By plotting resistivity—determined by soil conductivity probe in the laboratory—of the cored samples versus their cation exchange capacity of 32 samples from various depths throughout BH5 and BH7, it is possible to differentiate between the formations present based solely on their electrical properties. Figure 7 presents cored soil resistivity versus CEC in semi-log space and shows the presence of two clustered groups of results. The first cluster of results shows a range of electrical resistivities and CEC values of between 28–115 Ωm and 7–14 meq/100 g and corresponds to sand flow deposits, slumped material and in situ SSF and are represented on the resistivity–CEC plot as red, green and orange points, respectively. The second cluster produced resistivities and CEC values of between 8–14 Ωm and 25–30 meq/100 g, respectively. This cluster is composed of WMF-derived flow deposits as low resistivity and high CEC values are indicative of clay-rich material.

Located between clusters 1 and 2 are five data points which do not clearly belong to either the SSF or WMF clusters and are attributed to clay-rich layers located towards the top of SSF-derived slump deposits. In addition, two data points from clay flow material (BH5, 1.5 and 2.0 m) also plot between the cluster and are

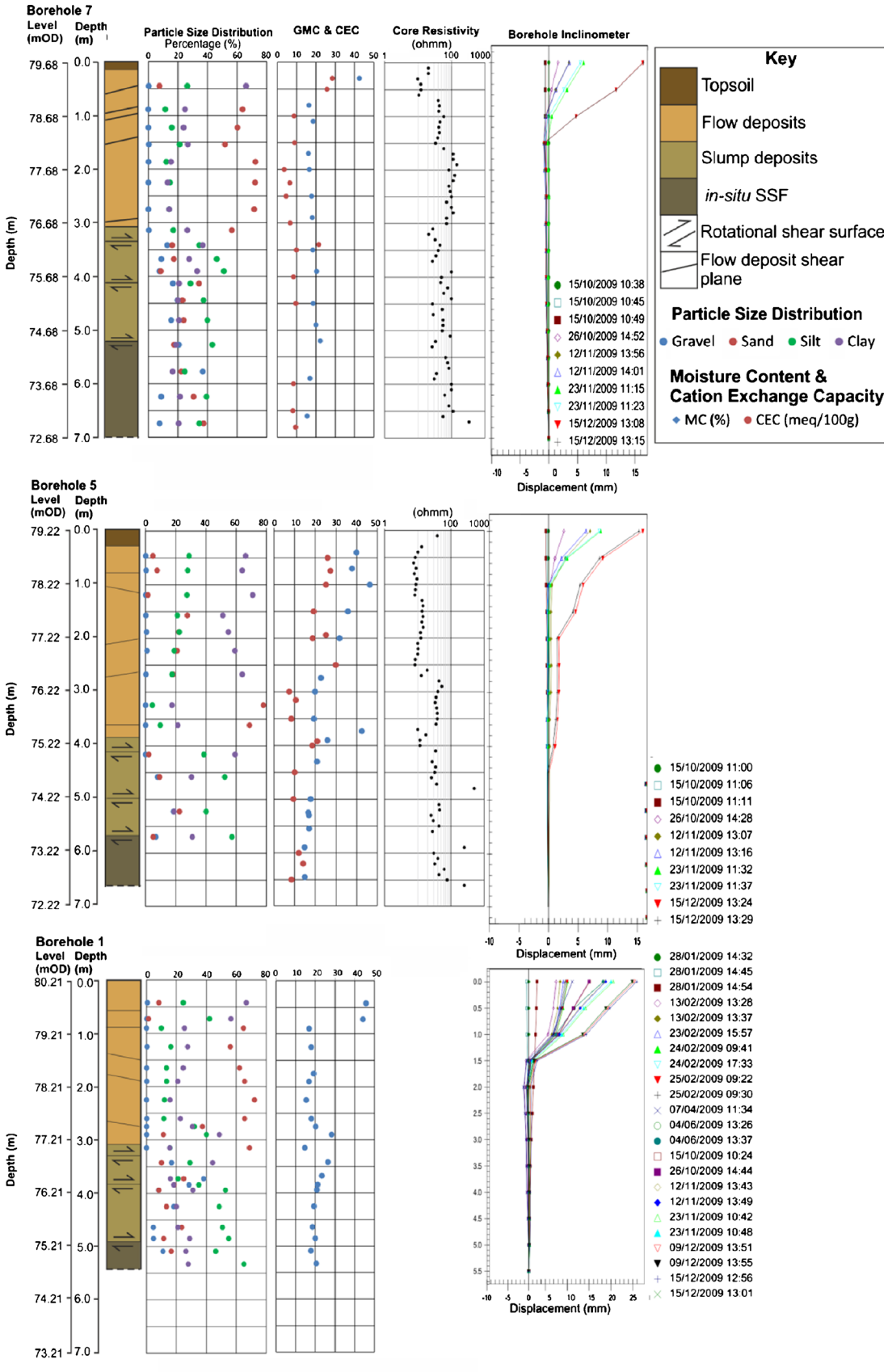

Fig. 5 Interpreted core logs including particle size analyses, moisture content, cation exchange capacity, core resistivity and inclinometer data of boreholes: BH1, BH5 and BH7. The cores, core logs and photos were analysed, and lithological layers were classified into one of four types: top soil, flow deposit, slump deposit or in situ SSF

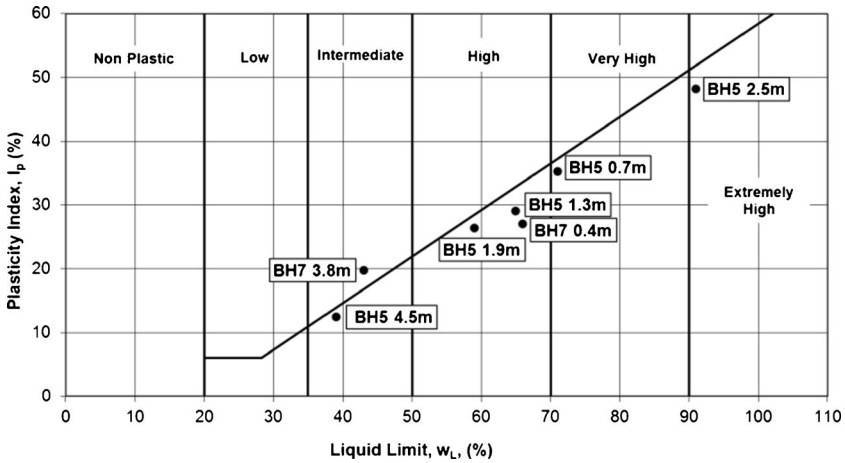

Fig. 6 Plot of Atterberg Limits results for soil samples from BH7 and BH5. A-line plot presents results as plasticity index versus liquid limit and shows the plasticity of soil samples

attributed to a WMF derived flow deposit with a higher sand content (~20 % sand) relative to the clay flow cluster (~5 % sand).

Soil resistivity

Borehole 7 is seen to contain several zones of varying resistivities, and good correlation exists between the various lithological and structural units found within the core. A thin layer of top soil exists from the surface to a depth of 0.2 m with a resistivity of 20 Ω m. The first clay-dominated flow exists between the top soil and 0.7 m depth, has a core resistivity of 10 Ωm and CEC value of 25–27 meq/100 g. Beyond the first flow deposit are a further three flows which have similar resistivities ranging between 40 and 60 Ω m, where the flow deposits are met by an abrupt increase in resistivity at 1.6 m. At this depth, the clay-dominated flow deposits give way to sand-dominated flows along with associated resistivity increase to between 70 and 120 Ωm. CEC results for this series of sandy flows are consistently lower than those of the clay flows at around 6 meq/100 g. The boundary between flow and slump deposits is marked by a decrease in resistivity at 3.0 m depth from ~100 Ωm to between 20 and 60 Ωm and with it comes a distinct change in lithology, as fines content increases from 30 to 70 %. The resistivity of the slump deposits and in situ SSF extending from 4.0 to 7.0 m (termination of borehole) show a range of values between 30 and 100 Ωm. This 3-m section of the borehole is composed of soil and weak rock layers along with an assortment gravels and sands. Despite the lithological variety shown by the slump and in situ SSF, cation exchange capacity remains constantly between 8 and 10 meq/100 g within this depth range.

Borehole 5 contains a thicker layer of clay-dominated flow deposits—ascertained through particle size analyses—and core resistivity measurements are persistently low from beyond the top soil (0.3 m) to the boundary with the rotational slump deposits at 3.9 m depth. Resistivity remains at 10 Ωm from 0.3 m until 2.7 m where it steps out for 1 m to 35 Ωm, between 2.7 and 3.7 m depth. Cation exchange capacity measurements within the clay flows between 0.3 and 2.8 m vary between 19 and 30 meq/100 g. Between 2.7 and 3.7 m the CEC is between 8 and 10 meq/100 g and coincides with a sand-dominated flow deposit possessing reduced clay content. The lowermost flow deposit and the uppermost slump deposit are located between 3.7 and 4.1 m depth and show a resistivity and CEC of 10–20 Ωm and 20 meq/100 g, respectively.

Slump deposits show an almost consistent resistivity from 4.1 to 5.7 m which marks the contact with in situ SSF and are between 25 and 45 Ωm, a much narrower range when compared to borehole 7. Core resistivity of in situ SSF gradually increases with depth from 30 Ωm at 6.0 m depth to 80 Ωm at 6.5 m. Two high resistivity outliers of over 250 Ωm exist within in situ SSF and are attributed to thin layers of weak siltstone. Between 4.1 and 6.5 m, the CEC measurement varies consistently between 9 and 14 meq/100 g.

Resistivity measurements made on soil cores show a range of values. This is due to the lithological variation within each soil type, which manifests as layers of more or less resistive material in core resistivity measurements. Accumulation and dissipation of soil moisture content also contribute to resistivity variability in subsurface material and varies both spatially and temporally within the subsurface.

Volumetric resistivity imaging (3D ERT)

Low resolution

The result of the large-scale ERT surveys of the landslide system is presented in Fig. 8. Three geological formations are present and are distinguished from one another by their relative differences in model resistivity (also see "Soil resistivity" section). High relative resistivities are expressed as warm colours such as browns, oranges and yellows, whereas relatively low resistivities appear blue and green. The low resistivity formation present at the top of the slope (*z*-axis, 100 m) is WMF and has a resistivity of 10–20 Ωm. Borehole-derived measurement of resistivity of the soil core samples recorded a resistivity of between 10 and 20 Ωm (Fig. 5). Clay-dominated flows can be seen between 0.2 and 0.7 m at BH7 and BH1 and 0.3 and 2.7 m at BH5. These resistivity values are in agreement with results of ERT surveys, thus confirming the presence and extent of clay-dominated flows—WMF derived—within both the survey and field site. This is the main formation which supplies material to form the flow lobes at Hollin Hill. The higher resistivity SSF is sandwiched between two low resistivity (blue) formations. When compared with WMF and RMF, SSF has a wider range of model resistivities, between 40 and 120 Ωm. Again, borehole-derived measurement of resistivity show similarity with ERT survey results as SSF exhibits core sample resistivities ranging between 30 and 100 Ωm (see Fig. 5).

Table 1 Results of X-ray diffraction analysis of six soil samples from BH7 which show the mineralogical composition of geological formation at the study site

Depth (m)	Soil Desc.	Quoted as % Quartz	Albite	Microline	Calcite	Dolomite	Mica	Illite–smectite	Kaolinite	Chlorite	Total
0.4 m	Flow	18.4	5.4	4.8	0.0	0.0	16.2	33.4	21.6	0.0	99.8
1.9 m	Flow	81.0	4.5	5.1	0.2	0.5	2.1	3.5	2.2	0.0	99.2
3.55 m	Slump	40.8	15.0	5.1	0.0	0.0	6.0	17.0	15.9	0.0	99.8
4.35 m	Slump	35.4	11.7	5.9	0.0	0.0	7.8	16.6	16.4	3.7	97.4
5.2 m	Slump: shear surface	32.9	9.9	5.8	0.0	0.0	4.3	26.6	11.2	7.4	98.1
5.70 m	In situ SSF	39.4	11.0	6.3	0.0	0.0	9.6	14.4	10.9	4.7	96.3

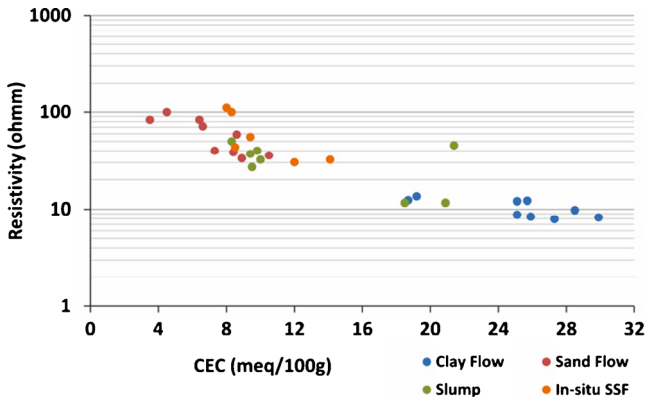

Fig. 7 Plot of core resistivity measurements versus cation exchange capacity of core samples from borehole BH5 and BH7. *Coloured points* represent different structural zones from the interpreted borehole logs (Fig. 5)

The stepped nature of the boundary between RMF with SSF in Fig. 8 is an artefact of the inversion process and increased sized of model blocks with depth. The more resistive regions of the tomogram are where the SSF crops out at the surface; this occurs towards the base of the slope, at the southern limits of the surveyed area. The uppermost ~4 m of Staithes Sandstone has relatively high resistivities in the order of 70–120Ωm; below this layer, the resistivity of the formation is lower at around 40Ωm. This unsaturated and free-draining layer is subjected to seasonal soil moisture content variation as a result of evapotranspiration. Below this more resistive zone, the formation appears to be reasonably homogeneous with respect to electrical resistivity. Finally, placed stratigraphically below SSF is a formation which appears dark blue in colour and is called Redcar Mudstone Formation. RMF, similarly to WMF, is a mudrock formation and has a model resistivity of 10–20Ωm. All three stratigraphical formations share a similar dip of between 5° and 10° to the north as can be seen from the layer boundaries in Fig. 8. An annotated cross section—parallel with the *y*-axis—is shown in Fig. 9 and has the interpreted core log of BH7 superimposed to aid the positioning of the three main rotational slip surfaces. Rotational slump shear surfaces were identified during core logging; however, no geomorphological evidence nor resistivity contrast exists within ERT survey images to suggest the exact orientation, length or form of these surfaces. The dearth of geomorphological evidence is due to the degradation of both the slumped SSF as a flow and the subsequent flowing of WMF up and over the SSF slumped material.

Rotational slip surfaces within WMF were matched with geomorphologic features picked out from LiDAR information and walkover survey. The material that composed the back scarp or slump block of that slump has since been activated, incorporated into a flow and deposited further down the slope. The boundary between the flow deposit of WMF—shown as a low resistivity (blue) mantle—with SSF-composed rotational slumps and in situ SSF is clearly marked by a change in resistivity from 10 to 20Ωm (WMF) to 50–65Ωm (SSF) and also correlates well with the interpreted borehole log of BH7. Flow deposits appear to thin in a southerly direction and show a maximum thickness of ~5–6 m. Two flow lobes can be seen in Fig. 8 and form the two pointed features at the sides of the image as the unstable WMF flows down the slope over the underlying SSF. The model cell versus resistivity plot (Fig. 8, right) is used to illustrate the range of resistivity

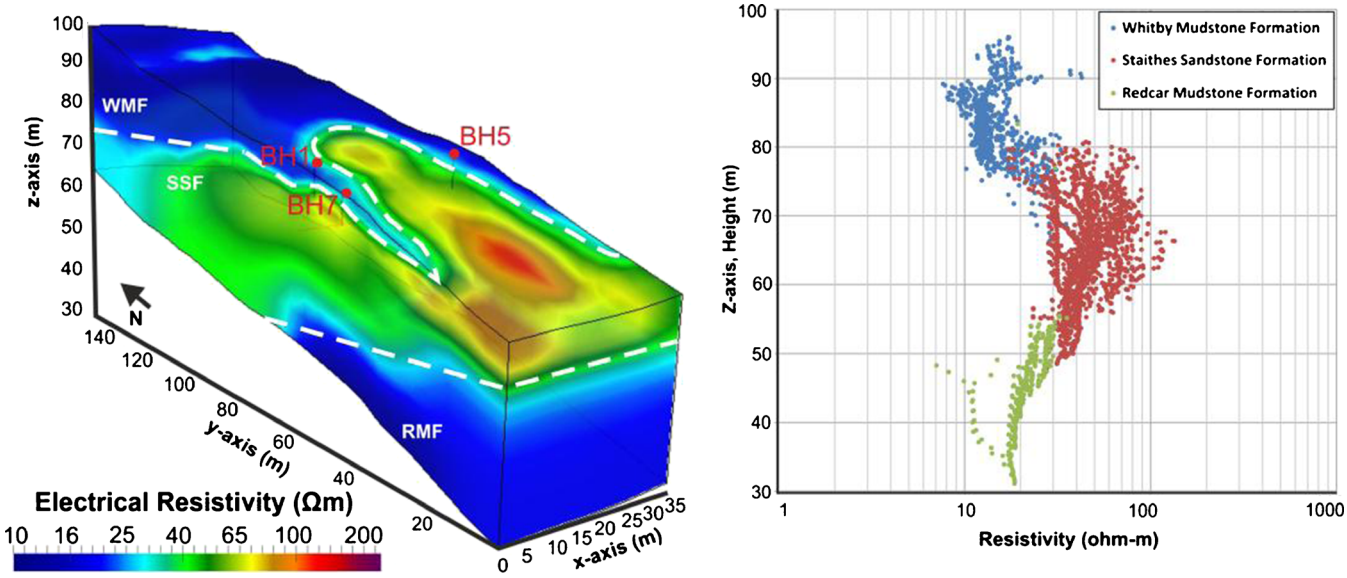

Fig. 8 3D volumetric image of resistivity from the low-resolution ERT survey (*red rectangle* on base map, Fig. 3) (*left*). Geological boundaries are marked with a *white dashed line* and formation names with *white text*. Plot of height of model cell (*z*-axis) versus resistivity for low-resolution ERT survey and shows distribution of lithological formations at Hollin Hill (*right*)

values for each lithological formation and acts as a guide—during ground model development—when applying ERT results to inform the ground model about spatial distribution of lithologies.

High resolution

Results of the high-resolution survey of the flow region are shown in Fig. 10 along with the positions of BH1 and BH7. Figure 10a shows the flow region at a higher resolution to the large-scale survey presented in Figs. 8 and 9, thus permitting the observation of additional subsurface features in the near surface. Much of the surface is dominated by the blue-coloured, lower resistivity unit which is composed of clay-dominated flow deposits of WMF. These flow deposits appear thinner in the high-resolution survey and have a maximum thickness of 3 m. In order to make the low-resistivity flow deposits more visible, Fig. 10b shows the blue flow deposits in 100 % opacity but with the underlying units which possess higher resistivities at 50 % opacity. From this figure, the spatial distribution of the clay-rich, low resistivity flow deposit is clear; it thins towards its periphery like a thin veneer over the underlying formation. This is in agreement with borehole data which suggests that clay-dominated flows exist from the surface to a depth of 0.5 and 0.8 m at BH7 and BH1, respectively. In the north of the survey area, the clay-dominated, blue-coloured, flow deposits appear thicker than to the south of the area. This thickening of the blue unit is attributed to stacking of flow deposits over one another as the landslide system evolved. Directly below the clay-dominated flow deposits is a more resistive, tabular shaped unit with an electrical resistivity of between 80 and 120Ωm. This silty sand unit is interpreted as a flow deposit which has experienced weathering-induced alteration. Boreholes 1 and 7 show that the lithology of the sand flow deposit is different to that seen elsewhere at the site, as the flows contain a greater sand content than WMF, in situ SSF and slumped SSF. This alteration could be attributed to weathering processes or mechanical reworking while in flow as the finer material has been preferentially removed from the soil. The sand content of the sand flow is between 50 and 70 %, yet the rest of the formations present at the hill slope contain a relatively low proportion of sand. It is therefore uncertain as to provenance of this sand flow; however, the weathering of a WMF-composed flow seems the most credible.

Figure 11 is a profile through the 3D volumetric image of model resistivity (Fig. 9) and is superimposed with interpreted borehole logs 1 and 7. Both 2D profiles offer good correlation with core logged data as all lithological and structural boundaries are identifiable and well constrained. Figure 10 identifies a small resistivity difference between the sand flow and the rotational slump deposits which are composed of SSF. The resistivity is seen to reduce across the boundary between the flow and slump deposits from 80 to 50Ωm.

Ground model development

The ground model of Hollin Hill was generated through the merging of results of many investigative methods and is presented as Fig. 12. This section aims to provide a summary of the contribution that each method provided to the process of ground model formulation.

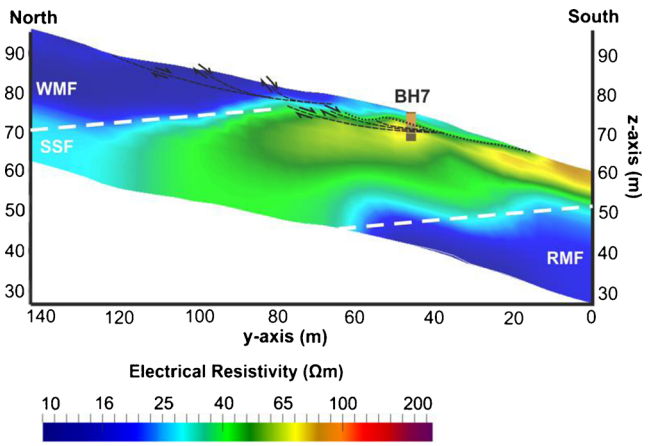

Fig. 9 2D ERT profile extracted from low-resolution 3D ERT survey. Profile runs parallel (approximately north–south) with *y*-axis and includes BH7. Rotational shear surfaces are represented by *black dashed lines*. Orientation and location of 2D ERT profile is indicated by an *orange profile line* on the base map (Fig. 2)

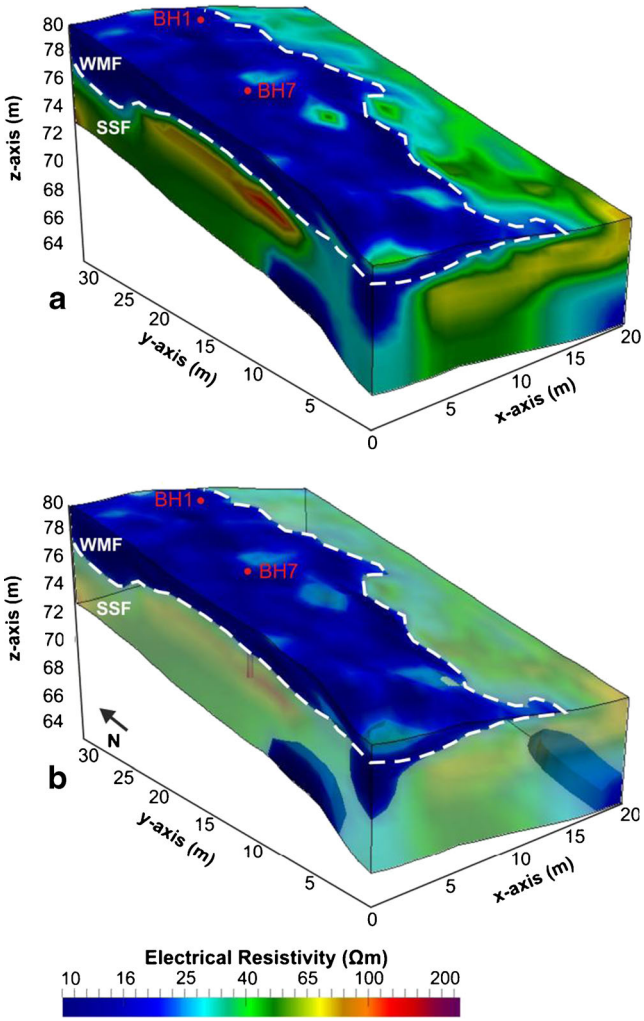

Fig. 10 3D volumetric image of resistivity from the high-resolution ERT survey (*purple rectangle* on the base map, Fig. 2). A *white dashed line* indicates the boundary between WMF and SSF, and *two red points* indicate borehole locations. **a** Resistivity model of earth flow region at 100 % opacity, **b** the higher resistivity zone at 40 % opacity and maintains the lower resistivity earth flow at 100 % opacity. N.B. Low resistivity features at the base of the image are likely to be artefacts of the inversion process associated with regions of very low sensitivity (and hence resolution)

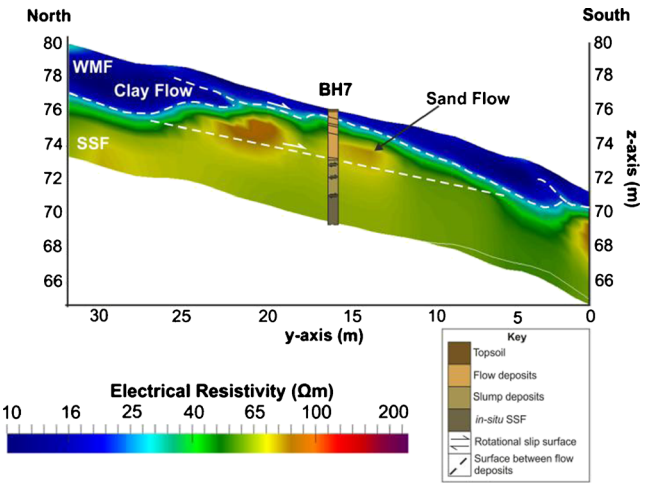

Fig. 11 Annotated profile through high-resolution ERT survey whose location is indicated by a *lilac profile line* on base map (Fig. 2). *White lines* represent flow surfaces with *arrows* indicating relative flow direction. The interpreted borehole log of BH7 shows structure of landslide system by landslide deposit type

Surface characterisation was performed through the interpretation of visualised airborne LiDAR remote sensing data. Remote sensing data permitted the interpretation of surface morphology—breaks in slope—and as a result identification (and location) of landslide type, such as the back scarp and back-rotated blocks indicative of rotational slumping. Visualisation of airborne LiDAR and production of geomorphology map allowed the spatial distribution of landslides to be determined, for example, a series of rotational slumps towards the top of the slope giving way to a number of flow deposits in the mid-slope region. By combining airborne LiDAR with aerial photography, the resulting DTM can be used to identify which areas of the landslide are most recently active by looking for surface features such as partially vegetated slopes/areas and abrupt or smoothed breaks in slope.

Low-resolution ERT determines the overall structure of the hill slope—at the formational scale—from beyond the back scarp to the relict flow deposits nearing the base of the slope. The low-resolution ERT survey picked out three lithological formations present at the field site (WMF, SSF and RMF), identified the nature of the flow deposits positioned over SSF and determined the regional dip of the formations. The low-resolution ERT is very much a reconnaissance survey, used to gain information quickly over a large area.

High-resolution ERT was performed to gain more information about active flow deposits and in particular their internal structure and lateral persistence. High-resolution surveying identified the resistivity contrasts which exist between flow deposits as a result of lithological variation. The blue, low resistivity uppermost flow deposits in contrast with deeper, higher resistivity flows. Core logging and index testing of boreholes performed at the field site shed further light on the reasons behind resistivity variation both between flow deposits and between lithological formations represented. ERT permits the interpolation of interpreted borehole information which can aid determining the landslide structure laterally.

Core logs were interpreted on the basis of mass movement type, so whether the soil cores were flow or slump deposits or in situ material. The task of differentiating between flow deposits and slump deposits required identification of features associated with each deposit type; for example, rotated bedding planes and presence of rip-up clasts are indications of slumping. Slip surfaces associated with flow deposits were identified as thin (~5 mm) bands of light brown clay between layers of highly disturbed dark brownish grey silty, sandy clay or silty sand.

Analysis of core soil samples allowed similarities to be drawn between core samples and ERT surveys. For example, core resistivity measurements can be used as a confirmatory tool when interpreting ERT surveys. In order to differentiate between clay and sand flow deposits in the high-resolution ERT survey, core resistivity measurements were utilised. Core resistivity measurements were then related to particle size analyses, and the resistivity variation could then be explained in terms of lithology. CEC versus core resistivity plot can inform about potential similarities in resistivities between lithological formations. In our example, differentiating between sand flow, slump and in situ SSF could be problematic, and as a result, any interpretation took this into account. For this reason, the differentiated between in situ SSF and slumped SSF was impossible and attributed to there being little to no lithological—and therefore

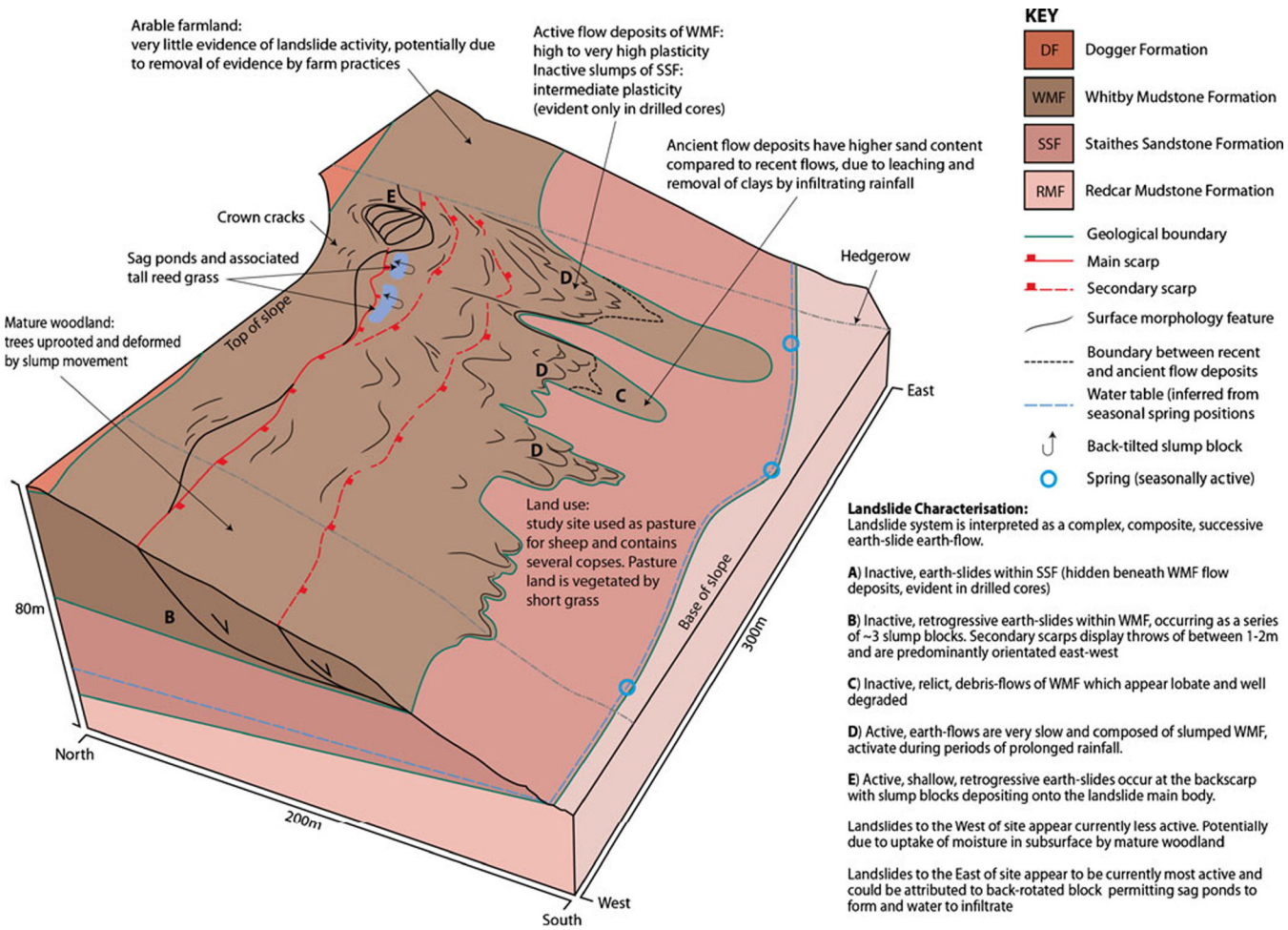

Fig. 12 Ground model of the Hollin Hill study site based on geophysical, geomorphological and geotechnical investigations

electrical property—variation between the two. XRD results also indicate the mineralogical similarities between slumped and in situ SSF, and dissimilarities with clay and sand dominated flows of WMF.

Implementation of peg displacement results along with ERT surveys and geomorphology studies made it possible to define active landslide regions, types of movement (flow or slump) and rate of displacement. With the addition of inclinometer results, the active shear surfaces were identified and incorporated into the ground model.

The concept and methodology of ground model development as outlined by Fookes (1997) was followed—where appropriate—and tried to inform about all the elements of a ground model: rock formation and modification processes. Fookes (1997) outlines that geophysical data must be thoughtfully interpreted and used to improve and refine a developing ground model. In our case, geophysical data complemented the earliest versions of Hollin Hill ground model which were based solely on intrusive information (borehole logs and inclinometer data).

Conclusions

Geoelectrical methods such as ERT can be usefully applied to landslide investigations where ground truth information is provided and where several lithological formations of contrasting resistivities exist within the area of interest. The investigation presented here informed to a high level of detail about subsurface conditions present within the hill slope by drawing upon many complementary information streams. Where one data set lacked the ability or resolution to inform about a feature or property another could be used to provide such information, an example being the inability of the large-scale ERT to differentiate between slumped and in situ SSF, instead the positions of the slump shear surfaces in SSF were identified in core logs.

A detailed ground model was developed based on additional high-resolution ERT information, remote sensing datasets and thorough interpretation of results from core logging, geotechnical testing and laboratory analysis of core samples. An integrated approach for ground model development, which takes into account both subsurface and surface investigative methods, is shown to improve the conclusions that can be drawn from a given site investigation. This is achieved by calibration of the geophysical results with direct physical property measurements of materials taken from the landslide and its environs. In particular, the use of 3D ERT at different spatial resolutions provides a means of volumetrically characterising the subsurface expression of both site scale (tens of metres) geological structure and finer (metre to sub-metre) scale earth-flow related structures, which were not effectively revealed by either the 1D information derived from discrete intrusive sampling, or the 2D surface data provided by remote sensing.

A key factor to be considered when designing a resistivity survey in the context of landslide investigation is the electrode spacing, as this has a profound effect on the resolution of the images returned. Resistivity images and profiles must be of a sufficient resolution and quality to permit the identification of the features of interest, in our case the

individual flow deposits, which were only detectable at the high-resolution afforded by closer electrode spacings.

Acknowledgments

We wish to convey our sincerest gratitude to Mr. And Mrs. Gibson (the landowners) for their involvement and cooperation throughout. This work was funded by the Natural Environment Research Council (NERC) (grant award NE/I1527988/1) and the University of Leeds. This paper is published with the permission of the Executive Director of the British Geological Survey (NERC) and the University of Leeds. Visualisation of airborne LiDAR data set using GeoVisionary was made possible by assistance from Mr Luke Bateson of British Geological Survey.

References

Baldo M, Bicocchi C, Chiocchini U, Giordan D, Lollino G (2009) LIDAR monitoring of mass wasting processes: the Radicofani landslide, Province of Siena, Central Italy. Geomorphology 105(3):193–201

Bichler A, Bobrowsky P, Best M, Douma M, Hunter J, Calvert T, Burns R (2004) Three-dimensional mapping of a landslide using a multi-geophysical approach: the Quesnel Forks landslide. Landslides 1:29–40. doi:10.1007/s10346-003-0008-7

BS1377 (1990) Methods of testing for soils for civil engineering purposes

BS5930 (1999) Code of practice for site investigation, British Standards Institution

Chambers JE, Wilkinson PB, Kuras O, Ford JR, Gunn DA, Meldrum PI, Pennington CVL, Weller AL, Hobbs PRN, Ogilvy RD (2011) Three-dimensional geophysical anatomy of an active landslide in Lias Group mudrocks, Cleveland Basin, UK. Geomorphology 125(4):472–484. doi:10.1016/j.geomorph.2010.09.017

Colangelo G, Lapenna, V., Loperte, A., Perrone, A., Telesca, L. (2008) 2D electrical resistivity tomographies for investigating recent activation landslides in Basilicata Region (Southern Italy). Ann Geophys 51:275–285

Colesanti C, Wasowski J (2006) Investigating landslides with space-borne Synthetic Aperture Radar (SAR) interferometry. Eng Geol 88(3):173–199

Cruden DM, Varnes, D.J. (1996) Landslide types and processes. In: Turner AK, Schuster RL (eds) Landslides, investigation and mitigation. Special report 247, Washington, DC

Dahlin T, Zhou B (2004) A numerical comparison of 2D resistivity imaging with 10 electrode arrays. Geophys Prospect 52(5):379–398

de Bari C, Lapenna V, Perrone A, Puglisi C, Sdao F (2011) Digital photogrammetric analysis and electrical resistivity tomography for investigating the Picerno landslide (Basilicata region, southern Italy). Geomorphology 133(1):34–46

Dewitte O, Jasselette JC, Cornet Y, Van Den Eeckhaut M, Collignon A, Poesen J, Demoulin A (2008) Tracking landslide displacements by multi-temporal DTMs: a combined aerial stereophotogrammetric and LIDAR approach in western Belgium. Eng Geol 99(1):11–22

Di Maio R, Piegari E (2011) Water storage mapping of pyroclastic covers through electrical resistivity measurements. J Appl Geophys 75(2):196–202. doi:10.1016/j.jappgeo.2011.07.009

Di Maio R, Piegari E (2012) A study of the stability analysis of pyroclastic covers based on electrical resistivity measurements. J Geophys Eng 9(2):191

Fookes PG (1997) Geology for engineers: the geological model, prediction and performance. Q J Eng Geol Hydrogeol 30(4):293–424. doi:10.1144/gsl.qjeg.1997.030.p4.02

Ford, J.R. (2013). Geological map of the High Stittenham Area (Sheet SE66NE). British Geological Survey, Nottingham

Godio A, Strobbia C, De Bacco G (2006) Geophysical characterisation of a rockslide in an alpine region. Eng Geol 83(1–3):273–286. doi:10.1016/j.enggeo.2005.06.034

Griffiths J, Stokes M, Stead D, Giles D (2012) Landscape evolution and engineering geology: results from IAEG Commission 22. Bull Eng Geol Environ 71:605–636. doi:10.1007/s10064-012-0434-7

Head KH (2006) Manual of Soil Laboratory Testing: soil classification and compaction tests. Whittles, Caithness

Heincke B, Günther T, Dalsegg E, Rønning JS, Ganerød GV, Elvebakk H (2010) Combined three-dimensional electric and seismic tomography study on the Åknes rockslide in western Norway. J Appl Geophys 70(4):292–306

Jaboyedoff M, Oppikofer T, Abellán A, Derron M-H, Loye A, Metzger R, Pedrazzini A (2012) Use of LIDAR in landslide investigations: a review. Nat Hazard 61(1):5–28. doi:10.1007/s11069-010-9634-2

Jomard H, Lebourg T, Binet S, Tric E, Hernandez M (2007) Characterization of an internal slope movement structure by hydrogeophysical surveying. Terra Nova 19(1):48–57. doi:10.1111/j.1365-3121.2006.00712.x

Jongmans D, Garambois S (2007) Geophysical investigation of landslides: a review. Bull Soc Géol Fr 178(2):101–112

Jordan C, Bateson L, Bow J, Newell A, Napier B, Sabine RJ, British Geological Survey, Tethys Petroleum (2009) GeovisionaryTM software for 3D visualisation and petroleum exploration in southern Tajikistan. Paper presented at the RSPSoc 2009: New Dimensions in Earth Observation, Leicester, UK

Lapenna V, Lorenzo P, Perrone A, Piscitelli S, Sdao F, Rizzo E (2003) High-resolution geoelectrical tomographies in the study of Giarrossa landslide (southern Italy). Bull Eng Geol Environ 62(3):259–268. doi:10.1007/s10064-002-0184-z

Lebourg T, Binet S, Tric E, Jomard H, El Bedoui S (2005) Geophysical survey to estimate the 3D sliding surface and the 4D evolution of the water pressure on part of a deep seated landslide. Terra Nova 17(5):399–406. doi:10.1111/j.1365-3121.2005.00623.x

McDowell P, Barker RD, Butcher A, Culshaw M, Jackson P, McCann D, Skipp B, Matthews S, Arthur J (2002) Geophysics in engineering investigations. Ciria, London

Perrone A, Iannuzzi A, Lapenna V, Lorenzo P, Piscitelli S, Rizzo E, Sdao F (2004) High-resolution electrical imaging of the Varco d'Izzo earthflow (southern Italy). J Appl Geophys 56(1):17–29. doi:10.1016/j.jappgeo.2004.03.004

Perrone A, Zeni G, Piscitelli S, Pepe A, Loperte A, Lapenna V, Lanari R (2006) Joint analysis of SAR interferometry and electrical resistivity tomography surveys for investigating ground deformation: the case-study of Satriano di Lucania (Potenza, Italy). Eng Geol 88(3–4):260–273. doi:10.1016/j.enggeo.2006.09.016

Powell J (1984) Lithostratigraphical nomenclature of the Lias Group in the Yorkshire Basin. In: Proceedings of the Yorkshire Geological and Polytechnic Society. Geological Society of London, 45, pp 51–57. doi:10.1144/pygs.45.1-2.51

Rawson PF, Wright JK (1995) Field geology of the British Jurassic. In: Taylor PD (ed) Jurassic of the Cleveland basin, North Yorkshire. Geological Society of London, London, pp 173–208

Revil A, Glover PWJ (1998) Nature of surface electrical conductivity in natural sands, sandstones, and clays. Geophys Res Lett 25(5):691–694. doi:10.1029/98gl00296

Reynolds J (2011) An introduction to applied and environmental geophysics. Wiley, New York

Sass O, Bell R, Glade T (2008) Comparison of GPR, 2D-resistivity and traditional techniques for the subsurface exploration of the Öschingen landslide, Swabian Alb (Germany). Geomorphology 93(1–2):89–103

Schmutz M, Guérin R, Andrieux P, Maquaire O (2009) Determination of the 3D structure of an earthflow by geophysical methods. The case of Super Sauze, in the French southern Alps. J Appl Geophys 68(4):500–507

Telford WM, Geldart LP, Sheriff RE (1990) Applied geophysics. Cambridge University Press, Cambridge

Topp G, Davis J, Annan AP (1980) Electromagnetic determination of soil water content: measurements in coaxial transmission lines. Water Resour Res 16(3):574–582

Udphuay S, Günther T, Everett ME, Warden RR, Briaud J-L (2011) Three-dimensional resistivity tomography in extreme coastal terrain amidst dense cultural signals: application to cliff stability assessment at the historic D-Day site. Geophys J Int 185(1):201–220. doi:10.1111/j.1365-246×.2010.04915.x

Wilkinson P, Loke MH, Meldrum PI, Chambers JE, Kuras O, Gunn DA, Ogilvy RD (2012) Practical aspects of applied optimised survey design for electrical resistivity tomography. Geophys J Int 189(1):428–440

A. J. Merritt (✉) · **W. Murphy** · **L. J. West**
School of Earth & Environment, Earth & Environment Building,
University of Leeds,
Woodhouse Lane, West Yorkshire, LS2 9JT, UK
e-mail: eeam@leeds.ac.uk

J. E. Chambers · **P. B. Wilkinson** · **D. A. Gunn** · **P. I. Meldrum** · **M. Kirkham**
Environmental Science Centre,
British Geological Survey,
Nottingham, UK

N. Dixon
School of Civil and Building Engineering,
Loughborough University,
Leicestershire, LE11 2TU, UK